Antarctic sedimentary basins and their influence on ice sheet dynamics

Alan R.A. Aitken[1], Lu Li[1], Bernd Kulessa[2], Dustin M Schroeder[3], Tom A. Jordan[4], Joanne M Whittaker[5], Sridhar Anandakrishnan[6], Eliza J Dawson[3], Douglas A Wiens[7], Olaf Eisen[8], and Martin J. Siegert[9]

[1]University of Western Australia
[2]Swansea University
[3]Stanford University
[4]British Antarctic Survey
[5]University of Tasmania
[6]Pennsylvania State University
[7]Washington University
[8]Alfred Wegener Institute Helmholtz Center for Polar and Marine Research
[9]Imperial College London

June 16, 2023

Antarctic sedimentary basins and their influence on ice-sheet dynamics

A.R.A. Aitken[1,2], L. Li[1], B. Kulessa[3,4], D. Schroeder[5,6], T.A. Jordan[7], J.M. Whittaker[8], S. Anandakrishnan[9], E.J. Dawson[5], D. A. Wiens[10], O. Eisen[11,12], M.J. Siegert[13,14]

1. School of Earth Sciences, The University of Western Australia, Perth, Western Australia, Australia
2. Australian Centre of Excellence for Antarctic Science, The University of Western Australia, Perth, Western Australia, Australia
3. School of Biosciences, Geography and Physics, Swansea University, Wales, UK
4. School of Geography, Planning and Spatial Sciences, The University of Tasmania, Hobart Tasmania, Australia
5. Department of Geophysics, Stanford University, Stanford, California, USA
6. Department of Electrical Engineering, Stanford University, Stanford, California, USA
7. British Antarctic Survey, Cambridgeshire, UK
8. Institute for Marine and Antarctic Studies, University of Tasmania, Hobart, Tasmania, Australia
9. College of Earth and Mineral Sciences, Pennsylvania State University, Pennsylvania, USA
10. Department of Earth & Planetary Sciences, Washington University, St. Louis, Missouri, USA
11. Glaciology, Alfred Wegener Institute, Helmholtz Centre for Polar and Marine Research, Bremerhaven, Germany
12. Department of Geosciences, University of Bremen, Bremen, Germany
13. Grantham Institute and Department of Earth Science and Engineering, Imperial College London, London, UK
14. Tremough House, University of Exeter, Penryn, Cornwall, UK

Corresponding author: Alan Aitken (alan.aitken@uwa.edu.au)

Key Points

- Recent advances in detection and characterization of subglacial sedimentary basins are reviewed
- A new map of Antarctic sedimentary basins is presented and implications for glacial processes are discussed
- Some future directions in Antarctic subglacial sedimentary basins research are explored

Abstract

Knowledge of Antarctica's sedimentary basins builds our understanding of the coupled evolution of tectonics, ice, ocean, and climate. Sedimentary basins have properties distinct from basement-dominated regions that impact ice-sheet dynamics, potentially influencing future ice-sheet change. Despite their importance, our knowledge of Antarctic sedimentary basins is restricted. Remoteness, the harsh environment, the overlying ice sheet, ice shelves and sea ice all make fieldwork challenging. Nonetheless, in the past decade the geophysics community has made great progress in internationally coordinated data collection and compilation with parallel advances in data processing and analysis supporting a new insight into Antarctica's subglacial environment. Here, we summarize recent progress in understanding Antarctica's sedimentary basins. We review advances in the technical capability of radar, potential fields, seismic and electromagnetic techniques to detect and characterize basins beneath ice and advances in integrated multi-data interpretation including machine-learning approaches. These new capabilities permit a continent-wide mapping of Antarctica's sedimentary basins and their characteristics, aiding definition of the tectonic development of the continent. Crucially, Antarctica's sedimentary basins interact with the overlying ice sheet through dynamic feedbacks that have the potential to contribute to rapid ice-sheet change. Looking ahead, future research directions include techniques to increase data coverage within logistical constraints, and resolving major knowledge gaps, including insufficient sampling of the ice-sheet bed and poor definition of subglacial basin structure and stratigraphy. Translating the knowledge of sedimentary basin processes into ice-sheet modelling studies is critical to underpin better capacity to predict future change.

Plain Language Summary

Antarctica is the keystone to the former supercontinent Gondwana and, because of its unique isolated location at the South Pole, it has important consequences for understanding changing global climate and ocean change. In several ways, sedimentary basins beneath the ice sheet interact with the ice sheet above and can potentially contribute to rapid ice-sheet changes that impact global sea level and climate. These sedimentary basins have not all been systematically mapped due to the challenge of studying them beneath thick ice. In this work we review technical progress towards the understanding of sedimentary basins in the subglacial environment, and we map out the sedimentary basins beneath Antarctica's ice. We explore how improved knowledge of Antarctica's basins helps to (1) understand important tectonic events in the continent, (2) unravel the evolution of the landscape and the ice sheet, and (3) contribute to improved predictions of future ice-sheet change. Remaining challenges to advance Antarctic sedimentary basins research are identified and some future directions for study are discussed.

1 Introduction

Sedimentary basins are widely preserved on all of Earth's continents and provide distinct environments for physical, chemical and biological processes (Evenick, 2021). Antarctica is no exception and possesses several major sedimentary basins and many smaller ones distributed across the continent. Seasonally ice-free marine regions, including the Ross, Weddell, and Amundsen seas, and much of the East Antarctic continental margin are relatively well surveyed (Fig 1). However, the unique challenge of ice-covered inland Antarctica, with very limited and spatially clustered outcrops (Fig 1), a kilometers-thick ice sheet and severe environmental and logistical challenges has meant that the distribution and nature of sedimentary basins is poorly known inland. On the continental shelf, ice shelves and perennial sea ice limit access to both marine and terrestrial techniques. Sedimentary basins are important not just for the understanding of Antarctic geology, but also because they provide key boundary conditions for glacial processes, with major impacts on the dynamics of the overlying ice sheet (Bell et al., 1998; Gooch et al., 2016; Kulessa et al., 2019; Li et al., 2022; Person et al., 2012; M. J. Siegert et al., 2018; M. Studinger et al., 2001; Tankersley et al., 2022; Zhang et al., 2018).

The discovery of sedimentary basins in Antarctica has been a continuing theme since the earliest Antarctic expeditions. The earliest explorations captured both the existence of extensive sedimentary rocks in outcrop (Ferrar, 1907; Mawson, 1940) and speculated on the presence of major sedimentary basins in the marine regions, especially the Ross, Weddell and Scotia Seas (Mawson, 1928). A more comprehensive record emerged in the second half of the 20th Century, in particular the period following the 1957/8 International Geophysical Year (IGY) (Naylor et al., 2008), when geophysical mapping of subglacial geology became a consistent feature of Antarctic exploration (Bailey et al., 1964; Bentley et al., 1960; S. Evans & Robin, 1966). Key techniques were developed and adapted to Antarctic requirements, including radio-echo sounding (RES), since the 1960s (R. G. Bingham & M. J. Siegert, 2007; Dustin M. Schroeder et al., 2020; Turchetti et al., 2008), active- and passive-seismic surveying, since the 1950s and 1990s respectively (Anandakrishnan et al., 2000; Bentley et al., 1960; Lawrence et al., 2006; Robin, 1958) and airborne magnetic and gravity surveys, since the 1960s and 1990s respectively (Behrendt et al., 1966; R. E. Bell et al., 1999). The data collected led to the first continent-scale compilations, including for ice thickness and bed elevation (BEDMAP; Lythe & Vaughan, 2001), magnetic data (ADMAP; A. Golynsky et al., 2001; A. Golynsky et al., 2006) and gravity data (ADGRAV; R. Bell et al., 1999).

The 21st Century has seen continued development and refinement of these approaches, and of course the broadening of coverage over the continent, and the last decade has seen the development of much more detailed and comprehensive compilations (Frémand, Fretwell, et al., 2022; Fretwell et al., 2013; A. V. Golynsky et al., 2018; Scheinert et al., 2016). New techniques for compilation have emerged including the integration of satellite gravity and magnetic data (Ebbing et al., 2021; Ebbing et al., 2018; Scheinert et al.,

2016), and for topography the inclusion of mass-conservation techniques (Mathieu Morlighem et al., 2020) and geostatistical approaches (Emma J. MacKie et al., 2021).

These advances in the coverage and quality of key geophysical datasets, coupled with the development of new data processing and analysis techniques, mean it is now feasible to map with some confidence the sedimentary basins of the Antarctic continent (Li et al., 2022). In this review, we explore the state of the art with respect to defining the subglacial sedimentary basins of Antarctica, and we summarize the extent and nature of these across the continent. The evolving tectonic setting of basin formation since Pangea is discussed. We explore the interactions of sedimentary basins with glacial processes and consider implications for ice sheet dynamics. Finally, we look ahead to the next set of challenges in defining the extent, characteristics and importance of sedimentary basins in Antarctica.

2 Defining Subglacial Sedimentary Basins

2.1 What is a sedimentary basin?

A sedimentary basin is defined by the development of accommodation space into which sediments have been deposited. This definition needs several concepts to align: first, the development of a topographic depression or shallow-sloped platform is required; second, there must be a source of sediment derived from mechanical erosion, or from chemical or biological processes; third the deposition and accumulation of sediments must occur and fourth, these must be preserved to the present day. The most common situation on continents is that sediments eroded from highlands are deposited and preserved in a topographic depression, forming a sedimentary basin (Allen et al., 2015).

Sedimentary and metasedimentary rocks are commonly interpreted to represent their sedimentary basin, potentially defining such properties as extent and thickness of fill and the depositional environment. Later uplift, erosion, deformation, intrusion by magmatic rocks, or other events may make the original depositional basin hard to define. Furthermore, in metamorphic rocks, physical properties may become dominated by crystal structures rather than fluid-filled pore networks, and this affects both the geophysical expression (Enkin et al., 2020) and the nature of their interaction with glacial processes (Krabbendam & Glasser, 2011). For these reasons we exclude exposed metasedimentary rocks of greenschist facies or above from consideration in this study. Recent sediment deposits are widely exposed in ice-free regions (Cox et al., 2023) and subglacial sediments are a prominent feature of the ice sheet bed across all environments. While these sediments are an important facet of subglacial geology, their presence does not intrinsically define a sedimentary basin in line with the definition above and so they are excluded from consideration in our classification.

We define two major classes of sedimentary basin. Type 1 basins exist where a substantial amount of basin-fill, including sediments and sedimentary rocks, is preserved in the original depositional basin, with no

evidence for substantial uplift, major deformation or metamorphism. A certain degree of compaction, diagenesis and deformation are expected in all basins. In contrast, Type 2 basins exist where exposures or other evidence indicate the presence of sedimentary rocks for which the original depositional basin is not preserved.

2.2 Recent progress in characterization of subglacial sedimentary basins

Globally, the analysis of sedimentary basins is commonly achieved through extensive use of outcrops, where available, supported by drill-core and high-resolution active seismic reflection studies allowing detailed basin characterization. In Antarctica these key data are available only in selected areas (Fig 1) and, in the general case, the major challenge is to define and characterize basins in the subglacial environment, for which specialized techniques are needed.

2.2.1 Direct geological characterization

Direct access to rocks through outcrop, detrital samples or drill core is fundamental to sedimentary basin analysis, permitting a full assessment of sedimentary characteristics and enabling application of detrital geochronology, thermochronology and other key analysis techniques. In marine and some sub-ice-shelf settings of Antarctica (Fig 1), drilling programs with linked seismic surveys have revealed many key features of sedimentary basins on the continental shelf, in particular in the Ross Sea, Prydz Bay and Amundsen Sea (K. Gohl et al., 2017; Marschalek et al., 2021; R. M. McKay et al., 2016; Whitehead et al., 2006). Ice-shelf and sea-ice cover is a major limitation for offshore studies, leading to a substantial data gap on the inner continental shelf (Fig 1). Developing offshore exploration technologies including autonomous underwater vehicles (Batchelor et al., 2020; Davies et al., 2017; Dowdeswell et al., 2008), seafloor drilling (K. Gohl et al., 2017) and sub-ice shelf drilling (Gong et al., 2019) are enabling these data gaps to be filled.

For onshore regions, Antarctica possesses high-quality sedimentary rock outcrops in numerous areas, and these can provide the key knowledge for basin studies in those regions. The collation of Antarctic geological data has progressed significantly, with continent-scale compilations of key data now accessible (Cox et al., 2023; Sanchez et al., 2021). While a great deal of knowledge has been gained by these approaches, a severe limitation is the tendency for outcrops to occur only on major highlands, isolated nunataks and coastal islands, leaving unsampled the low-lying regions that contain the bulk of sedimentary rocks. This leads to some undesirable bias towards older and/or uplifted sedimentary rocks and, therefore, the utility of outcrop-based data to infer subglacial geology is limited. Outcrop data are focused in spaced clusters (Fig 1), often with a high degree of internal complexity, meaning that interpolation between these clusters carries high uncertainty.

Detrital samples from much younger sediments can mitigate exposure bias (Maritati et al., 2019; Mulder et al., 2019; Thomson et al., 2013), but the lack of a precisely known source location for these samples renders

their use to characterize inland basins highly uncertain. Plainly, for a more representative sampling of the Antarctic bedrock, drilling is necessary. As with offshore drilling, onshore sub-ice drilling techniques are developing (Gong et al., 2019; J. W. Goodge et al., 2021; Hodgson et al., 2016; Kuhl et al., 2021; Talalay et al., 2021) and have seen operation in several locations (Fig 1), with an intent to expand towards more systematic coverage in the future. Notably, the alignment of these records with major ice-coring initiatives has strong potential to inform glacial evolution on multiple timescales.

2.2.2 Indirect characterization

Despite the benefits of direct characterization, a systematic coverage of Antarctica requires indirect characterization from geophysical data to survey the regions where no direct information exists. The major techniques include ground and/or ship-based techniques including active and passive seismic methods and magnetotellurics, as well as airborne techniques including radio-echo sounding (RES), gravity and magnetic methods.

2.2.2.1 Radio-echo sounding

RES is an efficient geophysical method to characterize the morphology and nature of the ice-sheet bed. In the context of basin studies, RES data can define both the large-scale morphology of topographic depressions, but also the detailed character of the bed, as defined by along-track roughness measures. While radar data can give a robust characterization of the bed at fine resolutions, hundreds of meters or less, the technique cannot directly indicate a sedimentary origin, nor is it able to define the thickness or properties of the sedimentary cover.

RES systems have been used for more than five decades to determine the thickness of ice sheets in an effective way (Dustin M. Schroeder et al., 2020). Over that period, more than 1.5 million line-kilometers of RES data have been collected in Antarctica, with airborne surveys predominating in recent times (Frémand, Fretwell, et al., 2022; Mathieu Morlighem et al., 2020). By subtracting the radar-defined ice thickness from surface-elevation data, bed topography can be determined. Surface elevation may be obtained from the RES data, from other sensors (e.g. LIDAR) on the same platform, or from remote-sensing products (e.g. DEMs from satellite studies). The final product is bed-elevation profiles of the ice-bed interface that are interpolated to produce gridded bed-topography products. Interpolation may be done in numerous ways, including direct spline-based interpolation (Fretwell et al., 2013) or geostatistical interpolation (Emma J. MacKie et al., 2021); with the inclusion of ice-sheet flow data, mass-conservation approaches may be used also (Mathieu Morlighem et al., 2020).

For the nadir-facing acquisition geometry of RES, specular and quasi-specular returns from the surface and bed are typically the most prominent features in a radar trace (Haynes et al., 2018), which allows for straightforward interpretation of along-profile ice thickness and bed topography. Although the earliest

196 systems were incoherent (Dustin M. Schroeder et al., 2019) the development of coherent systems (Gogineni
197 et al., 1998) and synthetic-aperture radar processing with range migration (Heliere et al., 2007; M. E. Peters
198 et al., 2007) improved the azimuth resolution of radargrams and the resulting extracted thickness profiles as
199 well as improving clutter mitigation in regions of high topographic relief and layover. More recently, swath
200 (Holschuh et al., 2020), tomographic (Paden et al., 2010), and array-based (T. J. Young et al., 2018) systems
201 as well as the availability of ultra-wideband systems (Arnold et al., 2020; Hale et al., 2016) have further
202 improved the geometric resolution of RES observations, with range resolution in the tens of centimeters and
203 along-track resolution in the tens of meters (Kjær et al., 2018).

204 The roughness of the bed encodes information on the morphologic and geologic character of the subglacial
205 interface (Jordan, Ferraccioli, Corr, et al., 2010; Rippin et al., 2014; Martin J. Siegert et al., 2005). This
206 roughness can be estimated directly from thickness profiles (Robert G. Bingham & Martin J. Siegert, 2007)
207 and – with assumptions on the fractal character of the bed – extrapolated to finer scales (T. M. Jordan et al.,
208 2017). Where perpendicular crossovers are available, the anisotropy of the bed roughness can also be
209 estimated (Cooper et al., 2019; Eisen et al., 2020). In addition to its resolvable along-profile signature, finer-
210 scale (i.e. wavelength-scale) roughness is also encoded in the bed-echo character including its abruptness (T.
211 M. Jordan et al., 2017), specularity (D. M. Schroeder et al., 2015; D. A. Young et al., 2016), and amplitude
212 distribution (Grima et al., 2019). Notably, these fine-scale relative metrics are insensitive to (even large)
213 absolute errors in ice thickness (e.g. from firn correction or surface registration). Finally, the radiometric
214 signature of bed echoes can also encode information on bed materials (Christianson et al., 2016; Tulaczyk &
215 Foley, 2020) and thermal state (Chu et al., 2018). These signatures are often difficult to interpret
216 unambiguously at the glacier to ice-sheet scale (Matsuoka, 2011), without multi-frequency (Broome &
217 Schroeder, 2022) or multi-static observations (Bienert et al., 2022) or polarimetric (Corr et al., 2007; Dall et
218 al., 2010; Frémand, Bodart, et al., 2022; Scanlan et al., 2022) observations. These approaches can
219 characterize and constrain the wavelength-scale roughness (tens of centimeters or smaller) and sub-Fresnel-
220 zone geometry (Haynes et al., 2018; T. M. Jordan et al., 2017) (meters to tens of meters) of the bed,
221 providing orders of magnitude finer-scale constraints than along-profile approaches (Bingham & Siegert,
222 2009).

223 #### 2.2.2.2 *Gravity and magnetic data*

224 These passive techniques measure the intensity and, in some cases, the direction of the Earth's naturally
225 occurring gravity and magnetic fields. Magnetic and gravity data do not require large power sources, nor a
226 coupling to the Earth's surface, and airborne surveys have been widely deployed across Antarctica, most
227 commonly in combination with RES surveys from the same platform (Fig 1).

228 Gravity data are sensitive to the summed effects of mantle and crustal masses, including sedimentary rocks.
229 Due to their porosity, sedimentary rocks typically have lower density than the crystalline basement, causing

relative gravity lows over sedimentary basins (A. R. A. Aitken et al., 2016; Bell et al., 1998; Frederick et al., 2016). Airborne gravity systems include several major types of gravity meter, with the conventional stabilized-platform air-sea gravimeter (R. E. Bell et al., 1999) and derivations of this technology (M. Studinger et al., 2008) providing the majority of data. More recently, so-called "strapdown" systems have been used, which are based on inertial navigation sensors including triads of high-specification accelerometers and gyroscopes rigidly attached to the aircraft (Jordan & Becker, 2018). In either approach the observed accelerations are dominated by aircraft accelerations, and a well-constrained gravity solution is dependent on an accurate recording of the aircraft location and elevation, and careful removal from the recorded signal of aircraft accelerations and motion as well as temporal gravity variations such as tides. Accurate navigational systems such as differential GNSS are therefore essential to achieve the best quality data.

Older spring-based meters were restricted to straight and level flights, constraining operational logistics, and limiting the ability to collect other data types at the same time. This sensitivity to aircraft dynamics meant accuracies of 3-5 mGal were typical (Jordan, Ferraccioli, Vaughan, et al., 2010). In recent times advances in sensor technology and processing methods have allowed collection of gravity data during more dynamic draped flights and an overall improvement in data quality, with accuracies of 1-2 mGal now typical (Jordan & Becker, 2018; M. Studinger et al., 2008). Despite these improvements, gravity-data processing imposes a low-pass filter on the data, typically 70 seconds or more, that leads to spatial resolution of 5-10 km, depending on aircraft velocity. This velocity may be between 60 and 140 m/s for the fixed-wing platforms used in Antarctica. A recent innovation is the adoption of helicopter-borne operations, which promises further improvement in spatial resolution (Jensen & Forsberg, 2018; Wei et al., 2020). Future application of strapdown gravity on slower-flying Unmanned Aerial Vehicle (UAV) platforms also holds the promise of higher resolution and potentially lower-cost gravity surveys. An additional limit on the wavelengths resolved by gravity surveys is the ice thickness, which means observations are often made several kilometers from the bed interface, limiting the minimum resolvable wavelength. These factors limit the capacity for detection of abrupt spatial changes in gravity, such as may be associated with glacial landforms and fault-bounded sedimentary basins. Despite these residual limitations, the improved accuracy of gravity-sensor technology allows modern airborne-gravity data to be applied with confidence at length scales > 5 kilometers.

The observed gravity field is a summation of source components including topography and crustal thickness, as well as sedimentary-mass deficits, and to understand sedimentary basins the other factors must be accounted for. Ice, subglacial lake and ocean thicknesses and bed topography, where known, are corrected for using the Bouguer correction or an equivalent, which models the effect of topography and bathymetry, typically assuming reference densities for rock, ice and water (Hirt et al., 2016; Scheinert et al., 2016). In Antarctica, the thick ice-sheet load in the continental interior generates a Moho down-warp causing distinct negative Bouguer anomalies that do not reflect crustal geology, and it is desirable to correct for this.

Because topographic loads may be balanced by the Moho or other masses in the deep crust or uppermost mantle, for the isostatic residual anomaly, the condition is imposed that surface loads are balanced by variable crustal thickness, either locally in the Airy case, or via regional flexure using elastic or visco-elastic rheology (G. J. G. Paxman et al., 2017). Airy isostasy models are easy to apply and provide a consistent convention for interpretation, but are prone to overcorrection, whereas flexural models may provide superior removal of isostatic effects where the flexural rigidity is able to be constrained (Jordan, Ferraccioli, Armadillo, et al., 2013; G. J. G. Paxman et al., 2017). Negative isostatic-residual gravity anomalies often indicate sedimentary basins, although low-density basement rocks, such as granitic intrusions, can also give rise to negative anomalies, requiring differentiation with other data (Jordan, Ferraccioli, Vaughan, et al., 2010).

Despite the intricacies of processing and interpretation, sedimentary basin structure can potentially be defined from gravity data for wavelengths >10 km, and for sedimentary rock thicknesses greater than ca. 500 m, although larger and thicker basins are resolved with more confidence. Gravity-derived thicknesses are ambiguous, varying linearly with density contrast, and an inability to separate the basin source from other possible sources is a limiting factor to be overcome during interpretation.

For magnetic data, oxidation of magnetite to hematite during weathering means that sedimentary rocks, in general, have low magnetization relative to crystalline basement (Enkin et al., 2020). While low-magnetization rocks do not generate a magnetic anomaly, their presence increases the distance between a basement source and the aircraft sensor — this distance also includes the thickness of water and ice and the height of the aircraft above the surface. Increased source-sensor separation causes anomalies to have reduced amplitude and increased wavelength and sedimentary basins are characterized by reduced magnetic anomaly gradients (Reid, 1980; Reid et al., 1990). Analysis of the anomaly gradients using depth-to-magnetic-source estimation techniques is often applied to define the thickness and distribution of sedimentary rocks (A. R. A. Aitken et al., 2014; Fausto Ferraccioli et al., 2009; Tankersley et al., 2022).

Airborne magnetic data are collected from magnetometers that, most commonly, are attached to aircraft by a tail-boom, at wingtips, or in some cases towed. Fixed-wing surveys dominate modern data collection (A. R. A. Aitken et al., 2020; Jordan & Becker, 2018; Tinto et al., 2019) but helicopter surveys are also used in specific settings (Damaske et al., 2003; F. Ferraccioli et al., 2009; Fausto Ferraccioli & Bozzo, 2003; K. Gohl, Denk, et al., 2013; G. Wilson et al., 2007). In contrast to gravity surveys, instrument precision is not a major source of error, and improvements in practice have focused on managing the magnetic environment of Antarctica, being close to the magnetic pole, and so especially vulnerable to space weather and intense diurnal variations. In addition, the need for longer-range surveys and multi-year campaigns demands additional care in data processing. The most recent approaches consider more fully the complexities of the four-dimensional magnetic field yet (e.g. A. R. A. Aitken et al., 2020), yet the Antarctic geomagnetic

environment and logistical constraints remain substantial limitations on dataset accuracy relative to aeromagnetic data on other continents.

A limitation of both gravity and magnetic approaches is the inability for airborne surveys to recover field components at wavelengths longer than the scale of the survey (Scheinert et al., 2016). For this, the expansion of satellite-based gravity, gravity gradiometry and magnetic data, including the GRACE, GOCE and SWARM missions, has provided a crucial new understanding of the long-wavelength structure of the continent (Ebbing et al., 2021; Ebbing et al., 2018; Pappa, Ebbing, & Ferraccioli, 2019; Pappa, Ebbing, Ferraccioli, et al., 2019), these also underpinning more accurate compilations (Ebbing et al., 2021; A. V. Golynsky et al., 2018; Hirt et al., 2016). The GOCE mission in particular has allowed new understandings of crustal structure, including definition of sedimentary basins (Capponi et al., 2022; Haeger & Kaban, 2019).

Overall, the ability to define sedimentary basins through gravity and magnetic approaches has improved substantially in recent years, with particularly more accurate gravity recovery at shorter wavelengths, and the incorporation of satellite magnetic and gravity data at longer wavelengths. These improvements mean that, where airborne data exist, the identification of subglacial sedimentary basins is possible for basins with thicknesses greater than ca. 500m and with spatial resolutions of 10 kilometers or possibly less. These data are associated with physical non-uniqueness and, given other unknowns, they do not unambiguously define the geometry or physical properties of the basin fill. Unless these are otherwise constrained, these uncertainties limit their use for a quantitative 3D understanding of basin morphology.

2.2.2.3 Active and Passive Seismic

Seismic techniques record the propagation of elastic waves in the ground, with the two main types of survey being passive-seismic and active-seismic. Passive-seismic typically involves continuous observations from three-component seismometer arrays with sources that may be natural or non-specific anthropogenic origins (e.g. earthquakes, ambient noise). Active-seismic typically uses shorter-term, triggered observations with (usually single-component) geophones and artificial sources of a controlled and survey specific nature (e.g. explosives, airguns, vibrators), although hybrid approaches are also used. Seismometers or geophones must be deployed in or on the ground for on-ice surveys, or in the water for marine surveys. Of these methods active-seismic reflection approaches provide the more comprehensive image of basin architecture, although significant ambiguities remain, including uncertainties in constraining seismic velocities and geometrical biases stemming from the survey geometry.

Despite this, the application of active seismic techniques in Antarctica has several drawbacks. Active source marine surveys can cover hundreds of kilometers per day in open water, although around Antarctica, the presence of icebergs may disrupt surveying. By contrast, on-ice surveys that use explosive sources and individual geophones as receivers can cover only a few km per day in Antarctic conditions (Anandakrishnan

et al., 1998; Brisbourne et al., 2017; Johnston et al., 2008; L. E. Peters et al., 2006; A. M. Smith, 1997; David G. Vaughan et al., 2003). The use of the vibroseis method over snow with a towed streamer allows the collection of tens of kilometers per day, and by this approach it has become possible to obtain larger-scale surveys with several hundred kilometers per field season (Eisen et al., 2015; E. C. Smith et al., 2020). Nevertheless, on-ice active seismic data are currently very limited in spatial extent (Fig 1).

Unlike radio waves used in RES, seismic waves can penetrate subglacial environments such as water, sedimentary strata, and the basement beneath, providing crucial information necessary to understand glacial dynamics. In addition, due to the simpler timing requirements (relative to RES) sources and receivers can be separated, allowing for bi-static or multi-static configurations that can exploit angle-dependent information from reflections. Several seismic approaches have been employed to detect and define sedimentary basins in Antarctica. The tomographic approach determines the bulk velocity and thickness of a geologic unit underneath the ice. Because the seismic wave speed in sedimentary basins is significantly lower than in crystalline basement, the thickness and properties of such a unit can be estimated, especially with long-baseline (wide-angle) reflection and refracted-wave seismic surveys (Blankenship et al., 1986; Leitchenkov et al., 2016; Trey et al., 1999).

Seismic waves will reflect and refract at unit horizons where the acoustic impedance (defined as the product of seismic velocity and density) changes. The seismic wave speed and density of sedimentary basin fill is usually lower than that of crystalline basement, resulting in a generally lower acoustic impedance for sedimentary basins. Furthermore, as the acoustic impedance of ice is well known, the reflection from the subglacial interface can be used to determine the properties of that layer. Acoustic-impedance measurements along profiles can be used to discriminate between regions of hard bedrock from sediments or water at the bed. Of particular significance is the ability to discriminate different structures associated with tills and tillites that have a direct link to subglacial processes at the bed (Anandakrishnan et al., 1998; H. J. Horgan et al., 2021; A. Muto, Anandakrishnan, et al., 2019; Atsuhiro Muto et al., 2016; L. E. Peters et al., 2006; A. M. Smith et al., 2013).

Seismic reflection methods can be used to map the stratigraphy of the geological units underlying the ice sheet and ice shelves. The active seismic technique is especially important for resolving sub-ice-shelf bathymetry and basins (Rosier et al., 2018; E. C. Smith et al., 2020). These data can be used to constrain gravity-based approaches (Eisermann et al., 2020; Atsuhiro Muto et al., 2016). The identification of a geologic stratigraphy indicates that a subglacial unit is of probable sedimentary origin, and the details of its structure can be interpreted to understand the depositional environment, and age relationships with faults and volcanic edifices (e.g. H. Horgan et al., 2005; Johnston et al., 2008; Kristoffersen et al., 2014).

As seismic reflection surveys have high spatial resolution, they provide a very good estimate of the ice thickness and thus bed topography. In comparison to RES methods, ice-internal structure is not well resolved, but seismic techniques are better able to characterize subglacial properties. Seismic profiles can be analyzed in the same way as RES profiles for bed roughness, but because they very often record over a larger offset (source-to-receiver distance) spread than RES methods, they are less prone to the influence of side reflections and smoothing given that adequate processing is applied in the form of migration.

Our ability to detect and discriminate subglacial sedimentary basins in seismic reflection data is improving. Because seismic-reflection-data quality increases with the square root of the number of observations, more efficient data acquisition is key to improving resolution within logistical constraints. Over the last decade, progress in borehole-drilling techniques (e.g. the rapid-air-movement drill system (Gibson et al., 2020)), geophone design and deployment (e.g. Georods (Voigt et al., 2013)), and a combination of highly efficient source-receiver systems (e.g. vibroseis-snowstream combination (Eisen et al., 2015)) have all contributed to increasing the seismic data coverage and thus our ability to detect sub-ice properties (A. Muto, Alley, et al., 2019; A. M. Smith et al., 2013). Nevertheless, as active seismic surveys are logistically demanding, studies have been either only locally constrained or require considerable resources to cover regional distances.

Passive-seismic methods for detecting and studying sedimentary basins can estimate the seismic velocity structure of the upper few kilometers of the crust using seismograph arrays deployed for periods of time ranging from months to years. These techniques use naturally occurring seismicity within the ice sheet or from earthquakes around the world, as well as seismic 'noise' from ambient sources. These surveys are relatively simpler to deploy than active-source surveys as they do not require the source technology (drills and explosives or a vibroseis system). Passive seismic techniques can map the thickness of sedimentary rocks on a regional scale with a few seismic stations. Thus, passive techniques offer coverage of remote parts of Antarctica, but at lower resolution than is possible for active seismic methods. One common method to estimate the thickness of sedimentary basins is the so-called receiver function method that can be used to estimate basin properties with high sensitivity to acoustic impedance contrasts at structural interfaces located beneath the recording station (Ammon, 1991). Another method is to use the background signal, so-called ambient noise, that can resolve broader lateral changes in seismic velocity structure (Shapiro et al., 2005). Joint application of these (and other) methods has become common, providing the ability to resolve sedimentary basins(Lin et al., 2012).

Receiver-function analysis provides images of structural interfaces below a seismic station using processing that enhances seismic waves converted from S to P or P to S at structural interfaces (Ammon, 1991). The depth to the sediment-bedrock interface and thus the sediment thickness is determined from the time delay of the converted phase, after adjusting for ice thickness (Anandakrishnan & Winberry, 2004; Chaput et al., 2014). The use of higher frequencies compared to typical receiver-function analysis (4 Hz vs < 1 Hz) allows

detection of sediment thicknesses of a few hundred meters and can provide some approximate constraints on the velocity of the sediment layer (Dunham et al., 2020). While low-velocity relative to igneous or metamorphic basement, consolidated sedimentary rocks may not provide sufficient density and velocity contrast to be discernible in receiver functions.

Ambient-noise analysis uses short-period seismic surface waves obtained from the ambient-noise field derived from non-specific sources, in particular ocean waves. By correlating records from two seismic stations, the shallow structure beneath the ice sheet along the interstation path can be constrained (Pyle et al., 2010; W. Shen et al., 2018). The correlation yields the Green's Function for wave propagation between the stations, from which the phase and group velocity and ultimately the shear-wave velocity structure is obtained. If the distribution of seismic stations is dense enough, the phase and group velocity tomography maps can be used to map thicknesses of sediment and sedimentary rocks throughout the region and so results are not restricted to the locations of seismographs. The use of both Rayleigh and Love waves provides better results, since Love waves have superior resolution at shallow depths (Zhou et al., 2022). Constraints on shallow structure from ambient-noise Rayleigh waves can be improved by also measuring the ratio of horizontal to vertical displacement (Lin et al., 2012; Pourpoint et al., 2019). Joint inversion of several of these datasets using a Bayesian formalism, including receiver functions, surface-wave group and phase velocities, and horizontal to vertical ratios, can improve resolution of sedimentary material beneath the ice sheet (Dunham et al., 2020; Pourpoint et al., 2019).

Sedimentary basin thicknesses have been estimated using passive seismic techniques throughout West and Central Antarctica. Pourpoint et al. (2019) found thicknesses ranging from 0.1 to 1.5 km beneath seismic stations near the Thwaites Glacier drainage area, with the thickest sediment in the deep topography of the Byrd Basin and Thwaites Glacier bed. Dunham et al. (2020) found sediment thicknesses ranging from 0.1 to 0.9 km beneath seismographs in the West Antarctic Rift System (WARS) and Ellsworth Mountains region. Zhou et al. (2022) mapped sedimentary basin thicknesses throughout West and Central Antarctica with ambient-noise surface-wave methods. They found 4-5 km-thick basins beneath the Ross Ice Shelf but in other regions of the study area maximum thicknesses were at most about 1.5 km, except in small regions where spatial resolution is lacking. They interpreted the lack of thick sedimentary basins, dissimilar to intracratonic basins in other continents, as indicating that basins in this region of Antarctica may have been sediment starved throughout most of their post-Gondwana geological history, although erosion may also have been significant.

2.2.2.4 Electromagnetic and magnetotelluric

Electromagnetic techniques also include active and passive techniques. Due to their limited depth penetration, airborne approaches are not widely applicable to subglacial geology, although can be applied in ice-free regions (Foley et al., 2015). Ground-based electric and electromagnetic techniques have seen limited

use in Antarctica with the most broadly applied approach in recent times being passive magnetotellurics (Hill, 2020), although geomagnetic depth sounding has also been applied (Armadillo et al., 2004). The magnetotelluric technique provides the capacity to image deep within the Earth and is generally applicable to detect and image sedimentary basins through their electrical properties, which are commonly related to water content, salinity and temperature (Gustafson et al., 2022; P. E. Wannamaker et al., 2004). Assuming that subglacial sediments and sedimentary rocks are water-saturated, the key expected controls on bulk resistivity values are the connected porosity of the pore space and the salinity of the waters within them, defined empirically (see Glover, 2016).

Although a relatively old technique, the magnetotelluric method has been increasingly applied, due in large part to improved ability to generate robust model solutions with high-performance computing and improved sensor technologies. Magnetotelluric applications to crustal and upper-the-mantle imaging in the polar regions are reviewed in Hill (2020). Building on the most recent relevant work (Gustafson et al., 2022; Key & Siegfried, 2017; Kulessa et al., 2019; M. J. Siegert et al., 2018) we focus here on examining the potential scope and limitations of magnetotelluric imaging of the hydrogeological and thermal properties of subglacial sedimentary basins.

The source fields of the magnetotelluric technique are inherently wideband, ranging from ca. 10^{-5} Hz to 10^{4} Hz, generated when electrical storms and interactions between the solar wind and the ionosphere produce fluctuations in Earth's magnetic field. These fluctuations then induce correspondingly wideband telluric currents in ice sheets and the underlying crust and mantle. Signal period is a proxy for depth, with longer-period signals representing structure deeper in the Earth. Under favorable circumstances, and depending on the bandwidth and collection procedure of the survey, temporally coincident measurements of magnetic and electric potential fields allow the bulk electrical-resistivity distributions to be estimated at depths from the near surface, resolved at the highest frequencies, to ca. 400 km at the lowest frequencies. Data collection is typically focused in the high frequencies for near-surface studies (audio-frequency MT 10^{0} Hz to 10^{4} Hz), across a central broad band (BBMT 10^{-3} Hz to 10^{2} Hz) for general crust and mantle studies, and long-period MT (LPMT 10^{-1} Hz to 10^{-4} Hz) for mantle-focused studies. For the investigation of subglacial sedimentary basins beneath the Antarctic Ice Sheet the higher-frequency band of the magnetotelluric spectrum is of most interest. This is attractive in that high-quality magnetotelluric data can be acquired with day-long station occupations if wind speeds are low ($<<$ 10 m s^{-1}), as compared with station occupations of a week or more required for upper-mantle studies.

Many challenges arise in ice-sheet settings related to potential violations of fundamental source-field assumptions owing to the proximity to the geomagnetic south pole, high contact resistances of electrodes buried in firn, and spindrift of charged snow particles generating strong broadband electrical noise (see Hill, 2020). The last is a particular challenge in the imaging of subglacial sediment basins because the broadband

frequencies exploited in doing so are particularly susceptible to noise contamination by drifting snow. A second specific challenge arises when firn is absent and ice is exposed at the surface instead, forming a major barrier to the deployment of electrodes and magnetometers and associated wiring. This is a problem especially in coastal regions where seasonal melting and refreezing are widespread.

Notwithstanding these challenges, a growing number of Antarctic campaigns have demonstrated that high-quality magnetotelluric data can be acquired with careful survey planning and using bespoke electrode pre-amplifiers (Hill, 2020). Subglacial sedimentary basins are particularly well suited for magnetotelluric exploration because they are expected to be several orders of magnitude less resistive (order of 10^{-1} – 10^{1} Ωm) than both the underlying crystalline crust (typically > 10^{2} Ωm) and the overlying ice. Cold Antarctic ice has typical bulk resistivities of ca. 10^{4} – 10^{6} Ωm but these can exceed 10^{8} Ωm for temperate clean-ice glaciers (Kulessa, 2007).

Magnetotelluric studies of subglacial sedimentary basins remain limited, with only a few studies in Antarctica. Although not yet widely applied, magnetotelluric surveying can reveal high-quality images of subglacial sediment basins and has unique potential for detecting and defining liquid groundwater within them (Gustafson et al., 2022). The use of seismic data to constrain magnetotelluric inversions with cutting-edge joint inversion schemes has not yet been attempted in Antarctica but will very likely result in improved resolution in the future (Key & Siegfried, 2017; Kulessa et al., 2019; M. J. Siegert et al., 2018).

There are two major complications for interpretation, however, in that Archie's law contains a cementation exponent that has never been calibrated for subglacial sediments; and even more significantly, Archie's law is not applicable where sediments have noticeable clay mineral contents requiring a significantly adapted formulation (Kulessa et al., 2006). This is likely a particular problem for coastal subglacial sedimentary basins where contents of marine clays are not normally negligible.

Finally, it is expected that a significant geothermal gradient will exist between the base and top of subglacial sedimentary basins, especially where they have a vertical extent of several kilometers and are buried beneath several kilometers of cold ice. Kulessa et al. (2019) demonstrated with a conceptual model that such temperature gradients will likely result in a multi-fold increase in bulk resistivity between the base and top of subglacial sediment basins, largely due to a temperature-controlled decrease in ionic mobility in sediment pore-waters. This inference suggests that bulk resistivity models can be used to infer temperature changes in subglacial sedimentary basins and implied geothermal heat flux into the ice-sheet base, a key unknown in ice sheet modelling, especially in high-heat flux settings.

Overall, magnetotelluric measurements are powerful tools to explore subglacial sedimentary basins, the associated groundwater and geothermal heat fluxes, and their interactions with the ice-sheet base. In most Antarctic situations, porosity, pore-fluid salinity, clay mineral contents and temperature changes will

combine to control bulk resistivity magnitudes, a complication that may be further compounded for coastal sediment basins. These ambiguities require external constraint to develop a quantitative interpretation of sedimentary properties from bulk resistivities.

2.2.3 Integrated Studies

As we have seen above, each of the listed methods has the capacity to define the existence of sedimentary basins beneath ice and, in many cases, also particular characteristics such as thickness, internal geometry, seismic velocity, density, and electrical conductivity. These characteristics each may resolve different aspects of the basin and, furthermore, each technique has different uncertainties and so the methods are complementary. In particular, the inherent ambiguities in most available data can lead to major errors when any single technique is used. For example, outcrops may be selected for erosion resistance through landscape-forming processes while low-roughness topography may be caused by glacial erosion (Stewart S. R. Jamieson et al., 2014) and low gravity anomalies and/or smooth magnetic gradients may be caused by low-density or non-magnetic basement rocks.

Integrated studies that use multiple datasets are necessary to resolve these ambiguities (Grikurov et al., 2003). For airborne geophysical surveys, the combination of RES, gravity and magnetic data has proved powerful, and this is especially enhanced where suitable ground observations are also collected. Major recent, ongoing, and upcoming data collection programs have sought to synergize multidisciplinary data collection and modelling (MacGregor et al., 2021; Scambos et al., 2017). The co-interpretation of multiple complex and sparse geoscience datasets has a high task-complexity, that may lead to difficulty making reliable judgements (Swink & Speier, 1999). As a human-led process which relies on interpreter skill, the background, knowledge and biases of the investigator can have substantial impacts on results (C. G. Wilson et al., 2019). Although clearly not without uncertainty, multi-data analyses provide the potential to manage subjectivity in interpretation and support the ability to make sound judgements (Alan R. A. Aitken et al., 2018).

A consistent data-based mapping at continental scale is challenged by highly variable data quality, resolution and availability, as well as the challenge of combining multiple datasets into a consistent map that accounts for all data. To define basal boundary conditions, we may seek initially to define the presence or absence of sedimentary basins, which is a prerequisite to understanding their thickness, age, and other properties. Geostatistical and machine-learning techniques provide relatively unbiased and data-based approaches to understanding this in a probabilistic sense. Li et al. (2022) applied the random forest approach with multiple data types to map for all Antarctica the likelihood of sedimentary basins at the bed. Emma J. MacKie et al. (2021) applied a trained logistic regression model to simulated topographic-roughness models to infer geological bed type associated with the presence of sediments. Such techniques are highly valuable with respect to their consistent response to data, provided those data are not too variable in their properties

(resolution, accuracy etc.), but they are not able always to accommodate irregularly sampled or sparse data, while non-numerical data such as lithological descriptions can be problematic to include. In this work we use the results of such techniques with a wide range of prior findings and datasets (Fig. 2) to develop a new understanding of sedimentary basins beneath the Antarctic Ice Sheet.

3 Antarctica's Sedimentary Basins

3.1 Methods & Validation

We have mapped the sedimentary basin distribution continent-wide using a flexible basin-classification approach applied in a GIS. The map presented here (Fig 3) is manually classified based on a wide range of continent-scale datasets and derivative products. To develop the map, an initial classification into basins and non-basins was automatically generated from the machine-learning-derived likelihood map (Fig 2a) of Li et al. (2022), using a threshold of 0.5. From this initial point, the polygons for individual basin regions were scrutinized and edited considering additional data including outcrop geology (Cox et al., 2023), along-track roughness (Fig 2b), bed elevation (Fig 2c) and its spatial variability (Fig 2d), gravity magnitudes (Fig 2e) and their spatial variability (Fig 2f), aeromagnetic intensities (Fig 2g) and their spatial variability (Fig 2h), and estimates of sedimentary basin thickness from passive and active seismic datasets. Data visualizations, maps and interpretations from many published studies were accommodated in the mapping process.

3.1.1 Geology classification

As discussed above, the principal distinction we wish to make here is between crystalline-basement-dominated regions and sedimentary basins. However, a binary classification is inadequate to cover the range of circumstances that the geology presents. Retaining simplicity, we classify the bed type into four main classes: crystalline basement, intra-basin volcanic, and Type 1 and Type 2 sedimentary basins (Fig 3). Often, the data contain characteristics of more than one of these types, due either to variable bed types present in small areas, or due to transitional conditions from one type to another, and so we also have three mixed-type classes, although their distribution is limited compared to the major types (Fig 3).

The crystalline-basement class indicates where the bed is interpreted to consist of igneous or metamorphic rocks (including high-grade metasedimentary rocks), with either no sedimentary cover, or a thin veneer that is below the detection thresholds of the datasets used. Typically, these regions possess the characteristics of high elevation and high gravity with high spatial variability in topography, gravity, and magnetic data. Along-track roughness tends to be high for this class. Type cases for this class include regions in the Transantarctic Mountains, Dronning Maud Land, Marie Byrd Land and the Gamburtsev Subglacial Mountains.

The Type 1 basin class represents regions where sedimentary basins are preserved in relatively unmodified basins, with typical characteristics of low elevation and low gravity, and low spatial variability in gravity and

magnetic data. Along-track roughness tends to be low. Type cases for this class include the Ross and Weddell embayments, and the Wilkes, Aurora and Pensacola-Pole subglacial basins.

The intra-basin volcanics class includes areas where volcanic rocks are interpreted to be emplaced within a Type 1 basin sequence; that is they are younger than the base of the basin and may interfinger with or overlie sedimentary rocks. Typically, this class relies on outcrop data and aeromagnetic data to define the extents of volcanic complexes where they are dominant. It is noted that basins may contain volcanic rocks without them being evident in geophysical data and the extent of volcanic rocks is likely underestimated (van Wyk de Vries et al., 2018). The type case for this class is the McMurdo Volcanic Complex in the Ross Sea.

We define the Type 2 basin class where sedimentary rocks are known or inferred but the original depositional basin is not preserved. These rocks tend to predate the formation of the present landscape, are often uplifted to high elevations, may be intruded by younger igneous rocks, may be heavily eroded and may have geophysical characteristics more similar to crystalline basement than Type 1 basins. The type case for this class is the Beacon Supergroup, with its characteristic high elevation exposures and mesa-like topography as a consequence of widespread Jurassic dolerite intrusions. Type 2 basins are prominent in the Transantarctic Mountains and in the Ellsworth-Whitmore Mountains, with subglacial examples inferred in Dronning Maud Land, and subglacial highlands in the Vostok and Aurora regions (Fig 3).

3.1.1.1 Class Validation

For validation, we may review this geological bed-type classification against the major numerical datasets available to the interpretation. Summary statistics for each input dataset were calculated for each class using a Zonal Statistics GIS tool. These statistics allow the distinctiveness of the class-level populations to be defined in terms of differences of means, factoring in standard deviation, and so illuminate the data that most strongly differentiate between classes. Figure 4 shows the extent to which the zonal mean for each class differs from the mean for the entire continent. Where these differ substantially, especially in sign, that dataset is a potential discriminant of the selected classes. Furthermore, we may directly compare the population-level distinctiveness between classes, for which we derive Cohen's effect size (Fig 4). Values above 0.8 may be considered a large effect, indicating a strong discriminant, while values below 0.5 may be considered a small effect, indicating a weak discriminant.

The primary classification we seek is the distinction between Type 1 basins and crystalline basement. For these two classes, large effect sizes are seen for topography elevation datasets, while medium effect sizes are seen for free air and Bouguer gravity, topography and gravity variation and satellite gravity-gradient components (Fig 4a). The ability to discriminate between crystalline basement and Type 2 basins is weaker, with medium effect sizes seen for Airy Isostatic Residual Anomaly (IRA) and satellite-gravity-gradiometry

components (Fig 4b). The distinction between Type 1 and Type 2 basins is strong, with large effect sizes for subglacial topography elevation datasets, Bouguer gravity datasets and variability measures for these, and medium effect sizes for Airy IRA and high-pass-filtered Bouguer gravity (Fig 4c). Finally, the in-basin volcanics class is sharply defined relative to all other classes, these being most clearly differentiated with large or medium effect sizes for magnetic data-products as well as high variability in topography and gravity data.

The relationships highlighted above support the following as key criteria for classifying subglacial geology: Type 1 basins are defined most by their low topography at large scales, accompanied by relatively high Bouguer gravity, perhaps counter to expectations (note the opposite sign to topography in Fig 4a, 4c). With respect to their differentiation from Type 1 basins, Type 2 basins show similar characteristics to crystalline-basement, but with a stronger effect-size from gravity data, reflecting their characteristic gravity lows. Type 2 basins can be separated from crystalline basement by their low response in Bouguer and Airy IRA gravity anomalies and satellite-gravity-gradiometry components. The magnetic dataset does not discriminate strongly between these three classes but is strongly linked to the in-basin volcanics class, which is also identified by high spatial variability in all datasets.

3.1.2 Age Classification

In addition to geological bed-type classification we seek to define the age of the basins which, besides their importance for tectonic understanding, may reveal changing conditions for the ice sheet formation and evolution through the Cenozoic, as well as differences in basal conditions associated with the age of the sedimentary rocks at the surface. The interpreted age distribution indicates the evolving tectonic conditions of Antarctica and its landscape, although due to the general paucity of robust age-dating outside of outcropping regions, and very limited capacity for stratigraphic correlation beneath the ice, these interpretations are on necessarily broad timescales.

For each basin, we define an interpreted age for the base and the top of the basin sequence (Fig. 5). The base-of-basin age (Fig. 5a) represents a maximum bound on basin age, either from a known maximum age (e.g. from a maximum deposition age), or from the interpreted age of the underlying crust. The top-of-basin age (Fig. 5b) represents a minimum bound on basin age, either from a known minimum age (e.g. cooling age), from a capping or intruding igneous unit or from geomorphological criteria including interpreted regions of glacial erosion and deposition.

3.1.3 Basin Thickness

Except for RES data, the data types in Section 2.2 can all be used to generate models of the thickness of sedimentary cover. It is possible to interpolate sedimentary thickness between existing data points, giving an estimate of the thickness of sedimentary cover across the continent (Baranov et al., 2021). However, the

fundamental differences between basin-sensing techniques, their differing resolution and accuracy, and specific features of individual surveys and models all lead to major uncertainty in defining basin thickness.

Figure 6 shows several models of sedimentary basin thickness, including models derived from gravity (Haeger & Kaban, 2019), interpolation of seismic data (Baranov et al., 2021), passive seismic models (Zhou et al., 2022), magnetic depth to basement tied to seismic-reflection data (Tankersley et al., 2022) and marine seismic-reflection data (K. Hochmuth et al., 2020; Lindeque, Gohl, Wobbe, et al., 2016; Straume et al., 2019). While there is some commonality between these models, there are also many differences and only the seismic-reflection models show strong consistency with each other.

Three major factors contribute to this discrepancy. First, the resolution of techniques differs and so distinctly separate features in one technique are likely to be merged in another. Consequently, thickness models will differ greatly in the presence of complexity (e.g. Ross Island in Fig. 6c). Second, the physical properties detected with each technique differ and, furthermore, not all techniques have agreed criteria for the definition of the basin-basement interface. Finally, the different techniques have different capacity to resolve deep basins, and to accurately define the base of basins accurately is challenging. For example, depth to magnetic basement commonly defines sills or volcanic horizons within the basin sequence, and there is often no solution possible for the basement beneath. Ultimately, while a general agreement can be reached on the extent of sedimentary basins, for now, their thicknesses remain poorly constrained in Antarctica, except where seismic-reflection data have been collected and analyzed alongside other techniques.

3.2 West Antarctic Basins

West Antarctica, in a geomorphological division, includes the continental regions on the Pacific-facing side of the chain of mountains extending from Northern Victoria Land through the Transantarctic and Pensacola Mountains to Coats Land (Fig 3). This region possesses several major basin-dominated regions, in particular the Ross, Amundsen and Weddell regions, and is characterized by the low-elevation topography associated with these. West Antarctica's crust has a varied history, but the majority has formed since the Cambrian as a result of accretionary tectonics at Gondwana's paleo-Pacific margin (Jordan et al., 2020). Older crust with an affinity to cratonic regions of East Antarctica or Southern Africa may extend beneath parts of West Antarctica. Precambrian basement is known to outcrop at Haag Nunataks (Riley et al., 2020) and is suggested to underlie part of the Ross Embayment (Tinto et al., 2019). This basement hosts a series of basins of diverse origin extending in age from the Cambrian to the Quaternary.

3.2.1 The Ross Embayment and Siple Coast

This sector of West Antarctica is bounded by the Transantarctic Mountains to the west and the West Antarctic Ice Sheet (WAIS) divide to the south with the basement-dominated Marie Byrd Land to the east. In

Marie Byrd Land, small Type 1 basins are interpreted in glacial troughs (Fig. 7) but the major known basin (Type 2) is defined by the variably metamorphosed <520 Ma to >440 Ma Swanson Formation, dominated by turbidites and flysch. These rocks represent a middle-Cambrian to Ordovician basin, with sediments derived from the Ross Orogen and a variety of Proterozoic sources (Yakymchuk et al., 2015). These sediments were deposited along the Gondwana margin, initially on the continental slope and rise in the Cambrian – lower Ordovician but possibly later in a fore-arc to accretionary-prism as a convergent-margin setting developed (Jordan et al., 2020).

The Ross Sea is one of the most well-studied regions in Antarctica and the existence of major sedimentary basins is well established, with their stratigraphy revealed in multi-channel seismic data as well as numerous drill cores (Fig 1, Fig S1). These studies define a thick sequence of late Cretaceous to Quaternary sedimentary rocks separated into several packages by regional unconformities (F. J. Davey & Brancolini, 1995; Lindeque, Gohl, Henrys, et al., 2016; Pérez et al., 2021).

The Ross Sea basin has four major depocenters (Fig 7), the Victoria Land Basin, the Central Trough, the Eastern Basin and the Northern Basin (F. J. Davey & Brancolini, 1995) separated by basement highs with thinner sedimentary cover, the Coulman High and Central High; only Roosevelt Island appears sediment-free (D. S. Wilson & Luyendyk, 2006). The West Antarctic Rift System (WARS) initiated in the late Cretaceous, but with relatively little basin-fill deposited (C.S. Siddoway, 2008; Christine Smith Siddoway et al., 2004). The first major sedimentary sequence (RSS-1) is discontinuous and is observed in isolated grabens in the eastern to central Ross Sea, and may represent this rifting event, with thermal subsidence perhaps extending into the early Cenozoic (Luyendyk et al., 2001). A later phase of Eocene to Oligocene rifting is interpreted in the Victoria Land Basin (Fielding et al., 2008). A basin-wide unconformity (RSU-6) indicates a period of erosion in the Oligocene, occurring not later than 26 Ma in the Eastern Basin (Kulhanek et al., 2019), potentially associated with sea-level fall associated with large-scale glaciation in Antarctica. Correlation of RSU-6 into the Victoria Land Basin has been problematic (cf. F. J. Davey et al., 2000; Fielding et al., 2008), but may align with a mid-Oligocene unconformity that marks the end of the early rift stage of Fielding et al. (2008). Subsequent to this, basin deposition was episodic, but with relatively little extension, the glacial evolution of the continent being the major driver of basin evolution in most of the Ross Sea (Anderson et al., 2019; De Santis et al., 1999; Kim et al., 2018; Lindeque, Gohl, Henrys, et al., 2016; Marschalek et al., 2021; Pérez et al., 2021)

Upper Oligocene to Lower Miocene strata (RSS-2) are preserved in the major basins of the Ross Sea, but are thin to absent on the basement highs (Pérez et al., 2021). These sediments are interpreted to be deposited in a glacio-marine setting associated with a fluctuating ice-sheet margin including glaciation of local bathymetric highs (De Santis et al., 1999). Early to middle Miocene (18-15 Ma) sedimentary deposition (RSS-3 & RSS-4) is interpreted in detail in Pérez et al. (2021). In contrast to the thick and structurally segmented

packages of the lower sequence, this package overall is laterally continuous across the southern Ross Sea, but with complex internal structure that is representative of changeable ice-sheet dynamics, as documented in several drill-core records (Levy et al., 2016; Marschalek et al., 2021; R. M. McKay et al., 2016). A major mid-Miocene erosional event (RSU-4), indicating the advance of a major ice sheet over the Ross Sea is interpreted associated with the Mid-Miocene Climate Transition (Philip J Bart, 2003; Pérez et al., 2021). The post mid-Miocene sedimentary basin record is similarly characterized by numerous and repeated ice-sheet advance and retreat cycles (Anderson et al., 2019; P. J. Bart et al., 2000; Halberstadt et al., 2018; R. McKay, Naish, Carter, et al., 2012; R. McKay, Naish, Powell, et al., 2012; Naish et al., 2009). Consequently, sediment thicknesses are relatively low, except in deeper water in the northeast where substantial progradation of the shelf edge is seen (Katharina Hochmuth & Gohl, 2019; Pérez et al., 2021), and in the west where the Terror Rift has substantially deepened the bathymetry (Sauli et al., 2021; Wenman et al., 2020).

The Terror Rift has generated the ca. 4 km thick rhombic Discovery Graben, extending from Cape Washington to, at least, Ross Island (Sauli et al., 2021), with a seismically-defined extension into the southern McMurdo Ice Shelf (Johnston et al., 2008), and possibly further south (Tankersley et al., 2022). Stratigraphic considerations suggest that after Eocene- Oligocene rifting, a period of thermal subsidence persisted until renewed extension from ca. 13 Ma drove the renewed tectonic development of accommodation space in the Discovery Graben (Fielding et al., 2008); however a more continuous evolution may be considered (Granot & Dyment, 2018; Sauli et al., 2021). Within the western Ross Sea, the McMurdo Volcanic Complex represents widespread and prominent volcanism, and some of these volcanoes are associated with flexural basin development (e.g. H. Horgan et al., 2005; Wenman et al., 2020) generating repositories of Neogene sedimentation and glacial development (R. McKay, Naish, Carter, et al., 2012; R. McKay, Naish, Powell, et al., 2012; R. M. McKay et al., 2016; Naish et al., 2009).

The northwestern Ross Sea has a distinct Cenozoic evolution. The Northern Basin is directly associated with the adjacent Adare Basin, which formed during seafloor spreading from 43 to 26 Ma, while the oceanic crust beneath the Central Basin, north of the Central Trough, may have formed from 61 to 53 Ma (Cande & Stock, 2004). The Northern Basin is offset from the Victoria Land Basin by the Polar 3 magnetic anomaly, inferred to represent 48-34 Ma alkaline intrusive rocks emplaced into a transcurrent fault zone (F. Ferraccioli et al., 2009). With the implication that this fault zone extends further offshore to the Iselin Bank, Fred J. Davey et al. (2021) presented a three-stage reconstruction of the northern Ross Sea involving: 10 to 26 Ma – Terror Rift opening and minor extension of WARS (Granot & Dyment, 2018), 26 to 43 Ma – Opening of the Adare Basin and Northern Basin; 53 to 61 Ma – Opening of the Central Basin and northern Central Trough, accommodated by the Polar-3 transfer and its extension to the Iselin Rift (Fred J. Davey et al., 2021).

The extension of the basin-forming events known from the southern Ross Sea beneath the Ross Ice Shelf is highly likely, although the structure of these basins has not been fully demonstrated, due to the lack of

extensive seismic data and ambiguous gravity signals (Karner et al., 2005). Recent geophysical data have begun to reveal the structure of this basin: airborne geophysical surveys across the Ross Ice Shelf have allowed the identification of several depocenters from depth to magnetic basement calibrated against seismic-reflection data in the southern Ross Sea (Tankersley et al., 2022). These show continuation of the Ross Sea systems into Eastern and Western depocenters separated by a mid-shelf high connecting with the Central High. The Eastern depocenter narrows inland to a distinct trough beneath Siple Dome. A smaller depocenter is located to the east of Roosevelt Island. The western depocenter beneath the Ross Ice Shelf is broad with a weakly defined ridge separating two sub-basins. In addition, recent passive-seismic models have mapped sedimentary thickness in the region using ambient-noise tomography, also revealing thick sedimentary basins beneath the Ross Ice shelf and southern Ross Sea (Zhou et al., 2022). The structure of these is different to the magnetic studies, likely reflecting the different spatial sensitivities of these techniques. Similarly, the mapping of Li et al. (2022) indicates a high likelihood of major basins beneath the Ross Ice Shelf (Fig 2a). Despite these first considerations being addressed, the absence of seismic-reflection constraints on basin geometry and stratigraphy limits the understanding of Cenozoic deposition and erosion patterns beneath the Ross Ice Shelf.

A further extension of the WARS into the Siple Coast region suggests a likely continuation of the basin-forming processes; however, the Siple Coast has distinctly different characteristics to the Ross Embayment. Although sedimentary cover is widely recognized in many geophysical surveys, sedimentary deposits are apparently thinner (in general < 1 km) and not ubiquitous. Ambient-noise tomography resolves a broad basin region extending ca. 400 km inland from the coast (Zhou et al., 2022). Aeromagnetic data at the coast suggest several ca. 75 km wide depocenters beneath Siple Dome aligned with the previously identified Trunk D Basin (Bell et al., 1998), the Crary Trough, and on the Amundsen Coast, respectively north and south of the Crary Ice Rise (Tankersley et al., 2022). The southernmost of these has recently been defined in detail using magnetotelluric and passive-seismic data (Gustafson et al., 2022). In the mapping of Li et al. (2022) the Siple Coast region returns sedimentary-bed likelihoods dominantly between 0.25 and 0.75, indicating the ambiguous nature of this region at large scales. High sedimentary-bed likelihood regions are identified for the MacAyeal Ice Stream, for the Siple Dome/Trunk D Basin, the Crary Trough and the Amundsen Coast. Inland, beyond the limit of the broad basin-dominated region (Zhou et al., 2022), a basement-dominated pattern is seen; however, four smaller basins are identified associated with the uppermost MacAyeal Ice Stream, Trunk D Basin (L. E. Peters et al., 2006), the Onset Basin linking to the Crary Trough (Bell et al., 1998; L. E. Peters et al., 2006) and a southern basin linking to the Amundsen Coast (M. Studinger et al., 2001). The rest of the region is here classified as mixed Type 1 basin/crystalline basement for which the exact configuration of sedimentary cover in this region is not well resolved. Nonetheless there is likely to be sufficient sedimentary cover for basin-influenced processes to occur widely.

The transition from the Ross Sea to the Siple Coast involves, in the west, several transitions in basin architecture (Fig 7) – one located from the Polar-3 anomaly to Iselin Bank, which separates the Northern Basin from the Victoria Land Basin and the Central Basin from the Central Trough (Fred J. Davey et al., 2021); another located at the Discovery Accommodation Zone, separating the Victoria Land Basin and Central Trough from the Western Ross Basin (T. J. Wilson, 1999), and a third located outboard of Shackleton Glacier separating this broad basin from the narrower basins of the Amundsen Coast and Crary Trough (Tankersley et al., 2022). The situation in the east is simpler, with the Eastern Basin separating at Roosevelt Island into two narrower depocenters – one extending to Siple Dome, the other to MacAyeal Ice Stream (Tankersley et al., 2022; Zhou et al., 2022). In general, the tendency is for narrower and more defined depocenters developing inland, likely indicating a deeper exposure level inland due to repeated glaciation events combined with reduced Cenozoic subsidence and sediment loading inland (Guy J. G. Paxman et al., 2019; D. S. Wilson et al., 2012), and potentially stronger lithosphere under the WAIS divide.

3.2.2 Interior West Antarctica

Interior West Antarctica (Fig 8) includes a prominent low-lying region east of the WAIS divide, the central West Antarctica region, including the Byrd Subglacial Basin and the Bentley Subglacial Trough (each extending > 2 km below sea level.) This region is bounded to three sides by high-standing regions, the Ellsworth-Whitmore and Haag regions to the west, the Thurston Island region to the north and Marie Byrd Land to the northeast. To the southwest, an indistinct transition leads to the Siple Coast.

The Ellsworth-Whitmore Mountains preserve the oldest known sedimentary rocks in West Antarctica, with a ca. 13 km-thick sequence of Cambrian to Permian sedimentary rocks (Paula Castillo et al., 2017; Craddock et al., 2017). The lowermost unit, the Heritage Group, comprises lower- to middle-Cambrian sedimentary rocks including a lower sequence of terrestrial volcaniclastic, shallow-marine clastic sediments and limestones, an overlying sequence of transitional terrestrial to marine sedimentary rocks and, overlying these, Late-Middle to Late Cambrian carbonate-dominated rocks (Curtis & Lomas, 1999). Thin transitional beds divide the Heritage Group from the Upper Cambrian to Devonian Crashsite Group, deposited in a fluvial to shallow-marine environment (Curtis & Lomas, 1999). The glacial-derived Whiteout Conglomerate is interpreted to represent the early Permian Gondwanide glaciation at ca. 300 Ma (Isbell et al., 2008) and is overlain by the Polarstar Formation including argillite, sandstone and coal measures, interpreted to represent post-glacial deposition in the Gondwana Basin (Elliot et al., 2017). Overall, this basin has been interpreted to represent a transition from a rift setting in the early Cambrian to a passive-margin setting extending into the Permian (Paula Castillo et al., 2017; Craddock et al., 2017). Isolated exposures elsewhere in the Ellsworth-Whitmore Block (Cox et al., 2023) also possess sedimentary rocks and we infer the unexposed region to be of mixed class, preserving the Paleozoic basin intruded by younger granite suites.

Seismic observations suggest that the central West Antarctica region is not occupied by a thick, broad low-velocity sedimentary basin (Zhou et al., 2022), but sedimentary rocks are likely to exist in low-lying regions (Li et al., 2022). The low-elevation areas possess markedly smooth beds, and in many cases low isostatic-residual gravity anomalies indicating relatively young sedimentary rocks are present (Jordan, Ferraccioli, Vaughan, et al., 2010). Three basins are interpreted in this region, each with different glacial catchments: the Pine Island Rift Basin underlies the upper Pine Island Glacier catchment (Jordan, Ferraccioli, Vaughan, et al., 2010); the Byrd Subglacial Basin underlies the upper portion of the Thwaites Glacier catchment (M. Studinger et al., 2001); and the Bentley Subglacial Trough flanks the Ellsworth-Whitmore block, connecting to the Ferrigno Rift Basin (Bingham et al., 2012). The thickness of sedimentary rocks in these is variable but locally may be up to 2 km thick. The geometry of these basins indicates several phases of extension, with ca. E-W oriented basins overprinted by later extension generating ca. NE-SW aligned basins (Fig 8). The former set may relate to structures in the southern Weddell Sea while the latter are aligned with WARS rift axis and the Siple Coast basins.

The nature of the bed in the glacial troughs connecting these inland basins to the coast is not clearly defined. Evidence from seismic and RES data suggests in each case a complex bed evolving with, in places, thick and partially lithified sedimentary deposits, and in other places basement rocks or volcanoes (Alley et al., 2021; Bingham et al., 2012; Brisbourne et al., 2017; A. Muto, Alley, et al., 2019; A. Muto, Anandakrishnan, et al., 2019; Atsuhiro Muto et al., 2016; A. M. Smith et al., 2013). These are classed as mixed-crust, similar to the Siple Coast region, implying a bed condition that is not well resolved within the trough, but likely contains enough sedimentary material to support enhanced till production and hydrogeology (Alley et al., 2021).

3.2.3 Pacific Margin

The Pacific margin of West Antarctica includes the basin regions of the Amundsen and Bellingshausen Seas, and the extension of this margin along the western Antarctic Peninsula (Fig 8). Each of these is characterized by a thick sequence of sedimentary rocks on the continental shelf, with up to 7 km in the Amundsen Sea and 5 km in the Bellingshausen Sea (K. Hochmuth et al., 2020; Lindeque, Gohl, Wobbe, et al., 2016). Based on a partial continuity of Cenozoic seismic stratigraphy extending from the eastern Ross Sea, the Pacific margin preserves, from west to east, a progressively younger base-of-basin, from 80-67 Ma in the Ross Sea to 36 Ma on the Antarctic Peninsula margin, and correspondingly a younger onset of transitional glacial conditions, from 34-30 Ma in the Ross Sea to 21 Ma in the eastern Amundsen Sea, and 25 Ma on the Antarctic Peninsula margin ,(Lindeque, Gohl, Wobbe, et al., 2016). In the transition to glacial Antarctica, and in subsequent glacial conditions, these basins record selective deposition focused especially in the Amundsen Sea Embayment and the eastern Bellingshausen Sea (K. Hochmuth et al., 2020; Lindeque, Gohl, Wobbe, et al., 2016). This margin has substantial shelf-edge progradation, since the middle to late Miocene in the

Amundsen Sea and since the late Miocene/early Pliocene for the Bellingshausen Sea, and the early Pliocene for the Antarctic Peninsula margin (K. Hochmuth et al., 2020).

The Amundsen Sea Embayment receives sediments from the Pine Island and Thwaites Glaciers and possesses the thickest accumulation of sedimentary rocks on the Pacific margin. The inner shelf, however, is dominated by exposed basement, extending 200 to 250 km from the coast (K. Gohl, Denk, et al., 2013). Within this region some minor basin regions are interpreted where both the bed and the magnetic data are relatively smooth. The middle and outer shelf are thickly sedimented, comprising basal strata from early Cretaceous rifting, a thick passive-margin sequence of Late Cretaceous to Oligocene sediments, and Early/Middle Miocene to Pleistocene characterized by episodic glacial advances and progradation of the shelf edge, especially during the Pliocene (K. Gohl, Denk, et al., 2013; Karsten Gohl et al., 2021; K. Gohl, Uenzelmann-Neben, et al., 2013).

3.2.4 South Shetland and South Orkney Shelf

At the northern Antarctic Peninsula, the Pacific margin of Antarctica changes from a passive margin to a convergent margin with the former Phoenix Plate (Antarctic Plate) descending under the South Shetland Islands. The main features of this margin are the South Shetland Trench and the active spreading center in Bransfield Strait behind, both associated with ongoing basin-forming processes. At the South Shetland Trench, the margin preserves a thick accretionary complex and fore-arc system imposed on the older continental shelf (Maldonado et al., 1994). These sediments were predominantly accumulated during subduction of the former Phoenix Plate, which ceased between 3.6-2.6 Ma, but also preserve evidence of younger deformation suggesting ongoing thrust faulting (Maldonado et al., 1994). Since ca. 4 Ma, the Bransfield Basin is actively subsiding through rifting with segmented depocenters up to 2 km thick, and with active volcanism and seismicity (Almendros et al., 2020).

On the opposite side of the Antarctic Peninsula shelf, the Powell Basin records rifting of the South Orkney microcontinent from the Antarctic Peninsula, with rifting commencing in the late Eocene or early Oligocene, progressing to seafloor spreading from ca. 30 to ca. 20 Ma (Eagles & Livermore, 2002). The adjacent Jane Basin opened in a back-arc setting from ca. 18 to ca. 14 Ma (Bohoyo et al., 2002). Across these basins, sediments are deposited in several sequences including syn- to post-rift packages initially in individual depocenters, transitioning to a broader shared sequence since the mid-Miocene (Lindeque et al., 2013; Maldonado et al., 2006).

3.2.5 Antarctic Peninsula and Weddell Sea

The Antarctic Peninsula and the Weddell Sea record the evolution of the Weddell Sea Rift with a partly shared basin evolution in the Mesozoic to Cenozoic. The oldest sedimentary rocks on the Antarctic Peninsula are preserved in the Trinity Peninsula Group, outcropping on the northern Antarctic Peninsula. These rocks

comprise an upper Carboniferous to Triassic sequence that formed on the margin of Gondwana in association with erosion of continental magmatic-arc material (P. Castillo et al., 2015). The Triassic LeMay Group outcropping on Alexander Island was deposited in a fore-arc accretionary complex coincident with ongoing Triassic arc-magmatism in the southern Antarctic Peninsula (Willan, 2003). The Late Jurassic to Early Cretaceous Fossil Bluff Group represents a thick sequence of fore-arc deposits derived from adjacent magmatic arcs (Riley et al., 2012). Considering their current setting, all these basins are classed as Type 2 basins.

The Jurassic-Cretaceous Latady Group outcrops on the southeastern Antarctic Peninsula, representing the formation of a progressively deepening basin from 185 to 140 Ma, with several kilometers of sediment deposited (M. A. Hunter & Cantrill, 2006). Early Jurassic to early-Middle Jurassic terrestrial to shallow-marine formations occupy smaller depocenters in grabens or half-grabens, with a transition to a deep-marine environment from the late-Middle Jurassic onwards associated with Weddell Sea rifting (M. A. Hunter & Cantrill, 2006). More sparse outcrops of similarly-aged rocks are found to the north in the Larsen Basin. Although a distinct depocenter, the Larsen Basin preserves a similar evolution from a terrestrial to shallow-marine syn-rift setting in the Early to Middle Jurassic, transitioning to a deep-marine setting from the Late Jurassic (Hathway, 2000). The northern Antarctic Peninsula preserves key upper Mesozoic to lower Cenozoic sequences exposed in the James Ross Basin. These sequences preserve a critical record of the high-latitude paleoenvironment at the Cretaceous-Tertiary boundary and also support a better knowledge of paleogeography of Antarctica (Bowman et al., 2016; Francis et al., 2006).

The formation of the Weddell Sea Rift System is interpreted to commence in line with the above transition from a magmatic-arc setting to back-arc extension at 180-177 Ma (Riley et al., 2020), with the onset of seafloor spreading by 147 Ma (König & Jokat, 2006). The Weddell Sea contains the thickest known sedimentary basin in Antarctica (Fig 6), with up to 15 km of sedimentary rocks (Leitchenkov & Kudryavtzev, 1997; Straume et al., 2019). T. A. Jordan et al. (2017) defined distinct northern and southern provinces from magnetic fabrics, indicating two distinct phases of rifting: in the south, east-west extension is interpreted due to the motion, and possibly rotation, of the Ellsworth-Whitmore and Haag blocks from a position adjacent to the East Antarctic margin, north of the Pensacola Mountains. Movement of the Haag/Ellsworth-Whitmore microcontinent likely ceased by ca. 175 Ma, based on the ages of granites emplaced along the marginal Pagano Shear Zone (Jordan, Ferraccioli, Ross, et al., 2013). Modelling of Bouguer gravity anomalies has resolved highly-thinned continental crust with a bowl-shaped basin geometry beneath the Ronne-Filchner Ice Shelf (T. A. Jordan et al., 2017; Leitchenkov & Kudryavtzev, 1997). Distinct positive Bouguer gravity anomalies occur around the margins of the Ronne-Filchner Ice Shelf (Fig 2e), including the Weddell Rift Anomaly, Filchner Rift and Evans-Rutford Rift Basin. The tectonic significance of these anomalies is not clear and they may represent crustal thinning, but with less thick sedimentary fill than is seen in the central

basin, or they may reflect regional isostatic compensation of sedimentary loads deposited after rifting when the crust had regained its strength, as suggested in the Ross Sea (Karner et al., 2005).

After development of the Southern Weddell Sea Rift System, continental rifting between Southern Africa and Antarctica became the dominant tectonic process (König & Jokat, 2006) forming the Northern Weddell Sea Rift System. The northern province possesses a NE-SW magnetic fabric, and potentially oceanic to transitional crust (Jordan et al., 2020). This phase of extension appears to crosscut the older back-arc system (T. A. Jordan et al., 2017) and is associated with magmatism giving rise to the Orion and Explora magnetic anomalies (Fig. 9). These magnetic anomalies approximately coincide with the continent-ocean transition, and they may reflect seaward-dipping reflector sequences (Kristoffersen et al., 2014), potentially emplaced ca. 150-138 Ma (König & Jokat, 2006). The onset-age of northern Weddell Sea rifting is not uniquely defined: in one model, onset of extension is suggested by 167 Ma with ocean-crust forming by 147 Ma (König & Jokat, 2006), but an alternative model suggests the Northern Weddell Sea Rift reflects separation of a single Skytrain Plate from Southern Africa and the Falkland Plateau between 180 and 156 Ma, followed by 90 degree rotation of the entire Skytrain Plate into its current position by ca. 126 Ma (Eagles & Eisermann, 2020).

Regardless of the tectonic model, interpreted sedimentary-rock thicknesses and gravity anomalies are continuous throughout the central part of the Weddell Embayment. This suggests that most of the sedimentary fill was deposited after tectonic motions ceased, likely due to thermal subsidence associated with ongoing slow spreading at the margin. The oldest sedimentary horizons were deposited over the seaward-dipping reflectors and the oceanic crust from ca. 160 to 145 Ma, with ongoing deposition continuing until at least ca. 114 Ma in the southeastern Weddell Sea (Rogenhagen et al., 2004). Progressively younger deposition proceeded toward the northwest, in line with the generation of oceanic crust and its subsidence (Lindeque et al., 2013). The youngest sediments of the pre-glacial regime may be as young as mid-Miocene, with deposition controlled by the proto-Weddell gyre (Lindeque et al., 2013).

Glacial influences on the northern Weddell Sea are substantial, with major sedimentary packages deposited associated with the transition to glacial conditions, in the Oligocene (in the southeast) to early Miocene (in the northwest), and to full glacial conditions in the mid-Miocene (Lindeque et al., 2013). Substantial shelf progradation has occurred since the late Miocene (Katharina Hochmuth & Gohl, 2019). The youngest cover relates to Quaternary sediments recovered in marine sediment cores which preserve normally consolidated, over-compacted sediments and glacial till (Hillenbrand et al., 2014) as well as glacio-marine landforms in seabed topography (Arndt et al., 2017). The distribution of these young units is not comprehensively mapped, and their thickness and age are likely to be highly variable. Nevertheless, we infer that the Weddell Sea has received sediment continuously since the Early Jurassic. To the south of the Ronne-Filchner Ice Shelf, accumulations of water-saturated sediments are identified beneath the Bungenstock Ice Rise and extending

into the Institute Ice Stream (M. J. Siegert et al., 2016). These sedimentary deposits overlie a relatively shallow basement but are associated with elevated ice velocity suggesting their potential to control ice-sheet dynamics (M. J. Siegert et al., 2016).

3.3 East Antarctic Basins

3.3.1 Weddell Coast

The continental shelf in the eastern Weddell Sea preserves a sedimentary basin extending along the shelf from the Filchner Rift to the Fimbul Ice Shelf. The basin is associated with a volcanic rifted margin that initiated in the Jurassic (Jokat & Herter, 2016; Kristoffersen et al., 2014), but also has upper Cenozoic to Quaternary sediment deposition recording repeated glacial advances (Hillenbrand et al., 2014; Huang & Jokat, 2016; Kristoffersen et al., 2014). Magnetic data indicate the geology of the underlying basement with high frequency content indicating relatively thin basin cover throughout this basin. Magnetic data also image the Explora anomaly (Fig 9), associated with Jurassic magmatism (R. J. Hunter et al., 1996) and a seaward-dipping reflector sequence, the Explora Wedge (Kristoffersen et al., 2014). Seismic exploration on the Ekström Ice Shelf has demonstrated the Explora Wedge to extend beneath the ice shelf, with overlying sedimentary rocks of up to 1 km thickness (Kristoffersen et al., 2014). The boundary is marked by a prominent magnetic gradient that extends along the entire basin, which we infer to delineate the extent of the seaward-dipping reflector sequence. Landward from this magnetic boundary, the basin is characterized by smooth topography with several ice rises interpreted as representing grounded ice on remnants of shelf sediments while adjacent troughs were eroded (Kristoffersen et al., 2014).

Inland, as well as extensive crystalline bed, several phases of basin formation are recorded. The oldest phase is preserved in outcrops in the Pensacola Mountains (Fig 9). The early Cambrian Hannah Ridge Formation was deposited after 563 Ma and prior to granite intrusion dated at 505 Ma (Curtis et al., 2004). The Hannah Ridge Formation is overlain by the Nelson Limestone and the Gambacorta Formation volcanics, dated at 501 Ma. Overlying these, the Late Cambrian Wiens Formation and Late Cambrian to Ordovician Neptune Group were deposited during and after the Ross Orogeny (Curtis et al., 2004). Similar rocks may also be preserved in the Argentina and Shackleton Ranges (K. R. Evans et al., 2018). The second major phase comprises the Devonian to Permian Beacon Supergroup, including the Upper Devonian Dover Sandstone, the Carboniferous-Permian Gale Mudstone and the Permian Pecora Formation (Curtis, 2002). As elsewhere, the Beacon Supergroup is preserved with characteristic mesa-like landforms in the Polar Gap Subglacial Highlands (G. J. G. Paxman et al., 2019) between Support Force and Recovery glaciers (Fig 9). Outliers of the Beacon Supergroup also occur on the Theron Mountains north of Slessor Glacier (Cox et al., 2023). There is no evidence for Beacon Supergroup to the north of the Theron Mountains, although the Paleozoic rocks of the Urfjell Group and Amelang Formation outcrop in western Dronning Maud Land (Cox et al., 2023).

Several Type 1 basins are inferred, with a dominant westerly trend, and characterized by low topography, negative isostatic residual gravity anomalies and smooth beds. Major basins exist to the northeast and to the south of the Polar Gap Subglacial Highlands extending to the Recovery Subglacial Highlands (Fig 9). The southern basin, the Pensacola-Pole Basin, occupies an elongate trough 150-200 km wide. Sedimentary rocks in this basin thicken inland reaching a thickness of 3.6±1.1 km (G. J. G. Paxman et al., 2019). The basin fill is interpreted to be dominated by the Beacon Supergroup, indicated by the presence of magnetic features interpreted to represent Jurassic dolerites, but also there is interpreted younger cover of up to 1 km thickness (G. J. G. Paxman et al., 2019). We define the Foundation Basin as a smaller aligned depocenter with similar characteristics. The northern Recovery Basin occurs inland from Recovery Glacier. No thickness for this basin is defined, but its geophysical character is similar to the Pensacola-Pole basin. We suggest that the topography and morphology of the Foundation, Pensacola-Pole and Recovery subglacial sedimentary basins formed during Jurassic-Cretaceous rifting. The topographic basins were later incised by glaciers, removing several kilometers of sediments from glacier troughs (G. J. G. Paxman et al., 2017). These troughs do not host major basin fill today. To the north, another major basin is interpreted associated with the Slessor Glacier (Shepherd et al., 2006). This basin (Fig 9) has a particularly smooth bed throughout (Bamber et al., 2006; Eisen et al., 2020) and models of magnetic data suggest 3 km of post-Jurassic fill (Bamber et al., 2006).

3.3.2 Dronning Maud Land and Enderby Land

Dronning Maud Land preserves evidence for a series of basin-forming events. The most prominent is the Jurassic rifting associated with the Jutul-Penck Graben system, associated with localized crustal thinning associated with the Jutulstraumen and Pencksokket troughs, with high isostatic residual gravity, and smooth magnetic-field patterns (F. Ferraccioli, Jones, Curtis, & Leat, 2005; F. Ferraccioli, Jones, Curtis, Leat, et al., 2005; Riedel et al., 2013). Interpreted Type 1 basins in the interior Dronning Maud Land region (Fig 9) are parallel and may also represent this event.

Sedimentary rocks of the ca. 1.1 Ga Ritscherflya Supergroup are exposed adjacent to Jutulstraumen, representing a ca. 2 km thick basin forming on the eastern edge of the Grunehogna Craton, in an interpreted arc-proximal setting (Marschall et al., 2013). A series of north-south oriented Type 2 basins is interpreted in interior Dronning Maud Land based on negative isostatic residual gravity and reduced subglacial roughness relative to their surroundings (Fig 3). One of these was modelled in the work of Eagles et al. (2018) who identified a sedimentary bed incised by a preserved fluvial landscape. The age of these basins is highly uncertain, although they overlie magnetic trends of the Tonian Ocean Arc Super Terrane (Ruppel et al., 2018), and are aligned with interpreted late Pan-African structures in the Sør Rondane region (Mieth & Jokat, 2014).

The Dronning Maud Land Escarpment (Eagles et al., 2018) separates the basins of the interior from interpreted Type 1 basins along the coastal plain and continental shelf (Fig 9). The coastal escarpment basin

is characterized by low, flat and smooth bed topography, sloping gently southward overall (Eisen et al., 2020) and, onshore, negative isostatic residual gravity. Numerous ice rises are present associated with sedimentary banks, interpreted as remnant shelf sediments following erosion of the adjacent troughs. These basins are interpreted to reflect depocenters formed initially during the late Jurassic to Cretaceous denudation of the escarpment, and received sediment as part of the sedimentary pathway to the major depocenters of the Riiser-Larsen Sea (Eagles et al., 2018). Further regions along the front of the escarpment, and in localized topographic lows, also have relatively high basin likelihood (Li et al., 2022), and may represent piedmont deposits.

The Ragnhild Trough (Fig 10) is a major topographic feature cutting through the Dronning Maud Land Escarpment. Its coastal portion is interpreted to possess a fill of low-density sedimentary material (Eagles et al., 2018), and is topographically smooth (Eisen et al., 2020) and is included here in the escarpment basin. Inland, the trough forms two ca. 100 km wide sub-troughs either side of Belgica Highlands (Belgicafjella), respectively called West and Central Ragnhild Troughs, with low gravity, low to moderate topographic roughness and low magnetic roughness. To the east is the crystalline bed of the Queen Fabiola Mountains block. These linear troughs are interpreted as rifts forming during Paleozoic to Mesozoic rifting. Similar troughs are interpreted in Enderby Land, connecting to the west branch of the Lambert Rift System (Fig 10).

The continental shelf fringing the Cosmonauts Sea is narrow, at ca. 70 km width (Davis et al., 2018). Two separate depocenters are defined with the western depocenter having less rugged topography and lower sediment volume relative to the eastern depocenter (Davis et al., 2018). Seismic data over the shelf edge image a relatively thin package (0.5 to 2 km) of pre- to syn-rift sediments, with a more voluminous post-rift sequence (Stagg et al., 2004). While sedimentation on the shelf may be relatively limited, a substantial sediment volume was transported to the continental rise since the late Miocene (K. Hochmuth et al., 2020).

3.3.3 Lambert Graben and Prydz Bay

Mac. Robertson Land is dominated by crystalline basement, with basins associated with the Lambert Rift System. The Lambert Rift System has a cruciform geometry, with the north-south-aligned main branch extending inland for over 1500 km, complemented by eastern and western branches (Fig 10). Subsidence is greatest in the northern portion of the main branch, with more limited subsidence to the south, suggesting that the eastern and western branches may have accommodated differential strain. Smaller aligned basins are found in Mac. Robertson Land, including the exposed Beaver Lake Basin. The Beaver Lake Basin preserves the mid-Permian to upper-Triassic Amery Group, comprising clastic sedimentary rocks, with coals in the lower sequence (McLoughlin & Drinnan, 1997). These rocks represent a terrestrial depositional setting with overall north-directed sediment transport. Seismic studies on the Amery Ice Shelf resolve multiple layers of sedimentary rocks, with a thin layer of young sediments overlying an older package of interpreted glaciomarine origin (McMahon & Lackie, 2006). In turn this overlies a > 5 km-thick sequence of rift-related

sedimentary rocks (Mishra et al., 1999). Cenozoic glaciomarine fjordal sedimentary rocks are mapped from within the Lambert Graben, indicating a series of glacial-retreat events since the Oligocene or younger, and also significant Cenozoic uplift, with exposures preserved at up to 1500 m elevation (Hambrey & McKelvey, 2000).

Inland, the southern branch of the Lambert Rift System occupies the trough to the Mellor Glacier, while the eastern branch occupies the trough to the Lambert Glacier, and the western branch occupies the catchment of the Fisher Glacier (F. Ferraccioli et al., 2011). Each has characteristics of low isostatic residual gravity anomalies and smooth topography. The southern branch has several further depocenters indicated upstream (Fig 10).

Offshore, the Prydz Bay Basin is well-surveyed with relatively dense seismic coverage and multiple drill cores (Fig 1). The inner shelf is dominated by thick accumulations of Permian to Early Cretaceous sediments, with a thin veneer of Cenozoic cover (Stagg et al., 2004). On the outer shelf a sequence is recorded prograding toward the northeast through the Cenozoic, marked by several erosion surfaces and marine deposition events (Whitehead et al., 2006). Quaternary deposition is inferred to be present throughout the region (Whitehead et al., 2006). The Mac. Robertson Shelf preserves a relatively thin cover of syn- to post-rift sedimentary rocks (Stagg et al., 2004), with a comparable Cenozoic sequence to the Prydz Bay Basin (Whitehead et al., 2006).

3.3.4 Princess Elizabeth Land and Queen Mary Land

The continental shelf offshore from Princess Elizabeth Land preserves a thin cover of upper Paleozoic to Cenozoic sedimentary rocks (Davis et al., 2018), with interpreted Precambrian basement at Drygalski Island (Fig 11), and, at Gaussberg, a volcano dated at 56±5ka (Smellie & Collerson, 2021). Inland, the Princess Elizabeth Land region is dominated by crystalline basement, but several regions are identified with subdued magnetic responses and relatively smooth topography that may represent remnant sedimentary basins. These are arrayed along the tectonic structure of the Gaussberg Rift, which may share an evolution with the Lambert Rift system (D. A. Golynsky & Golynsky, 2007). A large basin (the Wilhelm II Basin) is identified with similar characteristics to the better-known Knox Basin further east (Fig 11). The interior of Princess Elizabeth Land, until recently, had one of the largest data gaps in Antarctica (Cui et al., 2020). Early work identified a significant lake (Lake Snow Eagle) and associated canyon system (Stewart S.R. Jamieson et al., 2016) likely aligned with tectonic structures (Fig 10). More recent subglacial topography (Cui et al., 2020) identified a topographic depression that is aligned en-echelon with the Wilhelm II Basin and Lake Snow Eagle (Fig 10). We infer a sedimentary basin in this depression although other geophysical results are not yet available for corroboration.

Queen Mary Land has the well-resolved and substantial Knox Rift system including several sedimentary depocenters aligned perpendicular to the coast sedimentary (Maritati et al., 2016). The basin system may extend over 1000 km inland (Fig 11). This basin possesses up to 3 km of sedimentary-rock fill that is interpreted to date primarily to the Permian-Triassic (Maritati et al., 2016; Maritati et al., 2020). The region also preserves the Neoproterozoic to Ediacaran Sandow Group, exposed at the fringes of the Knox Basin (Mikhalsky et al., 2020). The coastal region is dominated by Precambrian crystalline basement, including beneath the Shackleton Ice Shelf, with moderate to thin sedimentary cover interpreted for the Bruce Rise and the Knox Coast shelf. The Knox coastal plain preserves a low-relief surface (Eisen et al., 2020) potentially indicative of a thin and relatively young sedimentary cover.

3.3.5 Vostok and Gamburtsev Highlands

The East Antarctic interior is defined by the subglacial highlands of the Vostok and Gamburtsev regions (Fig 11). Subglacial Lake Vostok has been investigated with seismic techniques that return equivocal results (M. Siegert et al., 2011). Receiver-function studies recorded a low-velocity zone beneath the lake bed, interpreted to represent a 4-5 km thickness of sedimentary rocks above a crystalline bed (Isanina et al., 2009). However, later seismic-refraction experiments suggested that the lake bed is instead characterized by a relatively thin cover of sediments over an acoustically-fast basement, likely to be crystalline basement (Leitchenkov et al., 2016). The latter study resolved a lower-velocity bedrock for the highlands to the west of Lake Vostok. Lake Vostok and its western shore possesses predicted moderate to high sedimentary basin likelihood (Li et al., 2022), indicated by low isostatic residual gravity anomalies and smooth magnetic-field anomalies (Michael Studinger et al., 2003). These characteristics notably do not extend to the eastern shore. While a thick Type 1 sedimentary basin in Lake Vostok may not be supported, a Type 2 basin is interpreted extending along the Vostok Subglacial Highland to the west of and beneath Lake Vostok (Fig 11). This may represent a flexural basin formed in response to collisional processes in the Neoproterozoic (Michael Studinger et al., 2003).

The Vostok Highlands are separated from the Gamburtsev Subglacial Mountains (GSM) by a prominent low-lying region with a relatively smooth bed, also including Lake Sovetskaya and Lake 90°E (Fig 11), forming the eastern branch of the East Antarctic Rift System (EARS) (F. Ferraccioli et al., 2011). This region is interpreted as a Type 1 sedimentary basin, although it is not associated with a gravity low, suggesting sedimentary fill is limited in thickness. The main range of the GSM is dominated by high-elevation topography, high along-track roughness, and high spatial variability in elevation and magnetic data (Fig 2), all indicative of crystalline basement. To the west, a broad area with low and smooth topography and low gravity separates the GSM from the Recovery Subglacial Highlands, suggesting a basin with substantial sedimentary fill, forming the western branch of the EARS (F. Ferraccioli et al., 2011). The southern flank of the GSM is also marked by a substantial gravity low, and relatively low roughness, indicating a possible sedimentary basin (Fig 3). The

origin of this basin is not known, but it is aligned parallel to the South Pole Basin, and it may be an uplifted remnant of that basin or part of an older basin system (cf McLean et al., 2008).

3.3.6 Wilkes Land and Terre Adelie

Wilkes Land preserves an extensive sedimentary basin system including several major depocenters including the Aurora, Vincennes and Sabrina basins (A. R. A. Aitken et al., 2014). These basins are characterized by thick accumulations of sedimentary rocks, with as much as 10 km of fill possible in the Aurora Basin, but more typically ca. 5 km in Aurora, ca. 4 km in Vincennes and ca. 2 km in Sabrina Basin (A.R.A. Aitken et al., 2016; A. R. A. Aitken et al., 2014). The Aurora and Vincennes basins are characterized most fundamentally by low gravity, a very smooth surface, and subdued magnetic signals- this same characteristic defining the southward extension of the Aurora Basin (Fig 11). The Sabrina Basin has less smooth topography and more variable magnetic data, nevertheless, geophysical models suggest a preserved sedimentary basin of up to 3 km thickness that has been variably eroded by ice-ice-sheet activity, exposing basement in places (A.R.A. Aitken et al., 2016). These inland basins are separated from the Sabrina Coast by a basement ridge, likely also a feature of glacial erosion.

Tonian to Ediacaran sedimentary rocks have been found in glacial erratics from the Windmill Islands, indicating an early basin forming phase in this region with potential links to the Centralian Superbasin of Australia (Maritati et al., 2019). The region preserves several subglacial highlands that are interpreted in gravity models to be sedimentary in nature, including Highlands A, B and C, the region north of the Aurora Basin, and the Belgica Subglacial Highlands (A.R.A. Aitken et al., 2016). Thermochronology suggests that the highlands were uplifted and peneplained in the Permian-Triassic (Maritati et al., 2020), with the main phase of rifting at this time. Although the region was potentially reactivated during Jurassic-Cretaceous rifting events, to date, no evidence of this exists locally.

Offshore, sedimentary sequences along the Australian-Antarctic margin define four major sequences separated by unconformities of age 95-80 Ma, 65-58 Ma, 50-45 Ma and 34 Ma (Sauermilch et al., 2019). The first sequence represents the rift-derived basin; the sequence is characterized by deltaic sediment deposition derived from continental river systems, while the third may derive from clockwise-circulating bottom currents developing in the Paleocene – Eocene with a decrease in sediment input (Sauermilch et al., 2019). The Sabrina Shelf sedimentary basin may have begun forming at this time, with a distinctive terrestrial palynoflora interpreted to date to the latest Paleocene to earliest Eocene (C. Smith et al., 2019). The Sabrina Shelf is covered by post-Cretaceous sedimentary cover with variable thickness up to 1.3 km seismically imaged (Gulick et al., 2017; Montelli et al., 2019). Paleocene to late-Miocene strata record a history of Cenozoic ice-sheet evolution including the identification of marine-terminating glaciers in the early to middle Eocene, a series of retreat and advance events in the Oligocene and Miocene, and an expanded East Antarctic Ice Sheet since the late Miocene (Gulick et al., 2017). The fourth offshore sequence represents

the glacial development of the margin with, in particular, the deposition of a high volume of sediments since the Oligocene, including apparently variable supply from glacial outlets through time (K. Hochmuth et al., 2020; Katharina Hochmuth et al., 2022).

The Terre Adelie Craton provides the eastern boundary to this basin region, with a basement-dominated ridge extending 1800 km inland from Porpoise Bay. Several smaller basins are identified within this ridge including the Frost, Astrolabe and Adventure subglacial troughs. Smooth beds (Eisen et al., 2020) and low gravity suggest these depressions host sedimentary basins, although their age is not known (A. R. A. Aitken et al., 2014; Frederick et al., 2016). Offshore Terre Adelie, seismic data record the transition from a deformed Cretaceous rift on the innermost shelf, through a Paleocene to Eocene transpressional phase, younging to Plio-Pleistocene strata at the shelf edge (De Santis et al., 2003), representing progradation of the shelf since the Eocene (Katharina Hochmuth & Gohl, 2019). Maximum observed sedimentary thickness is 1.6 km (De Santis et al., 2003). The Mertz and Adelie banks are prominent bathymetric features representing remnant shelf-sediments, with adjacent basins incised by past glacial action (Beaman et al., 2011).

3.3.7 Wilkes Subglacial Basin, South Pole Basin and Transantarctic Mountains

The Beacon Supergroup is prominent along the Transantarctic Mountains (Fig 12) extending from northern Victoria Land, where outcrops are relatively sparse, to prominent and near-continuous exposures extending from David Glacier to the Ohio Range (Elliot et al., 2017). The Beacon Supergroup comprises the basal Taylor Group and the overlying Victoria Group. The Taylor Group consists of Devonian clastic sedimentary rocks, predominated by shallow-marine sediments grading to fluvial sediments (Bradshaw, 2013). The unconformably overlying Victoria Group and regional equivalents consist of Permian-Triassic siliciclastic and volcaniclastic rocks also including glacial deposits and coal beds (Elliot et al., 2017). Ongoing sedimentation into the Jurassic is identified from younger rocks exposed along the Transantarctic Mountains including the Section Peak Formation of northern Victoria land, the Mawson Formation of southern Victoria Land and the Hanson Formation in the central Transantarctic Mountains (Elliot et al., 2017). The sequence is overlain and intruded by mafic magmatic rocks of the Ferrar Group, often forming the caps to mesa-like exposures. In the context of their exposed extent the Beacon Supergroup are classed as Type 2 basins.

Likely Beacon Supergroup correlatives are exposed at Horn Bluff, on the Wilkes Land coast, and magnetic-field anomalies consistent with Ferrar Group dolerite intrusions are found throughout the northern Wilkes Subglacial Basin (Fausto Ferraccioli et al., 2009). From these observations we may infer the Beacon Supergroup as the dominant sedimentary fill in the Wilkes Subglacial Basin. The Wilkes Subglacial Basin extends for 1600 km along the edge of the Terre Adelie Craton. The basin may be divided into a southern sub-basin, which consists of a single broad depocenter, with a substantial thickness of sedimentary rocks (ca. 5 km) extending to 81°S, in line with Byrd Glacier (Frederick et al., 2016). Thinner cover extends southwards to roughly 84°S, in line with the southern end of the Miller Range. The northern sub-basin consists of three

smaller depocenters and more variable sedimentary cover (Frederick et al., 2016). Magnetic analysis suggests possible rifting post-dating the intrusion of the Ferrar Group, and interpreted to be Cretaceous in age, possibly with Cenozoic reactivation (Fausto Ferraccioli et al., 2009; Jordan, Ferraccioli, Armadillo, et al., 2013). The discontinuity between these basin regimes (Fig 12) connects to David Glacier and is aligned with several right-lateral transcurrent faults in northern Victoria Land (Fausto Ferraccioli et al., 2009), that also influenced the Cenozoic evolution of the Ross Sea (Salvini et al., 1997). The Wilkes Subglacial Basin is continuous with a further subglacial sedimentary basin located near the South Pole (P. E. Wannamaker et al., 2004). The furthest extent of the South Pole Basin is aligned with a structural lineament extending from the South Pole through the Transantarctic Mountains near the Reedy Glacier (Fig 12).

Several Neoproterozoic to early Paleozoic sedimentary packages occur along the Transantarctic Mountains. Ediacaran sedimentary rocks are preserved including the Berg Group (northern Victoria Land) and the Beardmore Group (central and southern Transantarctic Mountains). Metasedimentary units along the Transantarctic Mountains include the Rennick Schist and Priestley Formation (northern Victoria Land) and Skelton Group (southern Victoria Land) (John W. Goodge, 2020). Detrital zircon populations indicate these units were deposited after ca 1000 Ma, while Ross Orogeny metamorphism and granite intrusions provide a lower bound of 600 – 550 Ma; volcanic horizons in the Skelton Glacier area and Beardmore Group return compatible ages of 670-650 Ma Transantarctic Mountains (John W. Goodge, 2020). The Transantarctic Mountains also preserve extensive lower Paleozoic successions. These include in northern Victoria Land the Bowers Supergroup, comprising the Sledgers, Mariners and Leap Year Groups, exposed in the Bowers Terrane and the Robertson Bay Group exposed in the Robertson Bay Terrane. The Bowers Supergroup was deposited in a marine to terrestrial setting in the Cambrian, deposition beginning prior to 520 Ma and ceasing after 480 Ma (John W. Goodge, 2020). The Robertson Bay Group was deposited in a deep marine setting in the early Ordovician, after 490-465 Ma.

The Transantarctic Mountains between David Glacier and Byrd Glacier does not preserve a comparable lower Paleozoic sequence, but south of Byrd Glacier the Cambrian-Ordovician Byrd Group is interpreted to extend to the Shackleton Glacier (John W. Goodge, 2020). The Byrd Group contains a lower sequence of carbonate rocks (Shackleton Limestone, 525-515 Ma) transitioning upwards to carbonate-clastics (Holyoake Formation) and then siliciclastic sedimentary rocks (Starshot Formation and Douglas Conglomerate, 515 – 480 Ma). These are interpreted to represent the transition from a pre-Ross Orogeny carbonate platform to syn-orogenic molasse deposit Transantarctic Mountains (John W. Goodge, 2020). The southern Transantarctic Mountains, extending from the Queen Maud Range to the Wisconsin Range, preserve the lower Paleozoic siliciclastic LaGorce Formation and Duncan Formation. These formations contain detrital zircons dated at ca. 560-550 Ma, suggesting they were deposited in the early Cambrian and are intruded by

hypabyssal volcanic rocks of the Liv Group dated at 526 Ma. The Liv Group preserves an early Cambrian lower sequence of silicic volcanics and a middle to late Cambrian upper sequence of bimodal volcanics.

4 Tectonic architecture, basin formation and the paleolandscape of Antarctica

Antarctica's sedimentary basins have developed in several key phases in accordance with the evolving plate-tectonic system. Early phases associated with Pre-Ediacaran tectonic events are well defined at the regional scale; however, their plate-tectonic setting remains in many cases cryptic with respect to the global plate system. The Type 1 basins recognized in this study have predominantly developed since the Ediacaran and we focus on these.

4.1 Tectonic structure of Antarctica's lithosphere

The development of sedimentary basins occurs in parallel with the development of the crust and the lithospheric mantle beneath. The structure of the crust and mantle have been investigated in a number of recent studies that reveal key features of relevance to understanding the basin distribution (An et al., 2015; Chaput et al., 2014; Hazzard et al., 2023; Lloyd et al., 2015; Lloyd et al., 2020; Pappa, Ebbing, & Ferraccioli, 2019; Weisen Shen et al., 2017; W. Shen et al., 2018). Most critical to basin forming is the development of accommodation space due to tectonic subsidence. Most commonly, the thinning of the lithosphere under extension is the main driver of tectonic subsidence.

Antarctica's crustal thickness (Fig 13a) reflects, to a large degree, the history of extension events that have occurred since Pangea times, and thinner crust is highly correlated with the presence of major basins, whereas basement-dominated regions tend to have substantially thicker crust. This is most notable in the Ross and Weddell regions where very thin crust (thickness < 15 km) is linked to the major basin systems in these regions. This relationship is not universal, with the southern Wilkes Basin and the Aurora Basin being underlain by thicker crust (thickness > 30 km), suggesting that subsidence for these basins potentially was not linked to intense crustal thinning. Type 2 basins often overlie thick crust including those in the Vostok Highlands, Transantarctic Mountains and Dronning Maud Land regions.

In addition to effects on crustal thickness, lithospheric thinning may lead to the upwelling of asthenospheric mantle. Initially, a surface uplift is typical due to mantle heating, and then a prolonged post-rift thermal subsidence phase as the mantle cools over hundreds of millions of years. Lithospheric thickness (Fig 13b) is closely associated with the thermal state of the mantle, and areas of thin lithosphere are associated with recent to ongoing tectonic events. Thin lithosphere in West Antarctica is associated with the WARS, and recent higher-resolution models (Hazzard et al., 2023) suggest it may be less than 30 km thick in regions with recent volcanism including the Terror Rift, Marie Byrd Land, the Siple Coast and the Antarctic Peninsula.

Thicker lithosphere is found through the Eastern Basin of the Ross Sea, central West Antarctica and Ellsworth-Whitmore and Haag regions. The Jurassic Weddell Sea Rift System has a lithosphere thickness of ca. 100 km.

In central East Antarctica the thickest lithosphere, exceeding 200 km thickness, is centered on the Recovery Subglacial Highlands, the Gamburtsev Subglacial Mountains and the Vostok Highlands (Fig 13b). The effect of the East Antarctic Rift System on the lithosphere is not clearly delineated, although narrow rifts of ca. 100 km width may be below the resolution of the seismic models for East Antarctica. The major basins of East Antarctica are not all clearly associated with thinned lithosphere and notably Aurora, Vincennes, South Pole and Southern Wilkes basins all overlie lithosphere exceeding 150 km thickness. The lack of basin-aligned thermal anomalies suggests that these basins are probably associated with rifting occurring prior to the Jurassic. The Lambert, Slessor Glacier and northern Wilkes basins are associated with thinner lithosphere, supporting a more recent (post-Triassic) rifting and thermal reactivation in those basins. Thinned lithosphere is observed around the East Antarctic margin including lithospheric embayments beneath northern Victoria Land, the southern Transantarctic Mountains, Dronning Maud Land, Enderby Land, the Sabrina Coast and Terre Adelie (Fig 13b).

In rifting, crustal- and lithospheric-scale structures control the locus of deformation, and strongly influence the shape and internal structure of basins. Integrated lithospheric-scale structures were investigated by Stål et al. (2019), who analyzed bed topography, gravity, and seismic tomography models to delineate the major boundaries of the lithosphere (Fig 13c). We apply a multiscale edge-detection approach to the Bouguer gravity anomaly (Fig 13d). Phase-congruent multiscale edges (Kovesi, 1999) were delineated for 6 scales with upward-continued datasets at 20, 30, 40, 50, 60 and 80 km height. At each height, three sub-scales were analyzed for phase congruency using windows of 3, 6 and 12 times the height. Ultimately, the analysis resolves phase-congruent structures between 60 km and 960 km width, including finer-scaled structures than the integrated lithospheric analysis.

Both analyses indicate major basin-bounding structures of the lithosphere including the WARS-bounding structures of the Transantarctic Mountains front and Bentley Subglacial Trough but also several more subtle basin-aligned features including in the Ross Sea, and along the Siple Coast, the Pine Island Rift and the Byrd Subglacial Basin (Fig 13c). The boundaries of the Weddell Sea Rift system are clearly defined including the boundary with Palmer Land (the Palmer Land Lineament) and the Filchner Trough (the Filchner Trough Lineament), again with several smaller structures associated with the internal structure of the basin. The gravity analysis defines additional lineaments associated with the Orion and Explora magnetic anomalies (Fig 13d)

In East Antarctica, the analyses delineate major basin-bounding structures including both the eastern and western edges of the northern Wilkes Subglacial Basin. The western boundary (the Wilkes Adelie Lineament) extends inland for at least 1200 km, while the eastern boundary (the Matusevich Glacier Lineament) is truncated against the Transantarctic Mountains front near David Glacier. Numerous cross-basin structures are seen including the division of northern and southern Wilkes Subglacial Basin, near David Glacier, the boundary with the South Pole Basin near Nimrod Glacier, and the truncation of the South Pole Basin near Reedy Glacier (Fig 13). Beyond, the Polar Gap Subglacial Highlands are bounded by lineaments associated with Support Force and Recovery Glaciers, and the final boundary of the Beacon Supergroup basin is seen aligned with Bailey Glacier. Beyond Bailey Glacier the north-south-oriented Coats Land lineament relates to basement structures, likely of Precambrian age, with a minor basin formed to its west.

The Adventure Subglacial Trench is bounded to the west by a prominent north-south oriented lineament (the Adventure Trough Lineament) while a parallel structure to the west bounds the Belgica Subglacial Highlands from the Aurora Subglacial Basin (the Concordia Lineament). The southern boundary of the Aurora Subglacial Basin possesses a substantial gravity boundary, linked to a topographic boundary and truncation of magnetic trends (A. R. A. Aitken et al., 2014). This boundary is not associated with a lineament in either analysis (Fig 13) indicating a diffuse gradient that is not phase-congruent and may indicate a shallow-dipping structure. The northern edge of the Aurora Subglacial Basin is associated with a lineament (the Aurora Lineament) trending northwest-southeast towards the Knox Coast. The northwest-southeast lineament is disrupted by the north-south-trending Highland B Lineament and a similar structure to the west defines the eastern boundary of the Knox Subglacial Basin (the Knox Basin Lineament). The Lambert region has a complex structure including, in the analysis of Stål et al. (2019) the main north-south graben, although this is less obvious in the gravity analysis, and secondary east-west to northwest-southeast boundaries aligned with basins (Fig 13c). In the gravity-data analysis, additional northeast-southwest lineaments are identified aligned with the Ruker magnetic anomaly (the Ruker Lineament) and the Gamburtsev Suture representing structures in the Precambrian basement (F. Ferraccioli et al., 2011; McLean et al., 2009).

At the largest scale, we can see in these analyses and models the division of East Antarctica into several major domains by prominent sets of lineaments along structural culminations, marked by dashed lines in Figure 13. The first lineament set is observed extending along the Terre Adelie Highlands, bounding the Wilkes Subglacial Basin from the Aurora Subglacial Basin region. This trend reflects fundamental boundaries in the geometry of the Mawson continent and its Neoproterozoic margin (A. R. A. Aitken et al., 2016; M. Studinger et al., 2004). The second lineament set extends from near Nimrod Glacier, along the Vostok Subglacial Highlands, where lineaments bound the Vostok Highlands Basin and Lake Vostok Basin, to the coast near the West Ice Shelf. A potential sub-set to the west extends along a similar trend transecting the Gamburtsev Subglacial Mountains, Princess Elizabeth Land and emerging into Prydz Bay. In part this trend

may represent the East Antarctcic Rift System (F. Ferraccioli et al., 2011) but also is aligned with a proposed fundamental lithospheric boundary associated with Neoproterozoic collision (Mulder et al., 2019; Michael Studinger et al., 2003). The third set of lineaments extends from Reedy Glacier, through South Pole, extending along the Recovery Subglacial Highlands, and then either side of the Fuji Subglacial Highlands, with branches emerging into Lutzow-Holm bay, the West Ragnhild Trough and possibly also Borchgrevinkisen. In its southern portion, this structure separates the South Pole Basin from the Pensacola-Pole Basin and is linked to the formation of the Pensacola Embayment, interpreted in the late Neoproterozoic (Jordan et al., 2022). To the north, the Fuji Subglacial Highlands culmination separates the basin-dominated regions to the west (Recovery, Slessor and interior Dronning Maud Land), and east (Lambert).

These lineament sets represent fundamental structures of the Antarctic lithosphere dating to at least the Neoproterozoic, but their impact on later tectonics and basins is profound. In a Gondwana reconstruction, the Fuji Subglacial Highlands lineament trend is aligned with the eventual Africa-Madagascar-Sri Lanka triple junction, the Vostok Highlands lineament trend is aligned with the Kerguelen Plateau, and the Terre Adelie Highlands trend is linked to the George V fracture zone of Australian-Antarctic basin (Fig 14). The four domains of East Antarctica have clearly different basin systems with distinct geometries and structural trends, with broadly, the Pensacola-Recovery-Slessor rift system (G. J. G. Paxman et al., 2017; G. J. G. Paxman et al., 2019), the EARS (F. Ferraccioli et al., 2011), the Aurora-Vincennes-Sabrina system (A. R. A. Aitken et al., 2014), and the Wilkes Subglacial Basin system (Fausto Ferraccioli et al., 2009; Jordan, Ferraccioli, Armadillo, et al., 2013; Jordan et al., 2022).

4.2 Basin forming phase 1- Ediacaran to Carboniferous

During the Ediacaran to early Cambrian, a continuous East Antarctica was formed as part of Gondwana, assembled through the East-African (ca. 650 to ca. 550 Ma) and Kuunga (ca. 550 to ca. 490 Ma) orogens. The exact locations of the associated lithospheric boundaries beneath the ice sheet are not known well. Type 2 basins in the continental interior potentially formed during these events, including in Dronning Maud Land, the Vostok Highlands, the Aurora/Sabrina region and the Knox region. In the same timeframe, the edge of East Antarctica was evolving as a passive margin (Jordan et al., 2022) with associated basin forming events (John W. Goodge, 2020). Ediacaran subduction was initiated along the paleo-Pacific margin of Gondwana. The onset of the Ross Orogeny, marked by metamorphism from 615 Ma and magmatism from 590- 565 Ma (John W. Goodge, 2020) and associated deformation events, saw a change in the locus and nature of basin formation towards the edge of the craton, with the orogeny ending ca. 470 Ma when the margin retreated (John W. Goodge, 2020).

Cambrian to Ordovician sedimentary basins deposited along this margin are interpreted to have formed in association with arc-related magmatism of the Ross Orogeny, continuing into the post-tectonic phase. Basins

typically include an Early to Middle Cambrian sequence of pre- to syn-orogenic units (e.g. Bowers Supergroup, Byrd Group, Hannah Ridge Formation, Heritage Group) and a Late Cambrian to Ordovician syn- to post-orogenic sequence (e.g. the Robertson Bay Group, the Swanson Formation, Neptune Group, Crashsite Group). Both the Ellsworth-Whitmore and western Marie Byrd Land blocks were probably adjacent to East Antarctica at this time (Jordan et al., 2020). Global tectonic reconstructions of this time period lack detail relative to those from the Devonian onwards, and for regional tectonic reconstructions of this time period the reader is referred to regional syntheses (e.g. Boger, 2011; John W. Goodge, 2020). Cambro-Ordovician basement exhumation occurred inland from the central Transantarctic Mountains region as recorded in low-temperature thermochronology data (Fitzgerald & Goodge, 2022).

The Devonian is marked by the deposition of the lower Beacon Supergroup in an interpreted continental retro-arc setting within Gondwana (Bradshaw, 2013). This basin is exposed as Type 2 in the mountains from Northern Victoria Land to the Theron Mountains and is preserved as Type 1 in the subglacial hinterland. The distinction of Type 1 and Type 2 in this case is primarily a consequence of later uplift of the Transantarctic Mountains and potentially also downfaulting of the hinterland (Fausto Ferraccioli et al., 2009). We infer for the Devonian a single sedimentary basin system (the Beacon Basin) with low elevation throughout. The system was divided along-strike into distinct depocenters with up to nine major divisions along its length (Fig 13). The internal divisions are marked by changing thickness and morphology of the Type 1 basins, while for Type 2 basins in the Transantarctic Mountains the variable extent of Beacon Supergroup exposures along-strike may represent initial thickness variations coupled with differential uplift in later events (Brenn et al., 2017; Weisen Shen et al., 2017; P. Wannamaker et al., 2017). Offsets to the basin margins and the uplifted parts are also seen (Fig 12). The end of this subsidence episode is not well constrained but must predate lower-Permian glaciogenic deposits that mark the onset of the second phase (Elliot et al., 2017).

4.3 Basin forming phase 2- Permian to Triassic

Following the amalgamation of Pangea at ca. 320 Ma, the Permian marked a distinct change in the tectonic setting of Antarctica. Permian-Triassic Antarctica saw ongoing subduction at the West Antarctic-Panthalassan margin, while the Tethyan margin was subjected to rifting from ca. 300 Ma to ca. 200 Ma (Müller et al., 2019; A. Young et al., 2019). During this period several microcontinents rifted at different times, but the main Cimmerian terranes separated from Pangea from 280 to 270 Ma (Fig 14a). The Antarctic Peninsula preserves arc-proximal sedimentary rocks from this period (P. Castillo et al., 2015), but the most extensive known sedimentary deposits are found along the Transantarctic Mountains, including exposures from Northern Victoria Land to the Shackleton Range (Elliot et al., 2017) which are all considered equivalents of the Victoria Group of the Beacon Supergroup. Similar rocks in the Ellsworth Mountains may also be stratigraphic correlatives, since relocated due to motion of the Ellsworth-Whitmore Block (T. A. Jordan et al., 2017) (Fig 14a). A continuation of Victoria Group equivalent sequences into the Wilkes Subglacial basin,

South Pole Basin and Pensacola-Pole Basin is likely (Fausto Ferraccioli et al., 2009; G. J. G. Paxman et al., 2019; P. E. Wannamaker et al., 2004).

Exhumation of the East Antarctic coast at least from Prydz Bay to George IV Land occurred between ca. 350 and ca. 200 Ma, likely in response to Tethyan rifting (Lisker et al., 2007; Maritati et al., 2020; Tochilin et al., 2012) although influenced by glacial erosion (Rolland et al., 2019). This was accompanied by formation of several major basins including Lambert, Knox and Aurora basins (Maritati et al., 2020) and likely an extensive network of smaller basins within East Antarctica (Fig 14a). The Pangean landscape and basins persisted until the Early Jurassic Karoo-Ferrar LIP (183 Ma) when Gondwana breakup commenced.

4.4 Basin forming phase 3 - Jurassic to Eocene

The Jurassic to Eocene tectonic setting of Antarctica was dominated by the protracted and progressive fragmentation of Gondwana (Fig 14), which led to the formation of marginal basins and ultimately led to an isolated Antarctic continent. Rifting progressed in a 'clockwise' direction with first South America and Africa (from 177 Ma), India, Sri Lanka and Madagascar (from 135 Ma), Australia (from 100 Ma), and Zealandia (from 82 Ma). This process is relatively well recorded in the sedimentary basins of the Antarctic margin.

Subsidence linked to Gondwana dispersal began in the Weddell Sea region ca. 180-177 Ma (Riley et al., 2020). The pre-cursor to continental breakup is thought to have been extensive magmatism and emplacement of the Karoo-Ferrar Large Igneous Province at ca. 183 Ma (Burgess et al., 2015). For the main Weddell Sea basins, one suite of models suggests a two-stage development with Early Jurassic motion of the Haag-Ellsworth-Whitmore microcontinent that led to the development of the Southern Weddell Sea Rift System (T. A. Jordan et al., 2017), including rifting at the margins of the Weddell Sea (Evans-Rutford Basin and Filchner Trough). Subsequently, rifting occurred in the Northern Weddell Sea Rift Basin and the Riiser-Larsen Sea, beginning associated with breakup between Southern Africa and Antarctica before ca. 167 Ma (König & Jokat, 2006). The Weddell and Riiser-Larsen seas continued to open together, with associated basin formation offshore, until 126 Ma after which time Atlantic Ocean (Fig 14b) opening led to separate kinematics for these regions (König & Jokat, 2006). In East Antarctica, the Jutul-Penck Graben system (F. Ferraccioli, Jones, Curtis, Leat, et al., 2005; Riedel et al., 2012) and the Slessor Glacier Basin experienced Jurassic to early Cretaceous extension in line with the departure of Africa and South America (Fig 14b). The thermal history of the Shackleton Range suggests a heating episode between 180 – 135 Ma indicating possible sedimentary burial during this time, before rapid cooling at ca 130 Ma (Krohne et al., 2016).

An alternative tectonic model for the Weddell Sea region suggests that the entire Weddell Sea Rift System is part of a single larger Skytrain tectonic plate, including much of the central and southern Antarctic Peninsula Plate (Eagles & Eisermann, 2020). In this model the Northern Weddell Sea Rift reflects separation of the Skytrain Plate from Southern Africa and the Falkland Plateau between 180 and 156 Ma, followed by 90°

counterclockwise rotation of the entire Skytrain Plate into its current position by ca. 126 Ma (Eagles & Eisermann, 2020). In contrast with the previous model this model does not include Jurassic opening of the southern Weddell Sea, and the plate motion implies 200-400 km of shortening between the Skytrain Plate and East Antarctica during the Cretaceous.

Rifting of Madagascar and greater India from Antarctica had commenced by the early Cretaceous with oceanic crust forming in the Enderby Basin from 133 Ma (Jokat et al., 2021). This process may have involved an initial separation between East Antarctica and the Elan Bank and Southern Kerguelen Plateau, with by ca. 115 Ma a ridge-jump to north of the Elan Bank associated with the Kerguelen Plume (Gaina et al., 2007; Gibbons et al., 2013), although an entirely pre-Kerguelen evolution is possible (Jokat et al., 2021). From 120 Ma, igneous rocks from the Kerguelen Plume formed much of the Southern Kerguelen Plateau and also are prominent in the basins of Enderby and Davis Seas (Davis et al., 2018). The potential effects of the rifting of greater India on East Antarctica's landscape and onshore basins remains ill-defined. Limited thermochronology detects early Cretaceous cooling in the Lambert region (Lisker et al., 2007), linked to brittle deformation structures (Phillips & Läufer, 2009), although later studies propose an igneous origin for thermal resetting (Tochilin et al., 2012), while the Shackleton range experienced rapid cooling at ca 130 Ma (Krohne et al., 2016).

The geometry of the Lambert Rift is characteristic of two distinct structural orientations that dominate this sector of East Antarctica: one is aligned parallel to the early-spreading isochrons in the Cosmonauts Sea margin, and the other is aligned to the early-spreading isochrons of the Enderby Basin (Fig 14b). These structural orientations may be associated with much older events, and reactivation may have occurred in response to events associated with the opening of the Enderby Basin (130 – 115 Ma (Gibbons et al., 2013)) and the Cosmonauts Sea (<120 Ma (Jokat et al., 2010)), either separately, or due to strain-partitioning associated with contemporaneous rifting.

The impact of greater India rifting on the margin of Western Australia, at the time contiguous with East Antarctica, is more well defined, and may form a key template to understand East Antarctica. After the end of Permian-Triassic rifting, renewed subsidence of the Perth and Mentelle basins occurred from the mid-Jurassic to early Cretaceous, with the breakup phase associated with oblique northwest-southeast extension aligned with spreading in the Perth Abyssal Plain (Williams et al., 2013). Onshore structures for this period include dextral strike-slip on north-south oriented structures, en-echelon folding and sinistral motion on northwest-southeast transfer faults (Song & Cawood, 2000). The late Jurassic sedimentary fill of the Mentelle Basin suggests dominant detrital sources located in East Antarctica during this time, indicating active erosion of inland regions (Maritati et al., 2021). Following these a widespread Valanginian unconformity and eruption of the Bunbury Basalt at 137- 130 Ma (Olierook et al., 2016) mark breakup and

widespread uplift. The Perth Basin is continuous with the Knox and Aurora subglacial basins, which are structurally similar (Fig 14b).

In the mid-Cretaceous the oblique motion of Australia from Antarctica (Fig 14c) commenced at ca. 100 Ma, but this did not proceed to separation until 83 Ma (Williams et al., 2019). In contrast to Africa and India, Australia did not move away rapidly, with slow spreading persisting until ca. 45 Ma (Williams et al., 2019), and the Tasman Gateway was not opened until 33 Ma (Howie D. Scher et al., 2015). Spreading on this margin west of the George V fracture zone between 57-50 Ma may have been accommodated by sinistral transtension in East Antarctica and tectonic deepening of the Adventure and Astrolabe subglacial troughs (Eagles, 2019). The adjacent margins preserve the evolution of this post-rift system including, since the early Paleogene, a major influence from evolving glacial and oceanographic systems (De Santis et al., 2003; Escutia et al., 2005; K. Hochmuth et al., 2020; Sauermilch et al., 2019).

Initial east-west extension in the Ross Sea is interpreted with a broad basin developing between 105 and 83 Ma (Jordan et al., 2020). This phase of rifting in the Ross Sea is characterized by lower-crustal exhumation along low-angle detachment faults (Christine Smith Siddoway et al., 2004). Up to 100 km of diffuse extension may be accommodated on these shear zones (C.S. Siddoway, 2008), and this phase of extension is associated with crustal thinning and magmatism but not the development of major accommodation space (Lindeque, Gohl, Henrys, et al., 2016). The predominance of crustal thinning over basin development may have been a consequence of weak lower crust (Karner et al., 2005). This wide rift event has also been associated with a potential plateau collapse (Bialas et al., 2007). With separation of Zealandia at 83 Ma the translation of Marie Byrd Land trends towards the northwest and the rift system is interpreted to extend southward into the Siple Coast and Amundsen regions (Jordan et al., 2020), also evolving from a more diffuse wide-rift to a more focused narrow-rift mode, likely due to increasing rheological strength (Harry et al., 2018; Huerta & Harry, 2007). The opening of the Tasman Sea and Pacific-Antarctic Ridge from 83 Ma to 52 Ma accommodated the majority of the relative motion of Zealandia and the Pacific Plate relative to Antarctica (Gibbons et al., 2013). In the northern Ross Sea, opening of the Central Basin is interpreted between 61- 53 Ma (Fred J. Davey et al., 2021). From 52 Ma, the opening of the Macquarie Ridge and Adare Basin is associated with translation and rotation of Marie Byrd Land and the Eastern Basin, initially to the northeast, and then to the east (Fig 14).

4.5 Basin forming phase 4 – Eocene to Present

Post mid-Eocene, plate-tectonic motions in Antarctica were restricted to a few key areas. The western Ross Sea was in extension with corresponding seafloor spreading in the Adare Basin from 43 to 26 Ma, and also extension in the Terror Rift (F. J. Davey et al., 2016; Granot & Dyment, 2018). Although the amount of extension was limited, the effects on the bathymetry of the continental shelf, and the association with

volcanism, were important local drivers of basin evolution. Neogene rifting is interpreted to extend into the interior West Antarctica including the Bentley Subglacial Trough (Lloyd et al., 2015), Pine Island Rift (Jordan, Ferraccioli, Vaughan, et al., 2010), Byrd Subglacial Basin (W. Shen et al., 2018) and the Ferrigno Rift (Bingham et al., 2012). Tectonic subsidence through this period has occurred in the Ross, Siple Coast and Central West Antarctica regions (Fig 15) (Guy J. G. Paxman et al., 2019).

Subduction of the Aluk Plate (part of the Phoenix Plate) progressively ceased from south to north over time, as the West Antarctic-Aluk Ridge moved north and ultimately ceased subduction in the Neogene (Burton-Johnson & Riley, 2015). The evolution of a more complex margin to the north occurred in line with complex tectonics of the Scotia Sea (van de Lagemaat et al., 2021). This included the opening of the Powell (30-20 Ma) and Jane (18-14 Ma) basins in a back-arc setting, and the convergent South Shetland margin, comprising a fore-arc basin and accretionary prism (Maldonado et al., 1994), and since 4 Ma, rifting in the Bransfield Basin (Almendros et al., 2020). In the Eocene, tectonic processes occurring to the north of Antarctica remained important as the Drake Passage allowed throughflow by 42 Ma (H. D. Scher & Martin, 2006) and the Tasman Gateway by 33 Ma (Howie D. Scher et al., 2015). Through the Oligocene these gateways developed more fully (van de Lagemaat et al., 2021), allowing by the Miocene a fully-developed Antarctic Circumpolar Current.

Despite these regional tectonic events, by far the major influence on Antarctica's basin-forming processes in this period was the glacial influence as the ice sheet developed, with many cycles of advance and retreat causing major unconformities, substantial onshore erosion (Guy J. G. Paxman et al., 2019) and fluctuating sediment volumes deposited around the margins (Katharina Hochmuth & Gohl, 2019; Pérez et al., 2021). Understanding the resulting landscape of eroded basement regions, post-glacial sedimentary basins and the geomorphological features from both tectonic and glacial processes is essential to constrain the past, present and future behavior of the Antarctic Ice Sheet.

5 Implications for Antarctic Ice Sheet dynamics

5.1 Basin-associated processes and their potential impact on the cryosphere

Ice sheets and glaciers flow by three main mechanisms: internal ice deformation, basal sliding and deformation of basal material. The first of these is ubiquitous among ice masses, but the second and third are conditional on the presence of basal water. Furthermore, the third is dependent on the availability of deformable sediments at the bed. For water to exist beneath an ice sheet basal heat is needed: this can come from geothermal sources and, especially if ice flow is rapid, from basal motion and internal ice deformation. Thus, the dynamics of fast-flowing ice are dominated by basal-flow processes that allow speeds more than 50 m yr^{-1}, and often several 100 m yr^{-1}.

The availability of subglacial water is essential to both basal sliding and sediment deformation. In addition to ice-sheet melting, for a permeable bed we must consider the potential for water to be exchanged between the ice-sheet/bed interface, any actively deforming till layer, and the strata beneath which may tap deep groundwater reserves (Gustafson et al., 2022). The role of groundwater in subglacial hydrological systems is important to ice flow for two main reasons. The first reason is that groundwater comprises a source of water in addition to that melted from ice. For example, Christoffersen et al. (2014) suggest groundwater may contribute up to half of the water available beneath ice streams in the Siple Coast. The second reason is that groundwater flow allows heat to be transported vertically and laterally through the subglacial system (Gooch et al., 2016; Kulessa et al., 2019) thus representing a governing mechanism of advective heat transport to the ice-sheet base.

Hydraulic gradients in subglacial sedimentary basins vary over glacial cycles during the growth and decay of the ice sheet. This process has a positive feedback with ice sheet retreat and advance: as retreating ice sheets thin, unloading of the basin causes groundwater to be discharged into the subglacial system (Gooch et al., 2016; Li et al., 2022; Person et al., 2012). The opposite may occur when the ice sheet thickens, directing water away from the ice-sheet base and storing it in subglacial sedimentary basins (Gooch et al., 2016). In this manner, the groundwater system modulates interactions between basal water systems and the underlying sedimentary basins to exert control on the lubrication of the ice-sheet base and thus impact ice flow. Numerical modelling indicates that, even in situations of fast retreat, the rate of groundwater discharge can be of comparable magnitude to the expected basal-melt rate, and this feedback is likely to contribute substantially to ice-sheet dynamics (Li et al., 2022). Furthermore, past retreat and advance events can store 'fossil' hydraulic head in aquifers for later release (Gooch et al., 2016; Person et al., 2012).

From what we understand from formerly-glaciated regions (D. J. A. Evans et al., 2006) and from geophysical observations of subglacial Antarctica (Alley et al., 2021; Anandakrishnan et al., 1998; Christianson et al., 2016; A. Muto, Alley, et al., 2019; M. J. Siegert et al., 2016; A. M. Smith, 1997; A. M. Smith et al., 2013), the deformation of basal material is a dominant process within major ice streams and, consequently, exerts control on ice-sheet flow. InSAR depiction of surface-ice-flow velocities (Mouginot et al., 2019) and geophysical measurements of the subglacial system (Anandakrishnan et al., 1998; Brisbourne et al., 2017; Christianson et al., 2016; A. Muto, Alley, et al., 2019; Atsuhiro Muto et al., 2016; L. E. Peters et al., 2006; A. M. Smith et al., 2013; David G. Vaughan et al., 2003) allow us to pinpoint the onset of enhanced ice flow and the basal boundary conditions that permit it: for example, the onset of Whillans Ice Stream coincides with the availability of sedimentary material identified through aerogeophysical (Bell et al., 1998) and seismic (Anandakrishnan et al., 1998) data. The mechanics of subglacial sediment are complex and time variable, with hydration and fluid overpressure in general leading to weaker rheology while compaction and de-watering lead to stiffer rheology. This sensitivity to water supply can lead to relatively abrupt changes in flow

(Catania et al., 2012; Christoffersen et al., 2014; A. M. Smith et al., 2013). Meanwhile, sediment deposition in a grounding zone wedge and subsequent compaction associated with tidal loading may stabilize the grounding zone (Christianson et al., 2016). The deformation of the sediment commonly involves two layers: a relatively thin upper active zone, at most a few meters thick dilated by high-pressure water within pores that acts to reduce its material strength; and a thicker over-compacted basal unit that is stiffer and contributes little to flow (D. J. A. Evans et al., 2006).

Basal sediments originate from two main sources: accumulations of marine sediments deposited during previous times of deglaciation, and from the erosion of bedrock either locally or upstream. Recent marine deposits are likely to be present at lower elevations and will often be widespread, prompting zones of more continuous bed deformation (D. J. A. Evans et al., 2006). Without recent marine sediments, sediment supply must be sustained through glacial erosion, and this may be a limiting factor on till continuity. Glacial erosion is accomplished through a variety of processes, and these are fundamentally reliant on heterogeneities in the bedrock, including joints, especially their spacing and orientation (Hooyer et al., 2012), and lithological variations including competency contrasts, layer thicknesses, and structural orientation relative to flow (Krabbendam & Glasser, 2011; Lane et al., 2015). In comparison to the competent and massive structure more typical of igneous and metamorphic basement, sedimentary rocks provide more opportunities for quarrying to occur, and a higher likelihood of abrasion where the rocks are less competent (Krabbendam & Glasser, 2011). Finally, to sustain a continuous till layer, sediments eroded upstream must be transported, which is predominantly achieved via the subglacial-hydrology system, which, depending on erosion rate and water flux, may be supply-limited or transport-capacity limited (Delaney et al., 2019).

Both subglacial water and thin horizons of weak basal sediments may be present in areas of crystalline basement as well as in sedimentary-basin regions. Before considering basin settings, it is instructive to consider an ice-stream catchment with a structurally massive and impermeable bed throughout, such as a granite or gneiss bedrock. For such a bed we may consider as a priority the supply of basal water, which must be derived from basal melting and/or surface melting transported to the bed via fractures and moulins (Schoof, 2010). The latter, while certainly important, depends on surface-melting conditions that, for now, are limited to certain coastal regions of Antarctica, although they may be more widespread in the future (Tuckett et al., 2019). For the former, a sustained high flow-speed and/or geothermal heat flux is needed. With an impermeable bed, geothermal heat flux for a given location will be near constant, and so temporal variations in basal-melt rate will depend solely on ice-stream flow processes. In addition to water, sediment must be supplied through erosion of the crystalline basement, which is likely to be highly resistant to erosion (Krabbendam & Glasser, 2011) potentially restricting supply. We may now consider how the presence of a sedimentary bed influences ice-sheet dynamics.

Several factors associated with sedimentary-basin formation increase the likelihood that regions containing sedimentary basins will possess enhanced ice flow. These are: 1) a favorable source for sustained supply of sediment from more erodible bedrock and/or recent marine sediments (Bell et al., 1998); 2) the supply of subglacial water through groundwater discharge, tied to glacial unloading (Christoffersen et al., 2014; M. J. Siegert et al., 2018); 3) different organization of subglacial water systems including transitions between distributed and channelized flow, and flow routing between catchments (Christoffersen et al., 2014; Dustin M Schroeder et al., 2013); 4) the opportunity through groundwater circulation to advect heat from depth to the ice-sheet bed (Gooch et al., 2016). In addition, the tendency for basin-dominated regions to possess relatively smooth topography at all scales promotes ice-stream boundaries defined by ice-sheet dynamics, including basal processes (Catania et al., 2012). Finally, we may consider the effects of ongoing basin-forming processes on the morphology of ice-shelf cavities that are critical for ice-sheet stability (J. A. Smith et al., 2019).

5.2 Antarctic sedimentary basins and ice sheet dynamics

Although the specifics of when, where and how sedimentary basins have influenced ice-sheet dynamics in Antarctica remain to be defined, the mechanisms listed above are enhanced in catchments containing sedimentary basins. Consequently, we may consider if the presence of subglacial sedimentary basins within a glacial catchment is associated with more dynamic behaviour, and if this impact on ice-sheet dynamics may be expressed for the modern-day ice sheet.

Sedimentary basins are an important modulating influence on geothermal heat flux (GHF) and can act either to inhibit or enhance surface GHF. In Antarctica, the overall statistical relationship with heat flux from deep-seated sources (Lösing & Ebbing, 2021) is almost null for Type 1 basins relative to crystalline basement, although Type 2 basins are systematically associated with lower GHF (small effect size). In West Antarctica, where heat flux is generally high, higher heat flux is found within basin regions (Fig 16a). These regions include the Siple Coast with highest high heat flux in the south, but less to the north. Extending from the Byrd Subglacial Basin to the Ferrigno Rift is an elevated high heat flux region, with concentrations beneath basins including the Byrd Subglacial Basin and the Pine Island Rift Basin. Tectonically-active regions including the Terror Rift and the Bransfield Strait region have high heat flux relative to tectonically older regions such as the Weddell Sea that have more moderate heat flux (Fig 16a). Variations in heat flux in East Antarctica are not clearly associated with basins except for the tendency for very low GHF to occur only in areas without Type 1 basins. Selected basins, including the Foundation Basin, South Pole Basin, the Northern Wilkes Basin, and the Prydz Bay Basin show elevated heat flux relative to their surrounding areas. In contrast the Aurora-Vincennes and southern Wilkes subglacial basins show reduced heat flux relative to their surrounding areas. The large-scale heat flux shown here represents the crustal and lithospheric structure beneath the basin and, excepting volcanism, is a stable boundary condition for ice-sheet dynamics. The time-variable influence

of basins on heat flux at the bed is likely to be substantial where fluid circulation is coupled with a high thermal gradient, and fluid conduits such as deformation zones are also important (Tankersley et al., 2022).

Fast flowing ice, as defined by surface-ice velocity (Mouginot et al., 2019) has overall only a weak spatial association with the presence of basins (Fig 16b). Type 1 basins have a higher average velocity (24 m yr^{-1}) than either crystalline bed (19 m yr^{-1}) or Type 2 basins (11 m yr^{-1}), but with very small effect size given the large spatial variability in velocity ($\sigma \approx 70$ m yr^{-1}). However, although many of Antarctica's fastest-flowing glaciers flow over crystalline bedrock or a mixed bed, many of these possess sedimentary basins preserved in the upper catchment (Fig 16b).

The slipperiness at the ice-bed interface is expressed by the basal-friction coefficient, which relates basal sliding velocity to basal shear stress. It is a direct measure of the subglacial environment and encapsulates the effect of both subglacial water and deformable sediment. The model-inferred basal-friction coefficient is generally lower where there is fast-flowing ice and higher near topographic divides, but also may associate with the presence of basins (Fig 16c). The model-inferred basal-friction coefficient is closely correlated with the basin distribution, with a mean for Type 1 basins of 93 (Pa yr/m)$^{1/2}$ contrasting with a mean of 127 and 134 (Pa yr/m)$^{1/2}$ in crystalline basement and Type 2 basins respectively. Overall, this relationship has a medium effect size given regional variability ($\sigma \approx 70$ (Pa yr/m)$^{1/2}$).

Basal-friction coefficient is related to basin coverage in several ways. In several ice-stream systems, sedimentary basins occur in the fast-flowing lower catchment and low basal-friction coefficient is seen. Examples include Mercer and Whillans; MacAyeal and Bindschadler; and Institute ice streams draining the West Antarctic Ice Sheet and Academy and Support Force; Jutulstraumen; West and Central Ragnhild; and Cook ice streams draining the East Antarctic Ice Sheet. Often however for major catchments ice in the fast-flowing lower catchment flows over a crystalline or mixed bed, with the basin confined to the upper catchment, the downstream part having been eroded (A.R.A. Aitken et al., 2016; G. J. G. Paxman et al., 2017). Examples include Thwaites and Pine Island; Recovery and Slessor; Lambert, Mellor and Fisher; Denman and Scott; Totten and the ice streams draining from the southern Wilkes Subglacial Basin through the Transantarctic Mountains including Byrd, Skelton and David glaciers. For these ice streams, low basal-friction coefficient extends far into the sedimentary-basin region despite the surface velocity being relatively slow, suggesting that basal sliding can propagate into the upstream basin. A final relationship is that for slow-moving ice such as at Kamb Ice Stream, and at drainage divides (e.g. for South Pole), we see basin regions associated with moderate to high basal-friction coefficient, indicating that basal sliding is limited.

We may also review the association of basins with the subglacial-hydrology system (Fig 16d). Subglacial lakes are found throughout Antarctica (Livingstone et al., 2022) and occur across all bed classes. Of 675 lakes, 260 (39%) occur over crystalline bedrock, while 239 (35%) occur over Type 1 basins, and 114 (17%) over Type 2

basins. For comparison, the area taken up by these bed classes is 40%, 47% and 8% respectively. Furthermore, of 140 hydraulically-active lakes we find 96 (69%) occur over Type 1 basins, while of 502 stable lakes only 137 occur over this class (27%.). This represents a tendency for stable lakes to occur close to ice divides, while active lakes occur more frequently towards the ice-sheet margins (Livingstone et al., 2022). Besides subglacial lakes, basal-fluid flux is driven by hydraulic-potential gradients from the high-potential divides towards the ice sheet margins. These networks do not necessarily follow the same flow-routing as the ice and can cross boundaries to ice flow (Fig 16d). Unless the ice-sheet-surface slope is steep and oriented transverse to the bed slope, the subglacial water flux will be preferentially concentrated into topographic basins and form highly dynamic flow networks (Dow et al., 2022; Le Brocq et al., 2013), and so there is a natural association of high-volume subglacial water flux and sedimentary basins (Fig 16d). Several notable examples include the Recovery Lakes that overlie the Recovery Basin with flow directed towards Recovery Glacier; the Pensacola-Pole Basin with flow directed to Academy and Support Force glaciers; and the Byrd Subglacial Basin with flow directed towards Thwaites Glacier. Lake Vostok drains into the Wilkes Subglacial Basin, and from there flow is directed towards Cook Glacier, and also through the Transantarctic Mountains. Finally, Dome C has flow directed into the Aurora Subglacial Basin and from there towards Vanderford Glacier.

At Thwaites Glacier, the transition from distributed to channelized flow may be correlated to the change from sedimentary basin to crystalline bed (Dustin M Schroeder et al., 2013) and bed-type transitions in other catchments (Fig 16d) may also be critical thresholds for the hydrology system. The interaction of high-flux hydrology networks, including active lakes, with higher-permeability sedimentary beds is fundamental to the subglacial hydrology of Antarctica and may exert a critical influence on ice-sheet dynamics. An important consideration is where subglacial hydrology follows different routing to the ice flow: ice retreat and unloading in one catchment, along with increased basal melting, may enhance water flux that is potentially routed into another catchment, and so may help propagate dynamic behavior from one catchment to another (Wright et al., 2008). In some regions, high sensitivity to variable subglacial-hydrology network structure may lead to cross-catchment vulnerabilities and the propagation of dynamic behavior between ice streams (Alley et al., 1994; D. G. Vaughan et al., 2008; Wright et al., 2008).

The preceding discussion indicates associations between the presence of sedimentary basins and enhanced ice-sheet flow. In a sedimentary-basin setting, this sliding may occur in deformable till layers facilitated by more extensive basal till and from hydrogeological processes that may provide substantial amounts of subglacial water. Enhanced groundwater discharge to the bed is associated with additional feedbacks, including heat advection within the basin and temporally-variable water discharge and recharge coupled with ice unloading and loading histories. The expected groundwater response includes an ongoing long-term response from deep aquifers activated by unloading since Last Glacial Maximum, and shorter-term

responses from shallower aquifers activated by more recent mass loss (Christoffersen et al., 2014; Gustafson et al., 2022; Li et al., 2022).

A substantial role for subglacial sedimentary basins in governing the basal conditions of the ice sheet is well supported by both models and data, but a well-defined relationship between subglacial sedimentary basins and ice-sheet flow remains elusive, with many cross-associations with other boundary conditions and complex time- and space-variable interactions. In particular, the potential effects of these basin-facilitated processes on large scale glacial flow are yet to be systematically assessed.

6 Future directions in Antarctic Subglacial Sedimentary Basins research

Knowledge of sedimentary basins beneath the Antarctic Ice Sheet has expanded greatly in recent decades, and key concepts relating to their influence on ice-sheet dynamics have been identified. Despite this, for a full realization of their value for understanding global tectonics, paleolandscape evolution and the dynamic behavior of ice sheets with changing climate, there is a pressing need to continue to progress several key themes.

6.1 Sedimentary basin definition and characterization

Despite substantial recent advances, mapping the presence of sedimentary rocks beneath thick ice remains a significant challenge. The more widely available datasets from airborne geophysics can provide a strong indication of the presence of a sedimentary basin, subject to certain ambiguities.

Small-scale variations in the solid earth, for example geothermal heat flux (McCormack et al., 2022) and topography (E. J. MacKie et al., 2020) may have large impacts on ice-sheet dynamics. For consistent mapping at a continent scale, improved coverage is needed to fill remaining data gaps, and to improve data quality in areas with, low resolution, less accurate or poorly geolocated data. The newest topographic compilation, Bedmap3 ,(Frémand, Fretwell, et al., 2022) is based on a 500m along-line resolution. Taking this as a benchmark, we consider the requirements for airborne data to resolve subglacial geology at this resolution. To maximize non-aliased signal, magnetic intensity data should be collected with a line-separation comparable to the source-sensor separation (Reid, 1980). Gravity data may be more widely separated without loss of non-aliased signal. In much of Antarctica, due to thick ice, the source-sensor separation is several kilometers, and sothere is little gain from closely-spaced magnetic and gravity surveys. Regions with thinner ice may benefit in principle but are limited by several additional factors, in particular a.irborne gravity systems require along-line data filtering that, for most fixed-wing platforms, limit along-line resolutions to 5-10 kilometers wavelength.

RES has no similar physical limitation on resolution and the bed can be sampled at fine scales along lines. Fine-scale along-line sampling allows for sub-survey resolution data products to be generated in 2D using

physical and/or statistical techniques (Frémand, Fretwell, et al., 2022; E. J. MacKie et al., 2020; Mathieu Morlighem et al., 2020). The need for closely-spaced RES data depends on the characteristics of the ice-sheet bed and the ice-sheet flow, and a variable radar line-spacing of 500 to 2.5 km across the continent is likely to improve the fidelity of bed-topography data products across all scales. Across all airborne data types, finer resolution demands a reduced aircraft velocity, for which helicopter surveys are one solution (Wei et al., 2020), or alternatively, slow-flying UAVs are an emerging technology for practical deployment in the future (Teisberg et al., 2022). Ship-based airborne operations may also allow surveys to reach coastal data gaps where onshore infrastructure is not available.

Ground-based geophysical-data collection, including active- and passive-seismic and magnetotelluric methods, remains limited in Antarctica and it is a significant challenge to achieve a systematic continent-wide coverage. Large-scale passive-seismic deployments, with stations spaced tens of kilometers apart or more, have been used with success to image the nature of the crust and the mantle including basins (W. Shen et al., 2018; Zhou et al., 2022). The current network of passive-seismic stations, mostly in West Antarctica (Fig 1), could feasibly be expanded to a continent-scale network with accompanying magnetotelluric data within a manageable logistical footprint. Smaller-scale deployments with station spacings of kilometers are capable of imaging the ic bedgeology conditions for individual ice streams and are fundamental to understanding the impact of sedimentary basins on ice sheet dynamics Active-(Anandakrishnan & Winberry, 2004; Gustafson et al., 2022; L. E. Peters et al., 2006). Active seismic experiments remain resource-intensive and logistically challenging although the implementation of vibrator sources and snow-streamer technologies is a substantial step forward to increase the efficiency, resolution and accuracy of data collection but an(Eisen et al., 2015). These more intensive approaches initially may be targeted towards key catchments, however expanded deployment of these technologies would be of immense benefit to understanding geologic bed conditions for ice dynamics.

Finally, it is necessary to enhance capability for field verification of bed characteristics to inform and constrain geophysical observations. Several initiatives are under way to develop further drilling technologies to access the subglacial geology, including systems designed with differing logistical footprints and with different capacity to reach the bed through thick ice (Gong et al., 2019; J. W. Goodge et al., 2021; Hodgson et al., 2016; Kuhl et al., 2021; Talalay et al., 2021). Maintaining strong engagement with ice-coring and hot-water-drilling communities is desirable to synergize efforts where feasible. In the context of basins research, and the study of their interactions with glacial systems, a critical problem remains that representative samples are likely to be found under thick and especially wet-based ice, for which drilling technologies are not yet optimized. The capacity to recover long stratigraphic cores is of particular value to basins research.

As well as the detection of basins, we may seek to better define the geometry of basins, including their thickness and overall morphology but also their internal structure. Defining the thickness of Antarctica’s

sedimentary basins is a clear next step that demands a new approach able to combine multiple diverse datasets so that all are accommodated in the problem formulation, and so the solution. Also important are faults and stratigraphy, which provide critical controls on fluid flow within the basins. Consequently, these dictate the hydrogeological response to changing glacial load and so advective heat transport to the ice-sheet bed (Tankersley et al., 2022). The sensitivity of gravity and magnetic data to internal basin structure may be limited by density and magnetization contrasts between sedimentary rocks which are relatively low in comparison to the contrast with the basement and other features such as intrusions and volcanic rocks. While passive-seismic and magnetotelluric data provide some additional constraints, active-seismic data have in other regions proved most effective for developing a good appreciation of intra-basin structure.

Finally, while the physical properties of the basins, including density, seismic velocity and its anisotropy, electrical conductivity and other characteristics may be defined from geophysical data, to define their relationship with ice-sheet dynamics it is necessary to translate these into mechanical and hydrogeological properties. A particular challenge is to define topological properties defined largely by orientations and connections (e.g. permeability, stratigraphic layering and its orientation, fracture density and orientation) that have most bearing on both the hydrogeological system (Person et al., 2012) and also the erodibility of sedimentary bedrock (Krabbendam & Glasser, 2011; Lane et al., 2015).

6.2 Sedimentary basins as a record of glacial change

A profound quality of sedimentary basins is their capacity to record sensitively the conditions of their formation which provides knowledge of tectonic and surface processes, and past ice, ocean, and climate conditions. Sampling of sedimentary records from basins provides key benchmarks and constraints on the behavior of the ice sheet in the past, which supports an improved capacity to define ice-sheet dynamic processes in models of potential future ice-sheet change. While many studies have investigated the Antarctic margin, these studies remain limited in extent and are clustered in a few areas (Fig 1). With dynamic instabilities dominating catchment-scale ice-stream behavior, more comprehensive coverage is required to understand the dynamic response of the Antarctic Ice Sheet logistically-sheet to changing climate. Innovative approaches to marine drilling (e.g. K. Gohl et al., 2017) may allow more agile, safer and less logistically demanding investigations.

In addition to obtaining records of changing conditions from drill cores, spatial patterns of erosion and sedimentation are closely linked to past glacial cycles (Anderson et al., 2019; K. Hochmuth et al., 2020; Pérez et al., 2021) and can be used to understand systematic instabilities within catchments (A.R.A. Aitken et al., 2016). The structure of sedimentary basins can be used for the reconstruction of paleo-landscapes, offshore and onshore, which is important for understanding the long-term stability of the ice-sheet structure (K. Hochmuth et al., 2020; S. S. Jamieson et al., 2010; Guy J. G. Paxman et al., 2019). Paleotopographic

reconstruction is also critical in the effort to model past ice-sheet behavior with realistic topographic and basal boundary conditions, rather than relying on modern-day formulations (Katharina Hochmuth & Gohl, 2019; Guy J. G. Paxman et al., 2020). An important factor here is not just the reconstruction of topographic elevation, but also the changing geology of the ice-sheet bed through time.

6.3 Understanding cryosphere interactions

While the fundamental principles of the interactions between sedimentary basins, sediments and water at the ice-sheet bed and ice-sheet flow have been known for some time ,(Alley et al., 1987; Bell et al., 1998; Blankenship et al., 1986; Christoffersen et al., 2014) their overall role in controlling Antarctic Ice Sheet dynamics remains ill-defined. Knowledge of these interactions in Antarctica is growing, but it is evident that much further work needs be done to provide a systematic understanding of how these complex boundary conditions interact with the ice sheet to focus, enhance, inhibit or otherwise influence glacial-change processes associated with a warming climate (Kennicutt et al., 2019).

Hydrogeologic interactions of sedimentary basins with subglacial hydrology and the cryosphere are understood largely through model studies (Christoffersen et al., 2014; Gooch et al., 2016; Li et al., 2022) and through studies of the former Northern H hemisphere ice sheets (Person et al., 2007). It is not clear yet how these model concepts may translate to Antarctic conditions, and a robust and Antarctic-specific understanding of their role in the dynamics of the Antarctic Ice Sheet is a core challenge requiring both targeted model studies and expanded observations of the bed. Critical concepts to be defined further include the role of sedimentary basins for sustaining subglacial water supply, and the interactions of aquifer systems with subglacial lakes and hydrological flow organization on different timescales. Understanding how Antarctica's aquifers respond to a changing ice sheet may be an essential factor in understanding their vulnerability in retreat, as the release of water during glacial unloading, if substantial, could be a critical positive feedback promoting accelerated ice-sheet flow (Schoof, 2010) and also ice-shelf destabilization (Le Brocq et al., 2013).

Sedimentary basins are an important factor in controllinggeothermal heat flux, firstly through the tendency to insulate the crust beneath, leading to warmer conditions beneath and secondly, through efficiently that may further enhance meltingice-the capacity for fluid circulation within the basin to efficiently transport heat from depth to the surface, also potentially accessing saline waters (Gustafson et al., 2022). Heat advection is especially important as a positive feedback associated with ice sheet unloading (Gooch et al., 2016). Essential concepts to be defined further include mapping temperature gradients, water contents and salinity within basins, as well as the association of these with high ambient temperatures associated with rifting, magmatism, or high crustal heat production. Perhaps the most limiting factor is the identification of

the internal basin structure, and so the necessary conduits for fluid circulation, their orientation and connectivity.

A sustained supply of flow-capable sediment is an important factor enabling sustained fast ice-sheet flow. This requires either a base of marine sediments, deposited during a past retreat, or a reliably erodible bedrock. In the latter case, while the presence of the sedimentary bed is known to be an important condition, studies of formerly-glaciated regions show there is a high degree of sensitivity to the nature of the sedimentary rocks, including the dip and strike of the strata, bedding-layer thicknesses, the competency of the different lithologies, and the intensity and spacing of joints and other fractures (Hooyer et al., 2012; Krabbendam & Glasser, 2011; Lane et al., 2015). Characterization of these fine-scale details in a subglacial setting is problematic in the absence of high-resolution data, however, an understanding of the depositional setting, large-scale structure and broad lithology variations within basins may allow these factors to be assessed in a probabilistic sense bearing in mind analogues from formerly glaciated regions.

6.4 Coupling mapping with ice-sheet models for predictive capacity

A major frontier for basins research in Antarctica is the coupling of the knowledge of subglacial geology with ice-sheet models to understand the influence of bed conditions on basal processes and to enable better predictions of sea level change and other impacts on ocean and climate. The first challenge in doing so is the identification of the basin characteristics and processes that are most relevant to dynamic ice-sheet behavior: in particular we may wish to understand more precisely the influence of basin location within the catchment relative to the grounding zone, the effects of variable basin thickness, and variations at different scales of properties such as porosity, lithology, permeability, structural orientation and mechanical erodibility. Incorporating representations of these factorsin ice-sheet models may be enabledin the future through inclusion of adaptive sliding laws and better coupled hydrology and hydrogeology modelling.

Other challenges include the successful representation in ice-sheet models of evolving sedimentary systems under ice, including spatially-variable and anisotropic bedrock erosion, the re-distribution of subglacial sediments through subglacial sediment transport and time-variable subglacial hydrology on ice-sheet flow, water outflux and sediment deposition on ice shelves and their cavities. Many ice-sheet models are now able to accommodate at least some of these processes in parameterized forms, allowing their influence to be assessed alongside other processes (e.g. Delaney et al., 2019; Lowry et al., 2020; Pollard & DeConto, 2020).

7 Conclusion

The presence of sedimentary basins in Antarctica, their potential impact on ice-sheet dynamics, and their ability to record change has long been known. Except in some regions with access to outcrops and/or ship-based science, a comprehensive understanding has been lacking due to ice cover and remoteness restricting access. In recent years, the geophysical community has developed improved approaches to characterize

subglacial geology, through improved equipment and data collection, and advances in data processing and analysis targeted to the unique environment of Antarctica. Large amounts of data have been collected, and crucially these are readily available to the broader community in compilations at continent-scale. Numerical data-analysis techniques including machine learning are providing advanced capability to map the distribution of sedimentary basins.

Key outcomes from the growing understanding of Antarctica's sedimentary basins are the definition of feedbacks with ice-sheet processes that have the capacity to influence the future Antarctic Ice Sheet, in particular through the potential supply of increased water and heat to the ice-sheet bed as a consequence of retreat. Around the continent, a system-level understanding is emerging that connects subglacial processes at the ice-sheet bed to marine-depositional systems (K. Hochmuth et al., 2020; Guy J. G. Paxman et al., 2019; Pollard & DeConto, 2020). A persistent finding beneath the ice sheet, on the continental shelf, and beyond, is that glacial processes are the dominant factor in the development of Antarctica's sedimentary basins since at least the Eocene, signifying the dynamic nature of the Antarctic Ice Sheet (Noble et al., 2020).

Despite the progress made it is notable that the records we havefor Antarctica are, relative to many other parts of the world, very limited in their distribution, resolution and scope. Across all data, critical gaps remain in our coverage of Antarctica's basins, and, due to high logistical thresholds, data redundancy and repeatability are often low. There is a critical need to define in expanded form the importance of subglacial sedimentary basins for controlling dynamic ice-sheet flow, especially to characterize the feedbacks and instabilities that may dictate the response of Antarctica's ice sheet to changing climate. Finally, it is essential that these findings are incorporated in numerical ice-sheet models to underpin a better predictive capacity for future ice-sheet change.

8 Acknowledgements

This work rests upon an enormous body of knowledge, and we thank all who have contributed to the acquisition, processing, analysis and modelling of data and to providing a rich base of interpretations to draw on. We thank a broad range of collaborators for conversations that helped to develop the manuscript, including Pippa Whitehouse, Jamin Greenbaum and Katharina Hochmuth. We thank the Editorial Board for the invitation for this review article. Reviews from Fausto Ferraccioli and an anonymous reviewer, and editorial comments from Associate Editor Rob Bingham helped to improve the manuscript. The authors acknowledge funding support from the following bodies Australian Research Council Special Research Initiative, Australian Centre for Excellence in Antarctic Science (Project Number SR200100008). China Scholarship Council–The University of Western Australia joint Ph.D. scholarship (201806170054). Natural Environment Research Council grants NE/S006621/1, NE/R010838/1 NE/G013071/2, NE/F016646/2. British

Antarctic Survey Palaeo Environments, Ice Sheets and Climate Change team. National Science Foundation Graduate Research Fellowship under Grant No. DGE-1656518.

9 Open Research

The map of Antarctic sedimentary basins as presented here (version 1.04) is available in GIS-ready format from the Zenodo repository [https://doi.org/10.5281/zenodo.7984586]. An updateable version for ongoing community development is available from GitHub [https://github.com/LL-Geo/AntarcticBasins/tree/main] or Zenodo [https://doi.org/10.5281/zenodo.7955584]. Data used in mapping are available from sources as cited in text.

10 References

Aitken, A. R. A., Betts, P. G., Young, D. A., Blankenship, D. D., Roberts, J. L., & Siegert, M. J. (2016). The Australo-Antarctic Columbia to Gondwana transition. *Gondwana Research, 29*(0), 136-152. https://doi.org/10.1016/j.gr.2014.10.019

Aitken, A. R. A., Occhipinti, S. A., Lindsay, M. D., & Trench, A. (2018). A role for data richness mapping in exploration decision making. *Ore Geology Reviews, 99*, 398-410. https://doi.org/10.1016/j.oregeorev.2018.07.002

Aitken, A. R. A., Ramos, L. N., Roberts, J. L., Greenbaum, J. S., Jong, L. M., Young, D. A., & Blankenship, D. D. (2020). A Magnetic Data Correction Workflow for Sparse, Four-Dimensional Data. *Journal of Geophysical Research: Solid Earth, 125*(10). https://doi.org/10.1029/2020jb019825

Aitken, A. R. A., Roberts, J. L., Van Ommen, T. D., Young, D. A., Greenbaum, J. S., Blankenship, D. D., & Siegert, M. J. (2016). Repeated large-scale retreat and advance of Totten Glacier indicated by inland bed erosion. *Nature, 533*, 385-389. https://doi.org/10.1038/nature17447

Aitken, A. R. A., Young, D. A., Ferraccioli, F., Betts, P. G., Greenbaum, J. S., Richter, T. G., et al. (2014). The subglacial geology of Wilkes Land, East Antarctica. *Geophysical Research Letters, 41*(7), 2390-2400. https://doi.org/10.1002/2014gl059405

Allen, P. A., Eriksson, P. G., Alkmim, F. F., Betts, P. G., Catuneanu, O., Mazumder, R., et al. (2015). Chapter 2 Classification of basins, with special reference to Proterozoic examples. *Geological Society, London, Memoirs, 43*(1), 5-28. https://doi.org/10.1144/m43.2

Alley, R. B., Anandakrishnan, S., Bentley, C. R., & Lord, N. (1994). A water-piracy hypothesis for the stagnation of Ice Stream C, Antarctica. *Annals of Glaciology, 20*, 187-194. https://doi.org/10.3189/1994AoG20-1-187-194

Alley, R. B., Blankenship, D. D., Bentley, C. R., & Rooney, S. T. (1987). Till beneath ice stream B: 3. Till deformation: Evidence and implications. *Journal of Geophysical Research: Solid Earth, 92*(B9), 8921-8929. https://doi.org/10.1029/JB092iB09p08921

Alley, R. B., Holschuh, N., MacAyeal, D. R., Parizek, B. R., Zoet, L., Riverman, K., et al. (2021). Bedforms of Thwaites Glacier, West Antarctica: Character and Origin. *Journal of Geophysical Research: Earth Surface, 126*(12). https://doi.org/10.1029/2021jf006339

Almendros, J., Wilcock, W., Soule, D., Teixidó, T., Vizcaíno, L., Ardanaz, O., et al. (2020). BRAVOSEIS: Geophysical investigation of rifting and volcanism in the Bransfield Strait, Antarctica. *Journal of South American Earth Sciences, 104*, 102834. https://doi.org/10.1016/j.jsames.2020.102834

Ammon, C. J. (1991). The isolation of receiver effects from teleseismic P waveforms. *Bulletin - Seismological Society of America, 81*(6), 2504-2510. https://doi.org/10.1785/BSSA0810062504

An, M., Wiens, D. A., Zhao, Y., Feng, M., Nyblade, A. A., Kanao, M., et al. (2015). S-velocity model and inferred Moho topography beneath the Antarctic Plate from Rayleigh waves. *Journal of Geophysical Research: Solid Earth, 120*(1), 2014JB011332. https://doi.org/10.1002/2014JB011332

Anandakrishnan, S., Blankenship, D. D., Alley, R. B., & Stoffa, P. L. (1998). Influence of subglacial geology on the position of a West Antarctic ice stream from seismic observations. *Nature, 394*(6688), 62-65. https://doi.org/10.1038/27889

Anandakrishnan, S., Voigt, D. E., Burkett, P. G., Long, B., & Henry, R. (2000). Deployment of a broadband seismic network in West Antarctica. *Geophysical Research Letters, 27*(14), 2053-2056. https://doi.org/10.1029/1999GL011189

Anandakrishnan, S., & Winberry, J. P. (2004). Antarctic subglacial sedimentary layer thickness from receiver function analysis. *Global and Planetary Change, 42*(1-4), 167-176. https://doi.org/10.1016/j.gloplacha.2003.10.005

Anderson, J. B., Simkins, L. M., Bart, P. J., De Santis, L., Halberstadt, A. R. W., Olivo, E., & Greenwood, S. L. (2019). Seismic and geomorphic records of Antarctic Ice Sheet evolution in the Ross Sea and controlling factors in its behaviour. *Geological Society, London, Special Publications, 475*(1), 223-240. https://doi.org/10.1144/sp475.5

Armadillo, E., Ferraccioli, F., Tabellario, G., & Bozzo, E. (2004). Electrical structure across a major ice-covered fault belt in Northern Victoria Land (East Antarctica). *Geophysical Research Letters, 31*(10). https://doi.org/10.1029/2004GL019903

Arndt, J. E., Hillenbrand, C. D., Grobe, H., Kuhn, G., & Wacker, L. (2017). Evidence for a dynamic grounding line in outer Filchner Trough, Antarctica, until the early Holocene. *Geology, 45*(11), 1035-1038. https://doi.org/10.1130/G39398.1

Arnold, E., Leuschen, C., Rodriguez-Morales, F., Li, J., Paden, J., Hale, R., & Keshmiri, S. (2020). CReSIS airborne radars and platforms for ice and snow sounding. *Annals of Glaciology, 61*(81), 58-67. https://doi.org/10.1017/aog.2019.37

Bailey, J. T., Evans, S., & Robin, G. D. Q. (1964). Radio echo sounding of polar ice sheets. *Nature, 204*(4957), 420-421. https://doi.org/10.1038/204420a0

Bamber, J. L., Ferraccioli, F., Joughin, I., Shepherd, T., Rippin, D. M., Siegert, M. J., & Vaughan, D. G. (2006). East Antarctic ice stream tributary underlain by major sedimentary basin. *Geology, 34*(1), 33-36. https://doi.org/10.1130/G22160.1

Baranov, A., Morelli, A., & Chuvaev, A. (2021). ANTASed – An Updated Sediment Model for Antarctica. *Frontiers in Earth Science, 9*. https://doi.org/10.3389/feart.2021.722699

Bart, P. J. (2003). Were West Antarctic ice sheet grounding events in the Ross Sea a consequence of East Antarctic ice sheet expansion during the middle Miocene? *Earth and Planetary Science Letters, 216*(1-2), 93-107. https://doi.org/10.1016/S0012-821X(03)00509-0

Bart, P. J., Anderson, J. B., Trincardi, F., & Shipp, S. S. (2000). Seismic data from the Northern basin, Ross Sea, record extreme expansions of the East Antarctic Ice Sheet during the late Neogene. *Marine Geology, 166*(1-4), 31-50. https://doi.org/10.1016/s0025-3227(00)00006-2

Batchelor, C. L., Montelli, A., Ottesen, D., Evans, J., Dowdeswell, E. K., Christie, F. D. W., & Dowdeswell, J. A. (2020). New insights into the formation of submarine glacial landforms from high-resolution Autonomous Underwater Vehicle data. *Geomorphology, 370*. https://doi.org/10.1016/j.geomorph.2020.107396

Beaman, R. J., O'Brien, P. E., Post, A. L., & De Santis, L. (2011). A new high-resolution bathymetry model for the Terre Adélie and George V continental margin, East Antarctica. *Antarctic Science, 23*(1), 95-103. https://doi.org/10.1017/S095410201000074X

Behrendt, J. C., Meister, L., & Henderson, J. R. (1966). Airborne geophysical study in the Pensacola Mountains of Antarctica. *Science, 153*(3742), 1373-1376. https://doi.org/10.1126/science.153.3742.1373

Bell, R., Small, C., & Arko, R. (1999). Development of a new generation gravity map of Antarctica: ADGRAV Antarctic Digital Gravity Synthesis. *Annali di Geofisica, 42*. https://doi.org/10.4401/ag-3720

Bell, R. E., Blankenship, D. D., Finn, C. A., Morse, D. L., Scambos, T. A., Brozena, J. M., & Hodge, S. M. (1998). Influence of subglacial geology on the onset of a West antarctic ice stream from aerogeophysical observations. *Nature, 394*(6688), 58-62. https://doi.org/10.1038/27883

Bell, R. E., Childers, V. A., Arko, R. A., Blankenship, D. D., & Brozena, J. M. (1999). Airborne gravity and precise positioning for geologic applications. *Journal of Geophysical Research: Solid Earth, 104*(B7), 15281-15292. https://doi.org/10.1029/1999jb900122

Bentley, C. R., Crary, A. P., Ostenso, N. A., & Thiel, E. C. (1960). Structure of West Antarctica. *Science, 131*(3394), 131-136. https://doi.org/10.1126/science.131.3394.131

Bialas, R., Buck, R., Studinger, M., & Fitzgerald, P. (2007). Plateau collapse model for the Transantarctic Mountains--West Antarctic Rift System: Insights from numerical experiments. *Geology, 35*, 687-690. https://doi.org/10.1130/G23825A.1

Bienert, N. L., Schroeder, D. M., Peters, S. T., MacKie, E. J., Dawson, E. J., Siegfried, M., et al. (2022). Post-Processing Synchronized Bistatic Radar for Long Offset Glacier Sounding. *IEEE Transactions on Geoscience and Remote Sensing*, 1-1. https://doi.org/10.1109/tgrs.2022.3147172

Bingham, R. G., Ferraccioli, F., King, E. C., Larter, R. D., Pritchard, H. D., Smith, A. M., & Vaughan, D. G. (2012). Inland thinning of West Antarctic Ice Sheet steered along subglacial rifts. *Nature, 487*(7408), 468-471. https://doi.org/10.1038/nature11292

Bingham, R. G., & Siegert, M. J. (2007). Radar-derived bed roughness characterization of Institute and Möller ice streams, West Antarctica, and comparison with Siple Coast ice streams. *Geophysical Research Letters, 34*(21). https://doi.org/10.1029/2007GL031483

Bingham, R. G., & Siegert, M. J. (2007). Radio-echo sounding over polar ice masses. *Journal of Environmental and Engineering Geophysics, 12*(1), 47-62. https://doi.org/10.2113/jeeg12.1.47

Bingham, R. G., & Siegert, M. J. (2009). Quantifying subglacial bed roughness in Antarctica: implications for ice-sheet dynamics and history. *Quaternary Science Reviews, 28*(3), 223-236. https://doi.org/10.1016/j.quascirev.2008.10.014

Blankenship, D. D., Bentley, C. R., Rooney, S., & Alley, R. B. (1986). Seismic measurements reveal a saturated porous layer beneath an active Antarctic ice stream. *Nature, 322*(6074), 54-57. https://doi.org/10.1038/322054a0

Boger, S. D. (2011). Antarctica — Before and after Gondwana. *Gondwana Research, 19*(2), 335-371. https://doi.org/10.1016/j.gr.2010.09.003

Bohoyo, F., Galindo-Zaldívar, J., Maldonado, A., Schreider, A. A., & Surinach, E. (2002). Basin development subsequent to ridge-trench collision: The Jane Basin, Antarctica. *Marine Geophysical Research, 23*(5-6), 413-421. https://doi.org/10.1023/b:mari.0000018194.18098.0d

Bowman, V., Ineson, J., Riding, J., Crame, J., Francis, J., Condon, D., et al. (2016). The Paleocene of Antarctica: Dinoflagellate cyst biostratigraphy, chronostratigraphy and implications for the palaeo-Pacific margin of Gondwana. *Gondwana Research, 38*, 132-148. https://doi.org/10.1016/j.gr.2015.10.018

Bradshaw, M. A. (2013). The Taylor Group (Beacon Supergroup): the Devonian sediments of Antarctica. *Geological Society, London, Special Publications, 381*(1), 67-97. https://doi.org/10.1144/SP381.23

Brenn, G. R., Hansen, S. E., & Park, Y. (2017). Variable thermal loading and flexural uplift along the Transantarctic Mountains, Antarctica. *Geology, 45*(5), 463-466. https://doi.org/10.1130/g38784.1

Brisbourne, A. M., Smith, A. M., Vaughan, D. G., King, E. C., Davies, D., Bingham, R. G., et al. (2017). Bed conditions of Pine Island Glacier, West Antarctica. *Journal of Geophysical Research: Earth Surface, 122*(1), 419-433. https://doi.org/10.1002/2016jf004033

Broome, A. L., & Schroeder, D. M. (2022). A Radiometrically Precise Multi-Frequency Ice-Penetrating Radar Architecture. *IEEE Transactions on Geoscience and Remote Sensing, 60*, 1-15. https://doi.org/10.1109/tgrs.2021.3099801

Burgess, S. D., Bowring, S. A., Fleming, T. H., & Elliot, D. H. (2015). High-precision geochronology links the Ferrar large igneous province with early-Jurassic ocean anoxia and biotic crisis. *Earth and Planetary Science Letters, 415*, 90-99. https://doi.org/10.1016/j.epsl.2015.01.037

Burton-Johnson, A., & Riley, T. R. (2015). Autochthonous v. accreted terrane development of continental margins: a revised in situ tectonic history of the Antarctic Peninsula. *Journal of the Geological Society, 172*(6), 822-835. https://doi.org/10.1144/jgs2014-110

Cande, S. C., & Stock, J. M. (2004) Cenozoic reconstructions of the australia-new zealand-south pacific sector of antarctica. In*: Vol. 151. Geophysical Monograph Series* (pp. 5-17).

Capponi, M., Sampietro, D., Ebbing, J., & Ferraccioli, F. (2022). Antarctica 3-D crustal structure investigation by means of the Bayesian gravity inversion: the Wilkes Land case study. *Geophysical Journal International, 229*(3), 2147-2161. https://doi.org/10.1093/gji/ggac036

Castillo, P., Fanning, C. M., Fernandez, R., Poblete, F., & Hervé, F. (2017). Provenance and age constraints of Paleozoic siliciclastic rocks from the Ellsworth Mountains in West Antarctica, as determined by detrital zircon geochronology. *GSA Bulletin, 129*(11-12), 1568-1584. https://doi.org/10.1130/b31686.1

Castillo, P., Lacassie, J. P., Augustsson, C., & Hervé, F. (2015). Petrography and geochemistry of the Carboniferous-Triassic Trinity Peninsula Group, West Antarctica: Implications for provenance and tectonic setting. *Geological Magazine, 152*(4), 575-588. https://doi.org/10.1017/S0016756814000454

Catania, G., Hulbe, C., Conway, H., Scambos, T. A., & Raymond, C. F. (2012). Variability in the mass flux of the Ross ice streams, West Antarctica, over the last millennium. *Journal of Glaciology, 58*(210), 741-752. https://doi.org/10.3189/2012JoG11J219

Chaput, J., Aster, R. C., Huerta, A., Sun, X., Lloyd, A., Wiens, D., et al. (2014). The crustal thickness of West Antarctica. *Journal of Geophysical Research: Solid Earth, 119*(1), 378-395. https://doi.org/10.1002/2013JB010642

Christianson, K., Jacobel, R. W., Horgan, H. J., Alley, R. B., Anandakrishnan, S., Holland, D. M., & DallaSanta, K. J. (2016). Basal conditions at the grounding zone of Whillans Ice Stream, West Antarctica, from ice-penetrating radar. *Journal of Geophysical Research: Earth Surface, 121*(11), 1954-1983. https://doi.org/10.1002/2015JF003806

Christoffersen, P., Bougamont, M., Carter, S. P., Fricker, H. A., & Tulaczyk, S. (2014). Significant groundwater contribution to Antarctic ice streams hydrologic budget. *Geophysical Research Letters, 41*(6), 2003-2010. https://doi.org/10.1002/2014GL059250

Chu, W., Schroeder, D. M., Seroussi, H., Creyts, T. T., & Bell, R. E. (2018). Complex Basal Thermal Transition Near the Onset of Petermann Glacier, Greenland. *Journal of Geophysical Research: Earth Surface, 123*(5), 985-995. https://doi.org/10.1029/2017JF004561

Cianfarra, P., & Salvini, F. (2016). Origin of the Adventure Subglacial Trench linked to Cenozoic extension in the East Antarctic Craton. *Tectonophysics, 670*, 30-37. https://doi.org/10.1016/j.tecto.2015.12.011

Cooper, M. A., Jordan, T. M., Schroeder, D. M., Siegert, M. J., Williams, C. N., & Bamber, J. L. (2019). Subglacial roughness of the Greenland Ice Sheet: relationship with contemporary ice velocity and geology. *The Cryosphere, 13*(11), 3093-3115. https://doi.org/10.5194/tc-13-3093-2019

Corr, H., Ferraccioli, F., Frearson, N., Jordan, T., Robinson, C., Armadillo, E., et al. (2007). Airborne radio-echo sounding of the Wilkes Subglacial Basin, the Transantarctic Mountains, and the Dome C region. 55-63.

Cox, S. C., Smith Lyttle, B., Elkind, S., Smith Siddoway, C., Morin, P., Capponi, G., et al. (2023). A continent-wide detailed geological map dataset of Antarctica. *Scientific Data, 10*(1), 250. https://doi.org/10.1038/s41597-023-02152-9

Craddock, J. P., Fitzgerald, P., Konstantinou, A., Nereson, A., & Thomas, R. J. (2017). Detrital zircon provenance of upper Cambrian-Permian strata and tectonic evolution of the Ellsworth Mountains, West Antarctica. *Gondwana Research, 45*, 191-207. https://doi.org/10.1016/j.gr.2016.11.011

Cui, X., Jeofry, H., Greenbaum, J. S., Guo, J., Li, L., Lindzey, L. E., et al. (2020). Bed topography of Princess Elizabeth Land in East Antarctica. *Earth Syst. Sci. Data, 12*(4), 2765-2774. https://doi.org/10.5194/essd-12-2765-2020

Curtis, M. L. (2002). Palaeozoic to Mesozoic polyphase deformation of the Patuxent Range, Pensacola Mountains, Antarctica. *Antarctic Science, 14*(2), 175-183. https://doi.org/10.1017/S0954102002000743

Curtis, M. L., & Lomas, S. A. (1999). Late Cambrian stratigraphy of the Heritage Range, Ellsworth Mountains: Implications for basin evolution. *Antarctic Science, 11*(1), 63-77. https://doi.org/10.1017/s0954102099000103

Curtis, M. L., Millar, I. L., Storey, B. C., & Fanning, M. (2004). Structural and geochronological constraints of early Ross orogenic deformation in the Pensacola Mountains, Antarctica. *Bulletin of the Geological Society of America, 116*(5-6), 619-636. https://doi.org/10.1130/B25170.1

Dall, J., Kristensen, S. S., Krozer, V., Hernández, C. C., Vidkjær, J., Kusk, A., et al. (2010). ESA'S POLarimetric Airborne Radar Ice Sounder (POLARIS): design and first results. *IET Radar, Sonar & Navigation, 4*(3), 488-496. https://doi.org/10.1049/iet-rsn.2009.0035

Damaske, D., Ferraccioli, F., & Bozzo, E. (2003). Aeromagnetic anomaly investigations along the Antarctic coast between Yule Bay and Mertz Glacier. *Terra Antartica, 10*, 85-96.

Davey, F. J., & Brancolini, G. (1995). The Late Mesozoic and Cenozoic structural setting of the Ross Sea region. *Geology and Seismic Stratigraphy of the Antarctic Margin, 68*, 167-182. https://doi.org/10.1029/AR068p0167

Davey, F. J., Brancolini, G., Hamilton, R. J., Henrys, S. A., Sorlien, C. C., & Bartek, L. R. (2000). A revised correlation of the seismic stratigraphy at the Cape Roberts drill sites with the seismic stratigraphy of the Victoria Land Basin, Antarctica. *Terra Antarctica, 7*(3), 215-220.

Davey, F. J., Cande, S., & Stock, J. (2021). Cenozoic continental rifting in the north-western Ross Sea. *New Zealand Journal of Geology and Geophysics*, 1-8. https://doi.org/10.1080/00288306.2021.1891942

Davey, F. J., Granot, R., Cande, S. C., Stock, J. M., Selvans, M., & Ferraccioli, F. (2016). Synchronous oceanic spreading and continental rifting in West Antarctica. *Geophysical Research Letters, 43*(12), 6162-6169. https://doi.org/10.1002/2016GL069087

Davies, D., Bingham, R. G., Graham, A. G. C., Spagnolo, M., Dutrieux, P., Vaughan, D. G., et al. (2017). High-resolution sub-ice-shelf seafloor records of twentieth century ungrounding and retreat of Pine Island Glacier, West Antarctica. *Journal of Geophysical Research: Earth Surface, 122*(9), 1698-1714. https://doi.org/10.1002/2017jf004311

Davis, J. K., Lawver, L. A., Norton, I., Dalziel, I., & Gahagan, L. M. (2018). The crustal structure of the Enderby Basin, East Antarctica. *Marine Geophysical Research, 40*, 1-16. https://doi.org/10.1007/s11001-018-9356-5

Dawson, E. J., Schroeder, D. M., Chu, W., Mantelli, E., & Seroussi, H. (2022). Ice mass loss sensitivity to the Antarctic ice sheet basal thermal state. *Nature Communications, 13*(1), 4957. https://doi.org/10.1038/s41467-022-32632-2

De Santis, L., Brancolini, G., & Donda, F. (2003). Seismo-stratigraphic analysis of the Wilkes Land continental margin (East Antarctica): Influence of glacially driven processes on the Cenozoic deposition. *Deep-Sea Research Part II: Topical Studies in Oceanography, 50*(8-9), 1563-1594. https://doi.org/10.1016/s0967-0645(03)00079-1

De Santis, L., Prato, S., Brancolini, G., Lovo, M., & Torelli, L. (1999). The Eastern Ross Sea continental shelf during the Cenozoic: Implications for the West Antarctic ice sheet development. *Global and Planetary Change, 23*(1-4), 173-196. https://doi.org/10.1016/s0921-8181(99)00056-9

Delaney, I., Werder, M. A., & Farinotti, D. (2019). A Numerical Model for Fluvial Transport of Subglacial Sediment. *Journal of Geophysical Research: Earth Surface, 124*(8), 2197-2223. https://doi.org/10.1029/2019JF005004

Dow, C. F., Ross, N., Jeofry, H., Siu, K., & Siegert, M. J. (2022). Antarctic basal environment shaped by high-pressure flow through a subglacial river system. *Nature Geoscience, 15*(11), 892-898. https://doi.org/10.1038/s41561-022-01059-1

Dowdeswell, J. A., Evans, J., Mugford, R., Griffiths, G., McPhail, S., Millard, N., et al. (2008). Autonomous underwater vehicles (AUVs) and investigations of the ice-ocean interface in Antarctic and Arctic waters. *Journal of Glaciology, 54*(187), 661-672. https://doi.org/10.3189/002214308786570773

Dunham, C. K., O'Donnell, J. P., Stuart, G. W., Brisbourne, A. M., Rost, S., Jordan, T. A., et al. (2020). A joint inversion of receiver function and Rayleigh wave phase velocity dispersion data to estimate crustal structure in West Antarctica. *Geophysical Journal International, 223*(3), 1644-1657. https://doi.org/10.1093/gji/ggaa398

Eagles, G. (2019). A little spin in the Indian Ocean plate circuit. *Tectonophysics, 754*, 80-100. https://doi.org/10.1016/j.tecto.2019.01.015

Eagles, G., & Eisermann, H. (2020). The Skytrain plate and tectonic evolution of southwest Gondwana since Jurassic times. *Scientific Reports, 10*(1), 19994. https://doi.org/10.1038/s41598-020-77070-6

Eagles, G., Karlsson, N. B., Ruppel, A., Steinhage, D., Jokat, W., & Läufer, A. (2018). Erosion at extended continental margins: Insights from new aerogeophysical data in eastern Dronning Maud Land. *Gondwana Research, 63*, 105-116. https://doi.org/10.1016/j.gr.2018.05.011

Eagles, G., & Livermore, R. A. (2002). Opening history of Powell Basin, Antarctic Peninsula. *Marine Geology, 185*(3-4), 195-205. https://doi.org/10.1016/s0025-3227(02)00191-3

Ebbing, J., Dilixiati, Y., Haas, P., Ferraccioli, F., & Scheiber-Enslin, S. (2021). East Antarctica magnetically linked to its ancient neighbours in Gondwana. *Scientific Reports, 11*(1). https://doi.org/10.1038/s41598-021-84834-1

Ebbing, J., Haas, P., Ferraccioli, F., Pappa, F., Szwillus, W., & Bouman, J. (2018). Earth tectonics as seen by GOCE - Enhanced satellite gravity gradient imaging. *Scientific Reports, 8*(1). https://doi.org/10.1038/s41598-018-34733-9

Eisen, O., Hofstede, C., Diez, A., Kristoffersen, Y., Lambrecht, A., Mayer, C., et al. (2015). On-ice vibroseis and snowstreamer systems for geoscientific research. *Polar Science, 9*(1), 51-65. https://doi.org/10.1016/j.polar.2014.10.003

Eisen, O., Winter, A., Steinhage, D., Kleiner, T., & Humbert, A. (2020). Basal roughness of the East Antarctic Ice Sheet in relation to flow speed and basal thermal state. *Annals of Glaciology, 61*(81), 162-175. https://doi.org/10.1017/aog.2020.47

Eisermann, H., Eagles, G., Ruppel, A., Smith, E. C., & Jokat, W. (2020). Bathymetry Beneath Ice Shelves of Western Dronning Maud Land, East Antarctica, and Implications on Ice Shelf Stability. *Geophysical Research Letters, 47*(12), e2019GL086724. https://doi.org/10.1029/2019GL086724

Elliot, D. H., Fanning, C. M., Isbell, J. L., & Hulett, S. R. W. (2017). The Permo-Triassic Gondwana sequence, central Transantarctic Mountains, Antarctica: Zircon geochronology, provenance, and basin evolution. *Geosphere, 13*(1), 155-178. https://doi.org/10.1130/ges01345.1

Enkin, R. J., Hamilton, T. S., & Morris, W. A. (2020). The Henkel Petrophysical Plot: Mineralogy and Lithology From Physical Properties. *Geochemistry, Geophysics, Geosystems, 21*(1), e2019GC008818. https://doi.org/10.1029/2019GC008818

Escutia, C., De Santis, L., Donda, F., Dunbar, R. B., Cooper, A. K., Brancolini, G., & Eittreim, S. L. (2005). Cenozoic ice sheet history from East Antarctic Wilkes Land continental margin sediments. *Global and Planetary Change, 45*(1), 51-81. https://doi.org/10.1016/j.gloplacha.2004.09.010

Evans, D. J. A., Phillips, E. R., Hiemstra, J. F., & Auton, C. A. (2006). Subglacial till: Formation, sedimentary characteristics and classification. *Earth-Science Reviews, 78*(1), 115-176. https://doi.org/10.1016/j.earscirev.2006.04.001

Evans, K. R., McKenna, L. W., Lieberman, B. S., Weichert, W. D., & Macleod, K. G. (2018). Geology of the Nelson Limestone, Postel Nunatak, Patuxent Range, Antarctica. *Antarctic Science, 30*(1), 29-43. https://doi.org/10.1017/S0954102017000396

Evans, S., & Robin, G. D. Q. (1966). Glacier depth-sounding from the air. *Nature, 210*(5039), 883-885. https://doi.org/10.1038/210883a0

Evenick, J. C. (2021). Glimpses into Earth's history using a revised global sedimentary basin map. *Earth-Science Reviews, 215*. https://doi.org/10.1016/j.earscirev.2021.103564

Ferraccioli, F., Armadillo, E., Jordan, T., Bozzo, E., & Corr, H. (2009). Aeromagnetic exploration over the East Antarctic Ice Sheet: A new view of the Wilkes Subglacial Basin. *Tectonophysics, 478*(1), 62-77. https://doi.org/10.1016/j.tecto.2009.03.013

Ferraccioli, F., Armadillo, E., Zunino, A., Bozzo, E., Rocchi, S., & Armienti, P. (2009). Magmatic and tectonic patterns over the Northern Victoria Land sector of the Transantarctic Mountains from new aeromagnetic imaging. *Tectonophysics, 478*(1-2), 43-61. https://doi.org/10.1016/j.tecto.2008.11.028

Ferraccioli, F., & Bozzo, E. (2003). Cenozoic strike-slip faulting from the eastern margin of the Wilkes Subglacial Basin to the western margin of the Ross Sea Rift: an aeromagnetic connection. *Geological Society, London, Special Publications, 210*(1), 109-133. https://doi.org/10.1144/GSL.SP.2003.210.01.07

Ferraccioli, F., Finn, C. A., Jordan, T. A., Bell, R. E., Anderson, L. M., & Damaske, D. (2011). East Antarctic rifting triggers uplift of the Gamburtsev Mountains. *Nature, 479*(7373), 388-392. https://doi.org/10.1038/nature10566

Ferraccioli, F., Forsberg, R., Olesen, A., Jordan, T., Matsuoka, K., Zakrajsek, A., & Ghidella, M. (2020). *Processed line aeromagnetic data over the Recovery Lakes region and interior Dronning Maud Land, East Antarctica (2013) [Data set]. UK Polar Data Centre, Natural Environment Research Council, UK Research & Innovation.* . https://doi.org/10.5285/849E2215-95B0-4275-88B8-50E18E3F8D56

Ferraccioli, F., Jones, P. C., Curtis, M. L., & Leat, P. T. (2005). Subglacial imprints of early Gondwana break-up as identified from high resolution aerogeophysical data over western Dronning Maud Land, East Antarctica. *Terra Nova, 17*(6), 573-579. https://doi.org/10.1111/j.1365-3121.2005.00651.x

Ferraccioli, F., Jones, P. C., Curtis, M. L., Leat, P. T., & Riley, T. R. (2005). Tectonic and magmatic patterns in the Jutulstraumen rift (?) region, East Antarctica, as imaged by high-resolution aeromagnetic data. *Earth, Planets and Space, 57*(8), 767-780. https://doi.org/10.1186/bf03351856

Ferrar, H. (1907). *Report on the field-geology of the region explored during the "Discovery" Antarctic Expedition, 1901-1904*. Retrieved from

Fielding, C. R., Whittaker, J., Henrys, S. A., Wilson, T. J., & Naish, T. R. (2008). Seismic facies and stratigraphy of the Cenozoic succession in McMurdo Sound, Antarctica: Implications for tectonic, climatic and glacial history. *Palaeogeography, Palaeoclimatology, Palaeoecology, 260*(1-2), 8-29. https://doi.org/10.1016/j.palaeo.2007.08.016

Fitzgerald, P. G., & Goodge, J. W. (2022). Exhumation and tectonic history of inaccessible subglacial interior East Antarctica from thermochronology on glacial erratics. *Nature Communications, 13*(1), 6217. https://doi.org/10.1038/s41467-022-33791-y

Foley, N., Tulaczyk, S., Auken, E., Schamper, C., Dugan, H., Mikucki, J., et al. (2015). Helicopter-borne transient electromagnetics in high-latitude environments: An application in the McMurdo Dry Valleys, Antarctica. *GEOPHYSICS, 81*, WA87-WA99. https://doi.org/10.1190/geo2015-0186.1

Forsberg, R., Olesen, A. V., Ferraccioli, F., Jordan, T. A., Matsuoka, K., Zakrajsek, A., et al. (2018). Exploring the Recovery Lakes region and interior Dronning Maud Land, East Antarctica, with airborne gravity, magnetic and radar measurements. *Geological Society, London, Special Publications, 461*(1), 23-34. https://doi.org/10.1144/SP461.17

Francis, J. E., Pirrie, D., & Crame, J. A. (2006). *Cretaceous–Tertiary High-Latitude Palaeoenvironments: James Ross Basin, Antarctica*: Geological Society of London. https://doi.org/10.1144/gsl.Sp.2006.258

Frederick, B. C., Young, D. A., Blankenship, D. D., Richter, T. G., Kempf, S. D., Ferraccioli, F., & Siegert, M. J. (2016). Distribution of subglacial sediments across the Wilkes Subglacial Basin, East Antarctica. *Journal of Geophysical Research F: Earth Surface, 121*(4), 790-813. https://doi.org/10.1002/2015jf003760

Frémand, A. C., Bodart, J. A., Jordan, T. A., Ferraccioli, F., Robinson, C., Corr, H. F. J., et al. (2022). British Antarctic Survey's aerogeophysical data: releasing 25 years of airborne gravity, magnetic, and radar datasets over Antarctica. *Earth Syst. Sci. Data, 14*(7), 3379-3410. https://doi.org/10.5194/essd-14-3379-2022

Frémand, A. C., Fretwell, P., Bodart, J., Pritchard, H. D., Aitken, A., Bamber, J. L., et al. (2022). Antarctic Bedmap data: FAIR sharing of 60 years of ice bed, surface and thickness data. *Earth Syst. Sci. Data Discuss., 2022*, 1-25. https://doi.org/10.5194/essd-2022-355

Fretwell, P., Pritchard, H. D., Vaughan, D. G., Bamber, J. L., Barrand, N. E., Bell, R., et al. (2013). Bedmap2: Improved ice bed, surface and thickness datasets for Antarctica. *Cryosphere, 7*(1), 375-393. https://doi.org/10.5194/tc-7-375-2013

Gaina, C., Müller, R. D., Brown, B., Ishihara, T., & Ivanov, S. (2007). Breakup and early seafloor spreading between India and Antarctica. *Geophysical Journal International, 170*(1), 151-169. https://doi.org/10.1111/j.1365-246X.2007.03450.x

Gibbons, A. D., Whittaker, J. M., & Müller, R. D. (2013). The breakup of East Gondwana: Assimilating constraints from Cretaceous ocean basins around India into a best-fit tectonic model. *Journal of Geophysical Research: Solid Earth, 118*(3), 808-822. https://doi.org/10.1002/jgrb.50079

Gibson, C., Boeckmann, G., Meulemans, Z., Kuhl, T., Koehler, J., Johnson, J., & Slawny, K. (2020). RAM-2 Drill system development: an upgrade of the Rapid Air Movement Drill. *Annals of Glaciology, 62*, 1-10. https://doi.org/10.1017/aog.2020.72

Glover, P. (2016). Archie's law – a reappraisal. *Solid Earth, 7*, 1157-1169. https://doi.org/10.5194/se-7-1157-2016

Gogineni, S., Chuah, T., Allen, C., Jezek, K., & Moore, R. K. (1998). An improved coherent radar depth sounder. *Journal of Glaciology, 44*(148), 659-669. https://doi.org/10.3189/s0022143000002161

Gohl, K., Denk, A., Eagles, G., & Wobbe, F. (2013). Deciphering tectonic phases of the Amundsen Sea Embayment shelf, West Antarctica, From a magnetic anomaly grid. *Tectonophysics, 585*, 113-123. https://doi.org/10.1016/j.tecto.2012.06.036

Gohl, K., Freudenthal, T., Hillenbrand, C. D., Klages, J., Larter, R., Bickert, T., et al. (2017). MeBo70 Seabed Drilling on a Polar Continental Shelf: Operational Report and Lessons From Drilling in the Amundsen Sea Embayment of West Antarctica. *Geochemistry, Geophysics, Geosystems, 18*(11), 4235-4250. https://doi.org/10.1002/2017GC007081

Gohl, K., Uenzelmann-Neben, G., Gille-Petzoldt, J., Hillenbrand, C.-D., Klages, J. P., Bohaty, S. M., et al. (2021). Evidence for a Highly Dynamic West Antarctic Ice Sheet During the Pliocene. *Geophysical Research Letters, 48*(14), e2021GL093103. https://doi.org/10.1029/2021GL093103

Gohl, K., Uenzelmann-Neben, G., Larter, R. D., Hillenbrand, C. D., Hochmuth, K., Kalberg, T., et al. (2013). Seismic stratigraphic record of the Amundsen Sea Embayment shelf from pre-glacial to recent times: Evidence for a dynamic West Antarctic ice sheet. *Marine Geology, 344*, 115-131. https://doi.org/10.1016/j.margeo.2013.06.011

Golynsky, A., Chiappini, M., Damaske, D., Ferraccioli, F., Finn, C., Ghidella, M., et al. (Cartographer). (2001). ADMAP – Magnetic anomaly map of the Antarctic, 1: 10 000 000 scale map

Golynsky, A., Chiappini, M., Damaske, D., Ferraccioli, F., Finn, C. A., Ishihara, T., et al. (2006). ADMAP — A Digital Magnetic Anomaly Map of the Antarctic. In D. K. Fütterer, D. Damaske, G. Kleinschmidt, H. Miller, & F. Tessensohn (Eds.), *Antarctica: Contributions to Global Earth Sciences* (pp. 109-116). Berlin, Heidelberg: Springer Berlin Heidelberg. https://doi.org/10.1007/3-540-32934-X_12

Golynsky, A. V., Ferraccioli, F., Hong, J. K., Golynsky, D. A., von Frese, R. R. B., Young, D. A., et al. (2018). New Magnetic Anomaly Map of the Antarctic. *Geophysical Research Letters, 45*(13), 6437-6449. https://doi.org/10.1029/2018gl078153

Golynsky, D. A., & Golynsky, A. V. (2007). Gaussberg rift - illusion or reality? In A. K. Cooper & C. R. Raymond (Eds.), *Antarctica: A Keystone in a Changing World--Online Proceedings of the 10th ISAES*: USGS Open-File Report 2007-1047, Extended Abstract 168, 5 p.

Gong, D., Fan, X., Li, Y., Li, B., Zhang, N., Gromig, R., et al. (2019). Coring of antarctic subglacial sediments. *Journal of Marine Science and Engineering, 7*(6). https://doi.org/10.3390/jmse7060194

Gooch, B. T., Young, D. A., & Blankenship, D. D. (2016). Potential groundwater and heterogeneous heat source contributions to ice sheet dynamics in critical submarine basins of East Antarctica. *Geochemistry, Geophysics, Geosystems, 17*(2), 395-409. https://doi.org/10.1002/2015gc006117

Goodge, J. W. (2020). Geological and tectonic evolution of the Transantarctic Mountains, from ancient craton to recent enigma. *Gondwana Research, 80*, 50-122. https://doi.org/10.1016/j.gr.2019.11.001

Goodge, J. W., Severinghaus, J. P., Johnson, J., Tosi, D., & Bay, R. (2021). Deep ice drilling, bedrock coring and dust logging with the Rapid Access Ice Drill (RAID) at Minna Bluff, Antarctica. *Annals of Glaciology*. https://doi.org/10.1017/aog.2021.13

Granot, R., & Dyment, J. (2018). Late Cenozoic unification of East and West Antarctica. *Nature Communications, 9*(1), 3189. https://doi.org/10.1038/s41467-018-05270-w

Grikurov, G., Leitchenkov, G., Kamenev, E. N., Mikhalsky, E., Golynsky, A., Masolov, V. N., & Laiba, A. A. (2003). Antarctic tectonic and minerogenic provinces. *Arctic and Antarctic, Russian Academy of Sciences, 2*, 26-47.

Grima, C., Koch, I., Greenbaum, J. S., Soderlund, K. M., Blankenship, D. D., Young, D. A., et al. (2019). Surface and basal boundary conditions at the Southern McMurdo and Ross Ice Shelves, Antarctica. *Journal of Glaciology, 65*(252), 675-688. https://doi.org/10.1017/jog.2019.44

Gulick, S. P. S., Shevenell, A. E., Montelli, A., Fernandez, R., Smith, C., Warny, S., et al. (2017). Initiation and long-term instability of the East Antarctic Ice Sheet. *Nature, 552*(7684), 225-229. https://doi.org/10.1038/nature25026

Gustafson, C. D., Key, K., Siegfried, M. R., Winberry, J. P., Fricker, H. A., Venturelli, R. A., & Michaud, A. B. (2022). A dynamic saline groundwater system mapped beneath an Antarctic ice stream. *Science, 376*(6593), 640-644. https://doi.org/10.1126/science.abm3301

Haeger, C., & Kaban, M. K. (2019). Decompensative Gravity Anomalies Reveal the Structure of the Upper Crust of Antarctica. *Pure and Applied Geophysics, 176*(10), 4401-4414. https://doi.org/10.1007/s00024-019-02212-5

Halberstadt, A. R. W., Simkins, L. M., Anderson, J. B., Prothro, L. O., & Bart, P. J. (2018). Characteristics of the deforming bed: Till properties on the deglaciated Antarctic continental shelf. *Journal of Glaciology, 64*(248), 1014-1027. https://doi.org/10.1017/jog.2018.92

Hale, R., Miller, H., Gogineni, S., Yan, J. B., Rodriguez-Morales, F., Leuschen, C., et al. (2016, 10-15 July 2016). *Multi-channel ultra-wideband radar sounder and imager.* Paper presented at the 2016 IEEE International Geoscience and Remote Sensing Symposium (IGARSS). https://doi.org/10.1109/igarss.2016.7729545

Hambrey, M. J., & McKelvey, B. (2000). Major Neogene fluctuations of the East Antarctic ice sheet: Stratigraphic evidence from the Lambert Glacier region. *Geology, 28*(10), 887-890. https://doi.org/10.1130/0091-7613(2000)28<887:MNFOTE>2.0.CO;2

Harry, D. L., Anoka, J. L., & Jha, S. (2018). Geodynamic models of the West Antarctic Rift System: Implications for the mantle thermal state. *Geosphere, 14*(6), 2407-2429. https://doi.org/10.1130/ges01594.1

Hathway, B. (2000). Continental rift to back-arc basin: Jurassic-Cretaceous stratigraphical and structural evolution of the Larsen Basin, Antarctic Peninsula. *Journal of the Geological Society, 157*(2), 417-432. https://doi.org/10.1144/jgs.157.2.417

Haynes, M. S., Chapin, E., & Schroeder, D. M. (2018). Geometric Power Fall-Off in Radar Sounding. *IEEE Transactions on Geoscience and Remote Sensing, 56*(11), 6571-6585. https://doi.org/10.1109/tgrs.2018.2840511

Hazzard, J. A. N., Richards, F. D., Goes, S. D. B., & Roberts, G. G. (2023). Probabilistic Assessment of Antarctic Thermomechanical Structure: Impacts on Ice Sheet Stability. *Journal of Geophysical Research: Solid Earth, 128*(5), e2023JB026653. https://doi.org/10.1029/2023JB026653

Heliere, F., Lin, C., Corr, H., & Vaughan, D. (2007). Radio Echo Sounding of Pine Island Glacier, West Antarctica: Aperture Synthesis Processing and Analysis of Feasibility From Space. *IEEE Transactions on Geoscience and Remote Sensing, 45*(8), 2573-2582. https://doi.org/10.1109/tgrs.2007.897433

Hill, G. J. (2020). On the Use of Electromagnetics for Earth Imaging of the Polar Regions. *Surveys in Geophysics, 41*(1), 5-45. https://doi.org/10.1007/s10712-019-09570-8

Hillenbrand, C. D., Bentley, M. J., Stolldorf, T. D., Hein, A. S., Kuhn, G., Graham, A. G. C., et al. (2014). Reconstruction of changes in the Weddell Sea sector of the Antarctic Ice Sheet since the Last Glacial

Maximum. *Quaternary Science Reviews, 100*, 111-136. https://doi.org/10.1016/j.quascirev.2013.07.020

Hirt, C., Rexer, M., Scheinert, M., Pail, R., Claessens, S., & Holmes, S. (2016). A new degree-2190 (10 km resolution) gravity field model for Antarctica developed from GRACE, GOCE and Bedmap2 data. *Journal of Geodesy, 90*(2), 105-127. https://doi.org/10.1007/s00190-015-0857-6

Hochmuth, K., & Gohl, K. (2019). Seaward growth of Antarctic continental shelves since establishment of a continent-wide ice sheet: Patterns and mechanisms. *Palaeogeography, Palaeoclimatology, Palaeoecology, 520*, 44-54. https://doi.org/10.1016/j.palaeo.2019.01.025

Hochmuth, K., Gohl, K., Leitchenkov, G., Sauermilch, I., Whittaker, J. M., Uenzelmann-Neben, G., et al. (2020). The Evolving Paleobathymetry of the Circum-Antarctic Southern Ocean Since 34 Ma: A Key to Understanding Past Cryosphere-Ocean Developments. *Geochemistry, Geophysics, Geosystems, 21*(8), e2020GC009122. https://doi.org/10.1029/2020GC009122

Hochmuth, K., Whittaker, J. M., Sauermilch, I., Klocker, A., Gohl, K., & LaCasce, J. H. (2022). Southern Ocean biogenic blooms freezing-in Oligocene colder climates. *Nature Communications, 13*(1), 6785. https://doi.org/10.1038/s41467-022-34623-9

Hodgson, D. A., Bentley, M. J., Smith, J. A., Klepacki, J., Makinson, K., Smith, A. M., et al. (2016). Technologies for retrieving sediment cores in Antarctic subglacial settings. *Philosophical Transactions of the Royal Society A: Mathematical, Physical and Engineering Sciences, 374*(2059). https://doi.org/10.1098/rsta.2015.0056

Holschuh, N., Christianson, K., Paden, J., Alley, R. B., & Anandakrishnan, S. (2020). Linking postglacial landscapes to glacier dynamics using swath radar at Thwaites Glacier, Antarctica. *Geology, 48*(3), 268-272. https://doi.org/10.1130/g46772.1

Hooyer, T. S., Cohen, D., & Iverson, N. R. (2012). Control of glacial quarrying by bedrock joints. *Geomorphology, 153-154*, 91-101. https://doi.org/10.1016/j.geomorph.2012.02.012

Horgan, H., Naish, T., Bannister, S., Balfour, N., & Wilson, G. (2005). Seismic stratigraphy of the Plio-Pleistocene Ross Island flexural moat-fill: A prognosis for ANDRILL Program drilling beneath McMurdo-Ross Ice Shelf. *Global and Planetary Change, 45*(1-3 SPEC. ISS.), 83-97. https://doi.org/10.1016/j.gloplacha.2004.09.014

Horgan, H. J., Van Haastrecht, L., Alley, R. B., Anandakrishnan, S., Beem, L. H., Christianson, K., et al. (2021). Grounding zone subglacial properties from calibrated active-source seismic methods. *Cryosphere, 15*(4), 1863-1880. https://doi.org/10.5194/tc-15-1863-2021

Huang, X., & Jokat, W. (2016). Sedimentation and potential venting on the rifted continental margin of Dronning Maud Land. *Marine Geophysical Research, 37*. https://doi.org/10.1007/s11001-016-9296-x

Huerta, A. D., & Harry, D. L. (2007). The transition from diffuse to focused extension: Modeled evolution of the West Antarctic Rift system. *Earth and Planetary Science Letters, 255*(1), 133-147. https://doi.org/10.1016/j.epsl.2006.12.011

Hunter, M. A., & Cantrill, D. J. (2006). A new stratigraphy for the Latady Basin, Antarctic Peninsula: Part 2, Latady Group and basin evolution. *Geological Magazine, 143*(6), 797-819. https://doi.org/10.1017/S0016756806002603

Hunter, R. J., Johnson, A. C., & Aleshkova, N. D. (1996). Aeromagnetic data from the southern Weddell Sea embayment and adjacent areas: Synthesis and interpretation. *Geological Society Special Publication, 108*, 143-154. https://doi.org/10.1144/GSL.SP.1996.108.01.10

Isanina, E., Krupnova, N., Popov, S., Masolov, V., & Lukin, V. (2009). Deep structure of the Vostok Basin, East Antarctica as deduced from seismological observations. *Geotectonics, 43*, 221-225. https://doi.org/10.1134/S0016852109030042

Isbell, J. L., Koch, Z. J., Szablewski, G. M., & Lenaker, P. A. (2008). Permian glacigenic deposits in the Transantarctic Mountains, Antarctica. In *Special Paper of the Geological Society of America* (Vol. 441, pp. 59-70). https://doi.org/10.1130/2008.2441(04)

Jamieson, S. S., Sugden, D. E., & Hulton, N. R. (2010). The evolution of the subglacial landscape of Antarctica. *Earth and Planetary Science Letters, 293*(1-2), 1-27. https://doi.org/10.1016/j.epsl.2010.02.012

Jamieson, S. S. R., Ross, N., Greenbaum, J. S., Young, D. A., Aitken, A. R. A., Roberts, J. L., et al. (2016). An extensive subglacial lake and canyon system in Princess Elizabeth Land, East Antarctica. *Geology, 44*(2), 87-90. https://doi.org/10.1130/g37220.1

Jamieson, S. S. R., Stokes, C. R., Ross, N., Rippin, D. M., Bingham, R. G., Wilson, D. S., et al. (2014). The glacial geomorphology of the Antarctic ice sheet bed. *Antarctic Science, 26*(6), 724-741. https://doi.org/10.1017/s0954102014000212

Jensen, T. E., & Forsberg, R. (2018). Helicopter Test of a Strapdown Airborne Gravimetry System. *Sensors (Basel, Switzerland), 18*(9), 3121. https://doi.org/10.3390/s18093121

Johnston, L., Wilson, G., Gorman, A., Henrys, S., Horgan, H., Clark, R., & Naish, T. (2008). Cenozoic basin evolution beneath the southern McMurdo Ice Shelf, Antarctica. *Global and Planetary Change, 62*, 61-76. https://doi.org/10.1016/j.gloplacha.2007.11.004

Jokat, W., Altenbernd, T., Eagles, G., & Geissler, W. H. (2021). The early drift of the Indian plate. *Sci Rep, 11*(1), 10796. https://doi.org/10.1038/s41598-021-90172-z

Jokat, W., & Herter, U. (2016). Jurassic failed rift system below the Filchner-Ronne-Shelf, Antarctica: New evidence from geophysical data. *Tectonophysics, 688*, 65-83. https://doi.org/10.1016/j.tecto.2016.09.018

Jokat, W., Nogi, Y., & Leinweber, V. (2010). New aeromagnetic data from the western Enderby Basin and consequences for Antarctic-India break-up. *Geophysical Research Letters, 37*(21). https://doi.org/10.1029/2010GL045117

Jones, P., Johnson, A., Frese, R. R. v., & Corr, H. F. J. (2002). Detecting rift basins in the Evans Ice Stream region of West Antarctica using airborne gravity data. *Tectonophysics, 347*, 25-41. https://doi.org/10.1016/S0040-1951(01)00236-0

Jordan, T. A., & Becker, D. (2018). Investigating the distribution of magmatism at the onset of Gondwana breakup with novel strapdown gravity and aeromagnetic data. *Physics of the Earth and Planetary Interiors, 282*, 77-88. https://doi.org/10.1016/j.pepi.2018.07.007

Jordan, T. A., Ferraccioli, F., Armadillo, E., & Bozzo, E. (2013). Crustal architecture of the Wilkes Subglacial Basin in East Antarctica, as revealed from airborne gravity data. *Tectonophysics, 585*, 196-206. https://doi.org/10.1016/j.tecto.2012.06.041

Jordan, T. A., Ferraccioli, F., Corr, H., Graham, A., Armadillo, E., & Bozzo, E. (2010). Hypothesis for mega-outburst flooding from a palaeo-subglacial lake beneath the East Antarctic Ice Sheet. *Terra Nova, 22*(4), 283-289. https://doi.org/10.1111/j.1365-3121.2010.00944.x

Jordan, T. A., Ferraccioli, F., & Forsberg, R. (2022). An embayment in the East Antarctic basement constrains the shape of the Rodinian continental margin. *Communications Earth & Environment, 3*(1), 52. https://doi.org/10.1038/s43247-022-00375-z

Jordan, T. A., Ferraccioli, F., & Leat, P. T. (2017). New geophysical compilations link crustal block motion to Jurassic extension and strike-slip faulting in the Weddell Sea Rift System of West Antarctica. *Gondwana Research, 42*, 29-48. https://doi.org/10.1016/j.gr.2016.09.009

Jordan, T. A., Ferraccioli, F., Ross, N., Corr, H. F. J., Leat, P. T., Bingham, R. G., et al. (2013). Inland extent of the Weddell Sea Rift imaged by new aerogeophysical data. *Tectonophysics, 585*, 137-160. https://doi.org/10.1016/j.tecto.2012.09.010

Jordan, T. A., Ferraccioli, F., Vaughan, D. G., Holt, J. W., Corr, H., Blankenship, D. D., & Diehl, T. M. (2010). Aerogravity evidence for major crustal thinning under the Pine Island Glacier region (West Antarctica). *Bulletin of the Geological Society of America, 122*(5-6), 714-726. https://doi.org/10.1130/b26417.1

Jordan, T. A., Riley, T. R., & Siddoway, C. S. (2020). The geological history and evolution of West Antarctica. *Nature Reviews Earth & Environment, 1*(2), 117-133. https://doi.org/10.1038/s43017-019-0013-6

Jordan, T. M., Cooper, M. A., Schroeder, D. M., Williams, C. N., Paden, J. D., Siegert, M. J., & Bamber, J. L. (2017). Self-affine subglacial roughness: consequences for radar scattering and basal water discrimination in northern Greenland. *The Cryosphere, 11*(3), 1247-1264. https://doi.org/10.5194/tc-11-1247-2017

Karner, G. D., Studinger, M., & Bell, R. E. (2005). Gravity anomalies of sedimentary basins and their mechanical implications: Application to the Ross Sea basins, West Antarctica. *Earth and Planetary Science Letters, 235*(3-4), 577-596. https://doi.org/10.1016/j.epsl.2005.04.016

Kennicutt, M. C., Bromwich, D., Liggett, D., Njåstad, B., Peck, L., Rintoul, S. R., et al. (2019). Sustained Antarctic Research: A 21st Century Imperative. *One Earth, 1*(1), 95-113. https://doi.org/10.1016/j.oneear.2019.08.014

Key, K., & Siegfried, M. R. (2017). The feasibility of imaging subglacial hydrology beneath ice streams with ground-based electromagnetics. *Journal of Glaciology, 63*(241), 755-771. https://doi.org/10.1017/jog.2017.36

Kim, S., De Santis, L., Hong, J. K., Cottlerle, D., Petronio, L., Colizza, E., et al. (2018). Seismic stratigraphy of the Central Basin in northwestern Ross Sea slope and rise, Antarctica: Clues to the late Cenozoic ice-sheet dynamics and bottom-current activity. *Marine Geology, 395*, 363-379. https://doi.org/10.1016/j.margeo.2017.10.013

Kjær, K. H., Larsen, N. K., Binder, T., Bjørk, A. A., Eisen, O., Fahnestock, M. A., et al. (2018). A large impact crater beneath Hiawatha Glacier in northwest Greenland. *Sci Adv, 4*(11), eaar8173. https://doi.org/10.1126/sciadv.aar8173

König, M., & Jokat, W. (2006). The Mesozoic breakup of the Weddell Sea. *Journal of Geophysical Research: Solid Earth, 111*(12). https://doi.org/10.1029/2006JB004035

Kovesi, P. (1999). Image Features from Phase Congruency. *VIDERE, 1*(3), 2-26.

Krabbendam, M., & Glasser, N. F. (2011). Glacial erosion and bedrock properties in NW Scotland: Abrasion and plucking, hardness and joint spacing. *Geomorphology, 130*(3), 374-383. https://doi.org/10.1016/j.geomorph.2011.04.022

Kristoffersen, Y., Hofstede, C., Diez, A., Blenkner, R., Lambrecht, A., Mayer, C., & Eisen, O. (2014). Reassembling Gondwana: A new high quality constraint from vibroseis exploration of the sub-ice shelf geology of the East Antarctic continental margin. *Journal of Geophysical Research: Solid Earth, 119*(12), 9171-9182. https://doi.org/10.1002/2014jb011479

Krohne, N., Lisker, F., Kleinschmidt, G., KlÜGel, A., LÄUfer, A., Estrada, S., & Spiegel, C. (2016). The Shackleton Range (East Antarctica): an alien block at the rim of Gondwana? *Geological Magazine, 155*(4), 841-864. https://doi.org/10.1017/S0016756816001011

Kuhl, T., Gibson, C., Johnson, J., Boeckmann, G., Moravec, E., & Slawny, K. (2021). Agile Sub-Ice Geological (ASIG) Drill development and Pirrit Hills field project. *Annals of Glaciology, 62*(84), 53-66. https://doi.org/10.1017/aog.2020.59

Kulessa, B. (2007). A Critical Review of the Low-Frequency Electrical Properties of Ice Sheets and Glaciers. *Journal of Environmental Engineering Geophysics, 12*, 23-36. https://doi.org/10.2113/jeeg12.1.23

Kulessa, B., Hubbard, B., & Brown, G. H. (2006). Time-lapse imaging of subglacial drainage conditions using three-dimensional inversion of borehole electrical resistivity data. *Journal of Glaciology, 52*(176), 49-57. https://doi.org/10.3189/172756506781828854

Kulessa, B., Key, K., Thompson, S., & Siegert, M. (2019). *Heat and groundwater transport between the Antarctic Ice Sheet and subglacial sedimentary basins from electromagnetic geophysical measurements*. Paper presented at the SEG Technical Program Expanded Abstracts https://doi.org/10.1190/segam2019-3215566.1

Kulhanek, D. K., Levy, R. H., Clowes, C. D., Prebble, J. G., Rodelli, D., Jovane, L., et al. (2019). Revised chronostratigraphy of DSDP Site 270 and late Oligocene to early Miocene paleoecology of the Ross Sea sector of Antarctica. *Global and Planetary Change, 178*, 46-64. https://doi.org/10.1016/j.gloplacha.2019.04.002

Kvas, A., Brockmann, J. M., Krauss, S., Schubert, T., Gruber, T., Meyer, U., et al. (2021). GOCO06s – a satellite-only global gravity field model. *Earth Syst. Sci. Data, 13*(1), 99-118. https://doi.org/10.5194/essd-13-99-2021

Lane, T. P., Roberts, D. H., Rea, B. R., Ó Cofaigh, C., & Vieli, A. (2015). Controls on bedrock bedform development beneath the Uummannaq Ice Stream onset zone, West Greenland. *Geomorphology, 231*, 301-313. https://doi.org/10.1016/j.geomorph.2014.12.019

Lawrence, J. F., Wiens, D. A., Nyblade, A. A., Anandakrishnan, S., Shore, P. J., & Voigt, D. (2006). Rayleigh wave phase velocity analysis of the Ross Sea, Transantarctic Mountains, and East Antarctica from a temporary seismograph array. *Journal of Geophysical Research: Solid Earth, 111*(B6). https://doi.org/10.1029/2005JB003812

Le Brocq, A. M., Ross, N., Griggs, J. A., Bingham, R. G., Corr, H. F. J., Ferraccioli, F., et al. (2013). Evidence from ice shelves for channelized meltwater flow beneath the Antarctic Ice Sheet. *Nature Geosci, 6*(11), 945-948. https://doi.org/10.1038/ngeo1977

Leitchenkov, G. L., Antonov, A. V., Luneov, P. I., & Lipenkov, V. Y. (2016). Geology and environments of subglacial Lake Vostok. *Philosophical Transactions of the Royal Society A: Mathematical, Physical and Engineering Sciences, 374*(2059). https://doi.org/10.1098/rsta.2014.0302

Leitchenkov, G. L., & Kudryavtzev, G. A. (1997). Structure and Origin of the Earth's Crust in the Weddell Sea Embayment (beneath the Front of the Filchner and Ronne Ice Shelves) from Deep Seismic Sounding data. *Polarforschung, 67*(3), 143-154.

Levy, R., Harwood, D., Florindo, F., Sangiorgi, F., Tripati, R., Eynatten, H. v., et al. (2016). Antarctic ice sheet sensitivity to atmospheric CO_2 variations in the early to mid-Miocene. *Proceedings of the National Academy of Sciences, 113*(13), 3453-3458. https://doi.org/10.1073/pnas.1516030113

Li, L., Aitken, A. R. A., Lindsay, M. D., & Kulessa, B. (2022). Sedimentary basins reduce stability of Antarctic ice streams through groundwater feedbacks. *Nature Geoscience, 15*(8), 645-650. https://doi.org/10.1038/s41561-022-00992-5

Lin, F.-C., Schmandt, B., & Tsai, V. C. (2012). Joint inversion of Rayleigh wave phase velocity and ellipticity using USArray: Constraining velocity and density structure in the upper crust. *Geophysical Research Letters, 39*(12). http://dx.doi.org/10.1029/2012GL052196

Lindeque, A., Gohl, K., Henrys, S., Wobbe, F., & Davy, B. (2016). Seismic stratigraphy along the Amundsen Sea to Ross Sea continental rise: A cross-regional record of pre-glacial to glacial processes of the West Antarctic margin. *Palaeogeography, Palaeoclimatology, Palaeoecology, 443*, 183-202. https://doi.org/10.1016/j.palaeo.2015.11.017

Lindeque, A., Gohl, K., Wobbe, F., & Uenzelmann-Neben, G. (2016). Preglacial to glacial sediment thickness grids for the Southern Pacific Margin of West Antarctica. *Geochemistry, Geophysics, Geosystems, 17*(10), 4276-4285. https://doi.org/10.1002/2016GC006401

Lindeque, A., Martos Martin, Y. M., Gohl, K., & Maldonado, A. (2013). Deep-sea pre-glacial to glacial sedimentation in the Weddell Sea and southern Scotia Sea from a cross-basin seismic transect. *Marine Geology, 336*, 61-83. https://doi.org/10.1016/j.margeo.2012.11.004

Lisker, F., Wilson, C. J. L., & Gibson, H. J. (2007). Thermal history of the Vestfold Hills (East Antarctica) between Lambert rifting and Gondwana break-up, evidence from apatite fission track data. *Antarctic Science, 19*(1), 97-106. https://doi.org/10.1017/S0954102007000144

Livingstone, S. J., Li, Y., Rutishauser, A., Sanderson, R. J., Winter, K., Mikucki, J. A., et al. (2022). Subglacial lakes and their changing role in a warming climate. *Nature Reviews Earth & Environment, 3*(2), 106-124. https://doi.org/10.1038/s43017-021-00246-9

Lloyd, A. J., Wiens, D. A., Nyblade, A. A., Anandakrishnan, S., Aster, R. C., Huerta, A. D., et al. (2015). A seismic transect across West Antarctica: Evidence for mantle thermal anomalies beneath the Bentley Subglacial Trench and the Marie Byrd Land Dome. *Journal of Geophysical Research: Solid Earth, 120*(12), 8439-8460. https://doi.org/10.1002/2015jb012455

Lloyd, A. J., Wiens, D. A., Zhu, H., Tromp, J., Nyblade, A. A., Aster, R. C., et al. (2020). Seismic Structure of the Antarctic Upper Mantle Imaged with Adjoint Tomography. *Journal of Geophysical Research: Solid Earth, 125*(3). https://doi.org/10.1029/2019JB017823

Lösing, M., & Ebbing, J. (2021). Predicting Geothermal Heat Flow in Antarctica With a Machine Learning Approach. *Journal of Geophysical Research: Solid Earth, 126*(6), e2020JB021499. https://doi.org/10.1029/2020JB021499

Lowry, D. P., Golledge, N. R., Bertler, N. A. N., Jones, R. S., McKay, R., & Stutz, J. (2020). Geologic controls on ice sheet sensitivity to deglacial climate forcing in the Ross Embayment, Antarctica. *Quaternary Science Advances, 1*, 100002. https://doi.org/10.1016/j.qsa.2020.100002

Luyendyk, B. P., Sorlien, C. C., Wilson, D. S., Bartek, L. R., & Siddoway, C. S. (2001). Structural and tectonic evolution of the Ross Sea rift in the Cape Colbeck region, Eastern Ross Sea, Antarctica. *Tectonics, 20*(6), 933-958. https://doi.org/10.1029/2000TC001260

Lythe, M. B., & Vaughan, D. G. (2001). BEDMAP: A new ice thickness and subglacial topographic model of Antarctica. *Journal of Geophysical Research: Solid Earth, 106*(B6), 11335-11351. https://doi.org/10.1029/2000jb900449

MacGregor, J. A., Boisvert, L. N., Medley, B., Petty, A. A., Harbeck, J. P., Bell, R. E., et al. (2021). The Scientific Legacy of NASA's Operation IceBridge. *Reviews of Geophysics, 59*(2). https://doi.org/10.1029/2020rg000712

MacKie, E. J., Schroeder, D. M., Caers, J., Siegfried, M. R., & Scheidt, C. (2020). Antarctic Topographic Realizations and Geostatistical Modeling Used to Map Subglacial Lakes. *Journal of Geophysical Research: Earth Surface, 125*(3), e2019JF005420. https://doi.org/10.1029/2019JF005420

MacKie, E. J., Schroeder, D. M., Zuo, C., Yin, Z., & Caers, J. (2021). Stochastic modeling of subglacial topography exposes uncertainty in water routing at Jakobshavn Glacier. *Journal of Glaciology, 67*(261), 75-83. https://doi.org/10.1017/jog.2020.84

Maggi, M., Cianfarra, P., & Salvini, F. (2016). Erosion by tectonic carving in the Concordia Subglacial Fault Zone, East Antarctica. *Earth and Planetary Science Letters, 433*, 99-108. https://doi.org/10.1016/j.epsl.2015.10.045

Maldonado, A., Bohoyo, F., Galindo-Zaldívar, J., Hernández-Molina, J., Jabaloy, A., Lobo, F. J., et al. (2006). Ocean basins near the Scotia-Antarctic plate boundary; influence of tectonics and paleoceanography on the Cenozoic deposits. *Marine Geophysical Researches, 27*(2), 83-107. https://doi.org/10.1007/s11001-006-9003-4

Maldonado, A., Larter, R. D., & Aldaya, F. (1994). Forearc tectonic evolution of the South Shetland margin, Antarctic Peninsula. *Tectonics, 13*(6), 1345-1370. https://doi.org/10.1029/94TC01352

Maritati, A., Aitken, A. R. A., Young, D. A., Roberts, J. L., Blankenship, D. D., & Siegert, M. J. (2016). The tectonic development and erosion of the Knox Subglacial Sedimentary Basin, East Antarctica. *Geophysical Research Letters, 43*(20), 10,728-710,737. https://doi.org/10.1002/2016gl071063

Maritati, A., Danišík, M., Halpin, J. A., Whittaker, J. M., & Aitken, A. R. A. (2020). Pangea Rifting Shaped the East Antarctic Landscape. *Tectonics, 39*(8), e2020TC006180. https://doi.org/10.1029/2020TC006180

Maritati, A., Halpin, J. A., Whittaker, J. M., & Daczko, N. R. (2019). Fingerprinting Proterozoic Bedrock in Interior Wilkes Land, East Antarctica. *Scientific Reports, 9*(1). https://doi.org/10.1038/s41598-019-46612-y

Maritati, A., Halpin, J. A., Whittaker, J. M., Daczko, N. R., & Wainman, C. C. (2021). Provenance of Upper Jurassic–Lower Cretaceous strata in the Mentelle Basin, southwestern Australia, reveals a trans-Gondwanan fluvial pathway. *Gondwana Research, 93*, 128-141. https://doi.org/10.1016/j.gr.2020.12.032

Marschalek, J. W., Zurli, L., Talarico, F., van de Flierdt, T., Vermeesch, P., Carter, A., et al. (2021). A large West Antarctic Ice Sheet explains early Neogene sea-level amplitude. *Nature, 600*(7889), 450-455. https://doi.org/10.1038/s41586-021-04148-0

Marschall, H. R., Hawkesworth, C. J., & Leat, P. T. (2013). Mesoproterozoic subduction under the eastern edge of the Kalahari-Grunehogna Craton preceding Rodinia assembly: The Ritscherflya detrital zircon record, Ahlmannryggen (Dronning Maud Land, Antarctica). *Precambrian Research, 236*, 31-45. https://doi.org/10.1016/j.precamres.2013.07.006

Matsuoka, K. (2011). Pitfalls in radar diagnosis of ice-sheet bed conditions: Lessons from englacial attenuation models. *Geophysical Research Letters, 38*(5). https://doi.org/10.1029/2010GL046205

Mawson, D. (1928). Unsolved Problems of Antarctic Exploration and Research. *American Geographical Society Special Publication, 7*, 253-266.

Mawson, D. (1940). *Sedimentary Rocks, Australasian Antarctic Expedition, 1911-1914, Sci. Rept., Ser. A, Geol., vol. 4, pt. 11, pp. 347-367*. Retrieved from

McCormack, F. S., Roberts, J. L., Dow, C. F., Stål, T., Halpin, J. A., Reading, A. M., & Siegert, M. J. (2022). Fine-Scale Geothermal Heat Flow in Antarctica Can Increase Simulated Subglacial Melt Estimates. *Geophysical Research Letters, 49*(15), e2022GL098539. https://doi.org/10.1029/2022GL098539

McKay, R., Naish, T., Carter, L., Riesselman, C., Dunbar, R., Sjunneskog, C., et al. (2012). Antarctic and Southern Ocean influences on Late Pliocene global cooling. *Proceedings of the National Academy of Sciences of the United States of America, 109*(17), 6423-6428. https://doi.org/10.1073/pnas.1112248109

McKay, R., Naish, T., Powell, R., Barrett, P., Scherer, R., Talarico, F., et al. (2012). Pleistocene variability of Antarctic Ice Sheet extent in the Ross Embayment. *Quaternary Science Reviews, 34*, 93-112. https://doi.org/10.1016/j.quascirev.2011.12.012

McKay, R. M., Barrett, P. J., Levy, R. S., Naish, T. R., Golledge, N. R., & Pyne, A. (2016). Antarctic Cenozoic climate history from sedimentary records: ANDRILL and beyond. *Philosophical Transactions of the Royal Society A: Mathematical, Physical and Engineering Sciences, 374*(2059). https://doi.org/10.1098/rsta.2014.0301

McLean, M. A., Rawling, T. J., Betts, P. G., Phillips, G., & Wilson, C. J. L. (2008). Three-dimensional inversion modelling of a Neoproterozoic basin in the southern Prince Charles Mountains, East Antarctica. *Tectonophysics, 456*(3-4), 180-193. https://doi.org/10.1016/j.tecto.2008.04.023

McLean, M. A., Wilson, C. J. L., Boger, S. D., Betts, P. G., Rawling, T. J., & Damaske, D. (2009). Basement interpretations from airborne magnetic and gravity data over the lambert rift region of east Antarctica. *Journal of Geophysical Research B: Solid Earth, 114*(6). https://doi.org/10.1029/2008JB005650

McLoughlin, S., & Drinnan, A. N. (1997). Revised stratigraphy of the Permian Bainmedart Coal Measures, northern Prince Charles Mountains, East Antarctica. *Geological Magazine, 134*(3), 335-353. https://doi.org/10.1017/S0016756897006870

McMahon, K. L., & Lackie, M. A. (2006). Seismic reflection studies of the Amery Ice Shelf, East Antarctica: delineating meteoric and marine ice. *Geophysical Journal International, 166*(2), 757-766. https://doi.org/10.1111/j.1365-246X.2006.03043.x

Mieth, M., & Jokat, W. (2014). New aeromagnetic view of the geological fabric of southern Dronning Maud Land and Coats Land, East Antarctica. *Gondwana Research, 25*(1), 358-367. https://doi.org/10.1016/j.gr.2013.04.003

Mikhalsky, E. V., Tkacheva, D. A., Skublov, S. G., Leitchenkov, G. L., Rodionov, N. V., Kapitonov, I. N., & Kunakkuzin, E. L. (2020). Low-grade Sandow Group metasediments of the Denman Glacier area (East Antarctica): Chemical composition, age and provenance from U–Pb detrital zircon data, with some palaeotectonic implications. *Polar Science, 26*, 100587. https://doi.org/10.1016/j.polar.2020.100587

Mishra, D. C., Chandra Sekhar, D. V., Venkata Raju, D. C., & Vijaya Kumar, V. (1999). Crustal structure based on gravity-magnetic modelling constrained from seismic studies under Lambert Rift, Antarctica and Godavari and Mahanadi rifts, India and their interrelationship. *Earth and Planetary Science Letters, 172*(3-4), 287-300. https://doi.org/10.1016/S0012-821X(99)00212-5

Montelli, A., Gulick, S. P. S., Fernandez, R., Frederick, B. C., Shevenell, A. E., Leventer, A., & Blankenship, D. D. (2019). Seismic stratigraphy of the Sabrina Coast shelf, East Antarctica: Early history of dynamic meltwater-rich glaciations. *GSA Bulletin, 132*(3-4), 545-561. https://doi.org/10.1130/b35100.1

Morlighem, M. (2020). *MEaSUREs BedMachine Antarctica, Version 2*. https://doi.org/10.5067/E1QL9HFQ7A8M

Morlighem, M., Rignot, E., Binder, T., Blankenship, D., Drews, R., Eagles, G., et al. (2020). Deep glacial troughs and stabilizing ridges unveiled beneath the margins of the Antarctic ice sheet. *Nature Geoscience, 13*(2), 132-137. https://doi.org/10.1038/s41561-019-0510-8

Mouginot, J., Rignot, E., & Scheuchl, B. (2019). Continent-Wide, Interferometric SAR Phase, Mapping of Antarctic Ice Velocity. *Geophysical Research Letters, 46*(16), 9710-9718. https://doi.org/10.1029/2019gl083826

Mulder, J. A., Halpin, J. A., Daczko, N. R., Orth, K., Meffre, S., Thompson, J. M., & Morrissey, L. J. (2019). A Multiproxy provenance approach to uncovering the assembly of East Gondwana in Antarctica. *Geology, 47*(7), 645-649. https://doi.org/10.1130/g45952.1

Müller, R. D., Zahirovic, S., Williams, S. E., Cannon, J., Seton, M., Bower, D. J., et al. (2019). A Global Plate Model Including Lithospheric Deformation Along Major Rifts and Orogens Since the Triassic. *Tectonics, 38*(6), 1884-1907. https://doi.org/10.1029/2018TC005462

Muto, A., Alley, R. B., Parizek, B. R., & Anandakrishnan, S. (2019). Bed-type variability and till (dis)continuity beneath Thwaites Glacier, West Antarctica. *Annals of Glaciology, 60*(80), 82-90. https://doi.org/10.1017/aog.2019.32

Muto, A., Anandakrishnan, S., Alley, R. B., Horgan, H. J., Parizek, B. R., Koellner, S., et al. (2019). Relating bed character and subglacial morphology using seismic data from Thwaites Glacier, West Antarctica. *Earth and Planetary Science Letters, 507*, 199-206. https://doi.org/10.1016/j.epsl.2018.12.008

Muto, A., Peters, L. E., Gohl, K., Sasgen, I., Alley, R. B., Anandakrishnan, S., & Riverman, K. L. (2016). Subglacial bathymetry and sediment distribution beneath Pine Island Glacier ice shelf modeled using aerogravity and in situ geophysical data: New results. *Earth and Planetary Science Letters, 433*, 63-75. https://doi.org/10.1016/j.epsl.2015.10.037

Naish, T., Powell, R., Levy, R., Wilson, G., Scherer, R., Talarico, F., et al. (2009). Obliquity-paced Pliocene West Antarctic ice sheet oscillations. *Nature, 458*(7236), 322-328. https://doi.org/10.1038/nature07867

Naylor, S., Dean, K., & Siegert, M. (2008). The IGY and the ice sheet: surveying Antarctica. *Journal of Historical Geography, 34*(4), 574-595. https://doi.org/10.1016/j.jhg.2008.07.001

Noble, T. L., Rohling, E. J., Aitken, A. R. A., Bostock, H. C., Chase, Z., Gomez, N., et al. (2020). The Sensitivity of the Antarctic Ice Sheet to a Changing Climate: Past, Present, and Future. *Reviews of Geophysics, 58*(4), e2019RG000663. https://doi.org/10.1029/2019RG000663

Olesen, A., Ferraccioli, F., Forsberg, R., Jordan, T., Matsuoka, K., Zakrajsek, A., & Ghidella, M. (2020). *Processed line aerogravity data over the Recovery Lakes region and interior Dronning Maud Land, East Antarctica (2013) [Data set]. UK Polar Data Centre, Natural Environment Research Council, UK Research & Innovation.* https://doi.org/10.5285/28E3B21F-BF4B-46A6-8559-F69D69C63A48

Olierook, H. K. H., Jourdan, F., Merle, R. E., Timms, N. E., Kusznir, N., & Muhling, J. R. (2016). Bunbury Basalt: Gondwana breakup products or earliest vestiges of the Kerguelen mantle plume? *Earth and Planetary Science Letters, 440*, 20-32. https://doi.org/10.1016/j.epsl.2016.02.008

Paden, J., Akins, T., Dunson, D., Allen, C., & Gogineni, P. (2010). Ice-sheet bed 3-D tomography. *Journal of Glaciology, 56*(195), 3-11. https://doi.org/10.3189/002214310791190811

Pappa, F., Ebbing, J., & Ferraccioli, F. (2019). Moho Depths of Antarctica: Comparison of Seismic, Gravity, and Isostatic Results. *Geochemistry, Geophysics, Geosystems, 20*(3), 1629-1645. https://doi.org/10.1029/2018GC008111

Pappa, F., Ebbing, J., Ferraccioli, F., & van der Wal, W. (2019). Modeling Satellite Gravity Gradient Data to Derive Density, Temperature, and Viscosity Structure of the Antarctic Lithosphere. *Journal of Geophysical Research: Solid Earth, 124*(11), 12053-12076. https://doi.org/10.1029/2019jb017997

Paxman, G. J. G., Gasson, E. G. W., Jamieson, S. S. R., Bentley, M. J., & Ferraccioli, F. (2020). Long-Term Increase in Antarctic Ice Sheet Vulnerability Driven by Bed Topography Evolution. *Geophysical Research Letters, 47*(20), e2020GL090003. https://doi.org/10.1029/2020GL090003

Paxman, G. J. G., Jamieson, S. S. R., Ferraccioli, F., Bentley, M. J., Forsberg, R., Ross, N., et al. (2017). Uplift and tilting of the Shackleton Range in East Antarctica driven by glacial erosion and normal faulting. *Journal of Geophysical Research: Solid Earth, 122*(3), 2390-2408. https://doi.org/10.1002/2016JB013841

Paxman, G. J. G., Jamieson, S. S. R., Ferraccioli, F., Jordan, T. A., Bentley, M. J., Ross, N., et al. (2019). Subglacial Geology and Geomorphology of the Pensacola-Pole Basin, East Antarctica. *Geochemistry, Geophysics, Geosystems, 20*(6), 2786-2807. https://doi.org/10.1029/2018gc008126

Paxman, G. J. G., Jamieson, S. S. R., Hochmuth, K., Gohl, K., Bentley, M. J., Leitchenkov, G., & Ferraccioli, F. (2019). Reconstructions of Antarctic topography since the Eocene–Oligocene boundary.

Palaeogeography, Palaeoclimatology, Palaeoecology, 535, 109346. https://doi.org/10.1016/j.palaeo.2019.109346

Pérez, L. F., Santis, L. D., McKay, R. M., Larter, R. D., Ash, J., Bart, P. J., et al. (2021). Early and middle Miocene ice sheet dynamics in the Ross Sea: Results from integrated core-log-seismic interpretation. *GSA Bulletin, 134*(1-2), 348-370. https://doi.org/10.1130/b35814.1

Person, M., Bense, V., Cohen, D., & Banerjee, A. (2012). Models of ice-sheet hydrogeologic interactions: A review. *Geofluids, 12*(1), 58-78. https://doi.org/10.1111/j.1468-8123.2011.00360.x

Person, M., McIntosh, J., Bense, V., & Remenda, V. H. (2007). Pleistocene hydrology of North America: The role of ice sheets in reorganizing groundwater flow systems. *Reviews of Geophysics, 45*(3). https://doi.org/10.1029/2006rg000206

Peters, L. E., Anandakrishnan, S., Alley, R. B., Winberry, J. P., Voigt, D. E., Smith, A. M., & Morse, D. L. (2006). Subglacial sediments as a control on the onset and location of two Siple Coast ice streams, West Antarctica. *Journal of Geophysical Research: Solid Earth, 111*(1). https://doi.org/10.1029/2005jb003766

Peters, M. E., Blankenship, D. D., Carter, S. P., Kempf, S. D., Young, D. A., & Holt, J. W. (2007). Along-Track Focusing of Airborne Radar Sounding Data From West Antarctica for Improving Basal Reflection Analysis and Layer Detection. *IEEE Transactions on Geoscience and Remote Sensing, 45*(9), 2725-2736. https://doi.org/10.1109/tgrs.2007.897416

Phillips, G., & Läufer, A. L. (2009). Brittle deformation relating to the Carboniferous–Cretaceous evolution of the Lambert Graben, East Antarctica: A precursor for Cenozoic relief development in an intraplate and glaciated region. *Tectonophysics, 471*(3–4), 216-224. http://dx.doi.org/10.1016/j.tecto.2009.02.012

Pollard, D., & DeConto, R. M. (2020). Continuous simulations over the last 40 million years with a coupled Antarctic ice sheet-sediment model. *Palaeogeography, Palaeoclimatology, Palaeoecology, 537*, 109374. https://doi.org/10.1016/j.palaeo.2019.109374

Pourpoint, M., Wiens, D., Shen, W., Aster, R. C., Nyblade, A., & Wilson, T. J. (2019). *Constraints on shallow subglacial structure beneath Thwaites Glacier from joint inversion of receiver function and surface wave data. abstract #NS11B-0632*. Paper presented at the AGU Fall Meeting 2019 Abstracts https://ui.adsabs.harvard.edu/abs/2019AGUFMNS11B0632P.

Pyle, M. L., Wiens, D. A., Nyblade, A. A., & Anandakrishnan, S. (2010). Crustal structure of the Transantarctic Mountains near the Ross Sea from ambient seismic noise tomography. *Journal of Geophysical Research: Solid Earth, 115*(11). https://doi.org/10.1029/2009jb007081

Reid, A. B. (1980). Aeromagnetic survey design. *GEOPHYSICS, 45*(5), 973-976. https://doi.org/10.1190/1.1441102

Reid, A. B., Allsop, J. M., Granser, H., Millett, A. J., & Somerton, I. W. (1990). Magnetic interpretation in three dimensions using Euler deconvolution. *GEOPHYSICS, 55*(1), 80-91. https://doi.org/10.1190/1.1442774

Riedel, S., Jacobs, J., & Jokat, W. (2013). Interpretation of new regional aeromagnetic data over Dronning Maud Land (East Antarctica). *Tectonophysics, 585*, 161-171. https://doi.org/10.1016/j.tecto.2012.10.011

Riedel, S., Jokat, W., & Steinhage, D. (2012). Mapping tectonic provinces with airborne gravity and radar data in Dronning Maud Land, East Antarctica. *Geophysical Journal International, 189*(1), 414-427. https://doi.org/10.1111/j.1365-246X.2012.05363.x

Riley, T. R., Flowerdew, M. J., & Whitehouse, M. J. (2012). Chrono- and lithostratigraphy of a Mesozoic-Tertiary fore- to intra-arc basin: Adelaide Island, Antarctic Peninsula. *Geological Magazine, 149*(5), 768-782. https://doi.org/10.1017/S0016756811001002

Riley, T. R., Jordan, T. A., Leat, P. T., Curtis, M. L., & Millar, I. L. (2020). Magmatism of the Weddell Sea rift system in Antarctica: Implications for the age and mechanism of rifting and early stage Gondwana breakup. *Gondwana Research, 79*, 185-196. https://doi.org/10.1016/j.gr.2019.09.014

Rippin, D. M., Bingham, R. G., Jordan, T. A., Wright, A. P., Ross, N., Corr, H. F. J., et al. (2014). Basal roughness of the Institute and Möller Ice Streams, West Antarctica: Process determination and landscape interpretation. *Geomorphology, 214*, 139-147. https://doi.org/10.1016/j.geomorph.2014.01.021

Robin, G. d. Q. (1958). Glaciology III: Seismic Shooting and Related Investigations. *Norwegian–British–Swedish Antarctic Expedition, 1949–52, Scientific Results, 5*.

Rogenhagen, J., Jokat, W., Hinz, K., & Kristoffersen, Y. (2004). Improved seismic stratigraphy of the Mesozoic Weddell Sea. *Marine Geophysical Research, 25*(3-4), 265-282. https://doi.org/10.1007/s11001-005-1335-y

Rolland, Y., Bernet, M., van der Beek, P., Gautheron, C., Duclaux, G., Bascou, J., et al. (2019). Late Paleozoic Ice Age glaciers shaped East Antarctica landscape. *Earth and Planetary Science Letters, 506*, 123-133. https://doi.org/10.1016/j.epsl.2018.10.044

Rosier, S. H. R., Hofstede, C., Brisbourne, A. M., Hattermann, T., Nicholls, K. W., Davis, P. E. D., et al. (2018). A New Bathymetry for the Southeastern Filchner-Ronne Ice Shelf: Implications for Modern Oceanographic Processes and Glacial History. *Journal of Geophysical Research: Oceans, 123*(7), 4610-4623. https://doi.org/10.1029/2018jc013982

Ruppel, A., Jacobs, J., Eagles, G., Läufer, A., & Jokat, W. (2018). New geophysical data from a key region in East Antarctica: Estimates for the spatial extent of the Tonian Oceanic Arc Super Terrane (TOAST). *Gondwana Research, 59*, 97-107. https://doi.org/10.1016/j.gr.2018.02.019

Salvini, F., Brancolini, G., Busetti, M., Storti, F., Mazzarini, F., & Coren, F. (1997). Cenozoic geodynamics of the Ross Sea region, Antarctica: Crustal extension, intraplate strike-slip faulting, and tectonic inheritance. *Journal of Geophysical Research B: Solid Earth, 102*(11), 24669-24696. https://doi.org/10.1029/97jb01643

Sanchez, G., Halpin, J. A., Gard, M., Hasterok, D., Stål, T., Raimondo, T., et al. (2021). PetroChron Antarctica: A Geological Database for Interdisciplinary Use. *Geochemistry, Geophysics, Geosystems, 22*(12). https://doi.org/10.1029/2021gc010154

Sandwell, D. T., Müller, R. D., Smith, W. H. F., Garcia, E., & Francis, R. (2014). New global marine gravity model from CryoSat-2 and Jason-1 reveals buried tectonic structure. *Science, 346*(6205), 65-67. https://doi.org/10.1126/science.1258213

Sauermilch, I., Whittaker, J. M., Bijl, P. K., Totterdell, J. M., & Jokat, W. (2019). Tectonic, Oceanographic, and Climatic Controls on the Cretaceous-Cenozoic Sedimentary Record of the Australian-Antarctic Basin. *Journal of Geophysical Research: Solid Earth, 124*(8), 7699-7724. https://doi.org/10.1029/2018JB016683

Sauli, C., Sorlien, C., Busetti, M., De Santis, L., Geletti, R., Wardell, N., & Luyendyk, B. P. (2021). Neogene Development of the Terror Rift, Western Ross Sea, Antarctica. *Geochemistry, Geophysics, Geosystems, 22*(3). https://doi.org/10.1029/2020GC009076

Scambos, T. A., Bell, R. E., Alley, R. B., Anandakrishnan, S., Bromwich, D. H., Brunt, K., et al. (2017). How much, how fast?: A science review and outlook for research on the instability of Antarctica's Thwaites Glacier in the 21st century. *Global and Planetary Change, 153*, 16-34. https://doi.org/10.1016/j.gloplacha.2017.04.008

Scanlan, K. M., Buhl, D. P., & Blankenship, D. D. (2022). Polarimetric Airborne Radar Sounding as an Approach to Characterizing Subglacial Röthlisberger Channels. *IEEE Journal of Selected Topics in Applied Earth Observations and Remote Sensing, 15*, 4455-4467. https://doi.org/10.1109/JSTARS.2022.3174473

Scheinert, M., Ferraccioli, F., Schwabe, J., Bell, R., Studinger, M., Damaske, D., et al. (2016). New Antarctic gravity anomaly grid for enhanced geodetic and geophysical studies in Antarctica. *Geophysical Research Letters, 43*(2), 600-610. https://doi.org/10.1002/2015gl067439

Scher, H. D., & Martin, E. E. (2006). Timing and climatic consequences of the opening of Drake Passage. *Science, 312*(5772), 428-430. https://doi.org/10.1126/science.1120044

Scher, H. D., Whittaker, J. M., Williams, S. E., Latimer, J. C., Kordesch, W. E. C., & Delaney, M. L. (2015). Onset of Antarctic Circumpolar Current 30 million years ago as Tasmanian Gateway aligned with westerlies. *Nature, 523*(7562), 580-583. https://doi.org/10.1038/nature14598

Schoof, C. (2010). Ice-sheet acceleration driven by melt supply variability. *Nature, 468*(7325), 803-806. https://doi.org/10.1038/nature09618

Schroeder, D. M., Bingham, R. G., Blankenship, D. D., Christianson, K., Eisen, O., Flowers, G. E., et al. (2020). Five decades of radioglaciology. *Annals of Glaciology, 61*(81), 1-13. https://doi.org/10.1017/aog.2020.11

Schroeder, D. M., Blankenship, D. D., Raney, R. K., & Grima, C. (2015). Estimating Subglacial Water Geometry Using Radar Bed Echo Specularity: Application to Thwaites Glacier, West Antarctica. *IEEE Geoscience and Remote Sensing Letters, 12*(3), 443-447. https://doi.org/10.1109/lgrs.2014.2337878

Schroeder, D. M., Blankenship, D. D., & Young, D. A. (2013). Evidence for a water system transition beneath Thwaites Glacier, West Antarctica. *Proceedings of the National Academy of Sciences, 110*(30), 12225-12228. https://doi.org/10.1073/pnas.1302828110

Schroeder, D. M., Dowdeswell, J. A., Siegert, M. J., Bingham, R. G., Chu, W., MacKie, E. J., et al. (2019). Multidecadal observations of the Antarctic ice sheet from restored analog radar records. *Proceedings of the National Academy of Sciences, 116*(38), 18867-18873. https://doi.org/10.1073/pnas.1821646116

Shapiro, N. M., Campillo, M., Stehly, L., & Ritzwoller, M. H. (2005). High-Resolution Surface-Wave Tomography from Ambient Seismic Noise. *Science, 307*(5715), 1615-1618. https://doi.org/10.1126/science.1108339

Shen, W., Wiens, D., Stern, T., Anandakrishnan, S., Aster, R., Dalziel, I., et al. (2017). Seismic evidence for lithospheric foundering beneath the southern Transantarctic Mountains, Antarctica. *Geology, 46*. https://doi.org/10.1130/G39555.1

Shen, W., Wiens, D. A., Anandakrishnan, S., Aster, R. C., Gerstoft, P., Bromirski, P. D., et al. (2018). The Crust and Upper Mantle Structure of Central and West Antarctica From Bayesian Inversion of Rayleigh Wave and Receiver Functions. *Journal of Geophysical Research: Solid Earth, 123*(9), 7824-7849. https://doi.org/10.1029/2017jb015346

Shepherd, T., Bamber, J. L., & Ferraccioli, F. (2006). Subglacial geology in Coats Land, East Antarctica, revealed by airborne magnetics and radar sounding. *Earth and Planetary Science Letters, 244*(1), 323-335. https://doi.org/10.1016/j.epsl.2006.01.068

Siddoway, C. S. (2008). Tectonics of the West Antarctic Rift System: new light on the history and dynamics of distributed intracontinental extension. *Antarctica: A keystone in a changing world*, 91-114. https://doi.org/10.3133/ofr20071047KP09

Siddoway, C. S., Baldwin, S. L., Fitzgerald, P. G., Fanning, C. M., & Luyendyk, B. P. (2004). Ross Sea mylonites and the timing of intracontinental extension within the West Antarctic rift system. *Geology, 32*(1), 57-60. https://doi.org/10.1130/G20005.1

Siegert, M., Popov, S., & Studinger, M. (2011). Vostok Subglacial Lake: A Review of Geophysical Data Regarding Its Discovery and Topographic Setting. *Washington DC American Geophysical Union Geophysical Monograph Series, 192*, 45-60. https://doi.org/10.1029/2010GM000934

Siegert, M. J., Kulessa, B., Bougamont, M., Christoffersen, P., Key, K., Andersen, K. R., et al. (2018). Antarctic subglacial groundwater: A concept paper on its measurement and potential influence on ice flow. *Geological Society Special Publication, 461*, 197-213. https://doi.org/10.1144/sp461.8

Siegert, M. J., Ross, N., Li, J., Schroeder, D. M., Rippin, D., Ashmore, D., et al. (2016). Subglacial controls on the flow of Institute Ice Stream, West Antarctica. *Annals of Glaciology, 57*(73), 19-24. https://doi.org/10.1017/aog.2016.17

Siegert, M. J., Taylor, J., & Payne, A. J. (2005). Spectral roughness of subglacial topography and implications for former ice-sheet dynamics in East Antarctica. *Global and Planetary Change, 45*(1), 249-263. https://doi.org/10.1016/j.gloplacha.2004.09.008

Smellie, J. L., & Collerson, K. D. (2021). Chapter 5.5 Gaussberg: volcanology and petrology. *Volcanism in Antarctica: 200 Million Years of Subduction, Rifting and Continental Break-up*, 0. https://doi.org/10.1144/m55-2018-85

Smith, A. M. (1997). Basal conditions on Rutford Ice Stream, West Antarctica, from seismic observations. *Journal of Geophysical Research: Solid Earth, 102*(B1), 543-552. https://doi.org/10.1029/96JB02933

Smith, A. M., Jordan, T. A., Ferraccioli, F., & Bingham, R. G. (2013). Influence of subglacial conditions on ice stream dynamics: Seismic and potential field data from Pine Island Glacier, West Antarctica. *Journal of Geophysical Research: Solid Earth, 118*(4), 1471-1482. https://doi.org/10.1029/2012jb009582

Smith, C., Warny, S., Shevenell, A. E., Gulick, S. P. S., & Leventer, A. (2019). New species from the Sabrina Flora: an early Paleogene pollen and spore assemblage from the Sabrina Coast, East Antarctica. *Palynology, 43*(4), 650-659. https://doi.org/10.1080/01916122.2018.1471422

Smith, E. C., Hattermann, T., Kuhn, G., Gaedicke, C., Berger, S., Drews, R., et al. (2020). Detailed Seismic Bathymetry Beneath Ekström Ice Shelf, Antarctica: Implications for Glacial History and Ice-Ocean Interaction. *Geophysical Research Letters, 47*(10), e2019GL086187. https://doi.org/10.1029/2019GL086187

Smith, J. A., Graham, A. G. C., Post, A. L., Hillenbrand, C.-D., Bart, P. J., & Powell, R. D. (2019). The marine geological imprint of Antarctic ice shelves. *Nature Communications, 10*(1), 5635. https://doi.org/10.1038/s41467-019-13496-5

Song, T., & Cawood, P. A. (2000). Structural styles in the Perth Basin associated with the Mesozoic break-up of Greater India and Australia. *Tectonophysics, 317*(1-2), 55-72. https://doi.org/10.1016/S0040-1951(99)00273-5

Stagg, H., Colwel, J., Direen, N., O'Brien, P., Bernardel, G., Borissova, I., et al. (2004). Geology of the Continental Margin of Enderby and Mac. Robertson Lands, East Antarctica: Insights from a Regional Data Set. *Marine Geophysical Researches, 25*, 183-219. https://doi.org/10.1007/s11001-005-1316-1

Stål, T., Reading, A. M., Halpin, J. A., & Whittaker, J. M. (2019). A Multivariate Approach for Mapping Lithospheric Domain Boundaries in East Antarctica. *Geophysical Research Letters, 46*(17-18), 10404-10416. https://doi.org/10.1029/2019GL083453

Straume, E. O., Gaina, C., Medvedev, S., Hochmuth, K., Gohl, K., Whittaker, J. M., et al. (2019). GlobSed: Updated Total Sediment Thickness in the World's Oceans. *Geochemistry, Geophysics, Geosystems, 20*(4), 1756-1772. https://doi.org/10.1029/2018GC008115

Studinger, M., Bell, R., & Frearson, N. (2008). Comparison of AIRGrav and GT-1A airborne gravimeters for research applications. *GEOPHYSICS, 73*(6), I51-I61. https://doi.org/10.1190/1.2969664

Studinger, M., Bell, R. E., Blankenship, D. D., Finn, C. A., Arko, R. A., Morse, D. L., & Joughin, I. (2001). Subglacial sediments: A regional geological template for iceflow in West Antarctica. *Geophysical Research Letters, 28*(18), 3493-3496. https://doi.org/10.1029/2000GL011788

Studinger, M., Bell, R. E., Buck, W. R., Karner, G. D., & Blankenship, D. D. (2004). Sub-ice geology inland of the Transantarctic Mountains in light of new aerogeophysical data. *Earth and Planetary Science Letters, 220*(3-4), 391-408. https://doi.org/10.1016/S0012-821X(04)00066-4

Studinger, M., Karner, G. D., Bell, R. E., Levin, V., Raymond, C. A., & A. Tikku, A. (2003). Geophysical models for the tectonic framework of the Lake Vostok region, East Antarctica. *Earth and Planetary Science Letters, 216*(4), 663-677. https://doi.org/10.1016/S0012-821X(03)00548-X

Swink, M., & Speier, C. (1999). Presenting geographic information: effects of data aggregation, dispersion, and users' spatial orientation. *Decision sciences, 30*(1), 169-195. https://doi.org/10.1111/j.1540-5915.1999.tb01605.x

Tabacco, I. E., Cianfarra, P., Forieri, A., Salvini, F., & Zirizotti, A. (2006). Physiography and tectonic setting of the subglacial lake district between Vostok and Belgica subglacial highlands (Antarctica). *Geophysical Journal International, 165*(3), 1029-1040. https://doi.org/10.1111/j.1365-246X.2006.02954.x

Talalay, P., Li, X., Zhang, N., Fan, X., Sun, Y., Cao, P., et al. (2021). Antarctic subglacial drilling rig: Part II. Ice and Bedrock Electromechanical Drill (IBED). *Annals of Glaciology, 62*(84), 12-22. https://doi.org/10.1017/aog.2020.38

Tankersley, M. D., Horgan, H. J., Siddoway, C. S., Caratori Tontini, F., & Tinto, K. J. (2022). Basement Topography and Sediment Thickness Beneath Antarctica's Ross Ice Shelf. *Geophysical Research Letters, 49*(10), e2021GL097371. https://doi.org/10.1029/2021GL097371

Teisberg, T. O., Schroeder, D. M., Broome, A. L., Lurie, F., & Woo, D. (2022, 17-22 July 2022). *Development of a Uav-Borne Pulsed ICE-Penetrating Radar System.* Paper presented at the IGARSS 2022 - 2022 IEEE International Geoscience and Remote Sensing Symposium. https://doi.org/10.1109/IGARSS46834.2022.9883583

Thomson, S. N., Reiners, P. W., Hemming, S. R., & Gehrels, G. E. (2013). The contribution of glacial erosion to shaping the hidden landscape of East Antarctica. *Nature Geoscience, 6*(3), 203-207. https://doi.org/10.1038/ngeo1722

Tinto, K. J., Padman, L., Siddoway, C. S., Springer, S. R., Fricker, H. A., Das, I., et al. (2019). Ross Ice Shelf response to climate driven by the tectonic imprint on seafloor bathymetry. *Nature Geoscience, 12*(6), 441-449. https://doi.org/10.1038/s41561-019-0370-2

Tochilin, C. J., Reiners, P. W., Thomson, S. N., Gehrels, G. E., Hemming, S. R., & Pierce, E. L. (2012). Erosional history of the Prydz Bay sector of East Antarctica from detrital apatite and zircon geo-and thermochronology multidating. *Geochemistry, Geophysics, Geosystems, 13*(11). https://doi.org/10.1029/2012GC004364

Trey, H., Cooper, A. K., Pellis, G., Della Vedova, B., Cochrane, G., Brancolini, G., & Makris, J. (1999). Transect across the West Antarctic rift system in the Ross Sea, Antarctica. *Tectonophysics, 301*(1-2), 61-74. https://doi.org/10.1016/s0040-1951(98)00155-3

Tuckett, P. A., Ely, J. C., Sole, A. J., Livingstone, S. J., Davison, B. J., Melchior van Wessem, J., & Howard, J. (2019). Rapid accelerations of Antarctic Peninsula outlet glaciers driven by surface melt. *Nature Communications, 10*(1). https://doi.org/10.1038/s41467-019-12039-2

Tulaczyk, S. M., & Foley, N. T. (2020). The role of electrical conductivity in radar wave reflection from glacier beds. *The Cryosphere, 14*(12), 4495-4506. https://doi.org/10.5194/tc-14-4495-2020

Turchetti, S., Dean, K., Naylor, S., & Siegert, M. (2008). Accidents and Opportunities: A History of the Radio Echo-Sounding of Antarctica, 1958-79. *The British Journal for the History of Science, 41*(3), 417-444. https://doi.org/10.1017/S0007087408000903

van de Lagemaat, S. H. A., Swart, M. L. A., Vaes, B., Kosters, M. E., Boschman, L. M., Burton-Johnson, A., et al. (2021). Subduction initiation in the Scotia Sea region and opening of the Drake Passage: When and why? *Earth-Science Reviews, 215*, 103551. https://doi.org/10.1016/j.earscirev.2021.103551

van Wyk de Vries, M., Bingham, R. G., Hein, A. S., Siegert, M. J., Jamieson, S. S. R., & White, D. A. (2018). A new volcanic province: an inventory of subglacial volcanoes in West Antarctica. In *Exploration of Subsurface Antarctica: Uncovering Past Changes and Modern Processes* (Vol. 461, pp. 0): The Geological Society of London. https://doi.org/10.1144/sp461.7

Vaughan, D. G., Corr, H. F. J., Smith, A. M., Pritchard, H. D., & Shepherd, A. (2008). Flow-switching and water piracy between Rutford ice stream and Carlson inlet, West Antarctica. *Journal of Glaciology, 54*(184), 41-48. https://doi.org/10.3189/002214308784409125

Vaughan, D. G., Smith, A. M., Nath, P. C., & Meur, E. L. (2003). Acoustic impedance and basal shear stress beneath four Antarctic ice streams. *Annals of Glaciology, 36*, 225-232. https://doi.org/10.3189/172756403781816437

Voigt, D. E., Peters, L. E., & Anandakrishnan, S. (2013). 'Georods': the development of a four-element geophone for improved seismic imaging of glaciers and ice sheets. *Annals of Glaciology, 54*(64), 142-148. https://doi.org/10.3189/2013AoG64A432

Wannamaker, P., Hill, G., Stodt, J., Maris, V., Ogawa, Y., Selway, K., et al. (2017). Uplift of the central Transantarctic Mountains. *Nature Communications, 8*(1), 1588. https://doi.org/10.1038/s41467-017-01577-2

Wannamaker, P. E., Stodt, J. A., Pellerin, L., Olsen, S. L., & Hall, D. B. (2004). Structure and thermal regime beneath the South Pole region, East Antarctica, from magnetotelluric measurements. *Geophysical Journal International, 157*(1), 36-54. https://doi.org/10.1111/j.1365-246X.2004.02156.x

Wei, W., Blankenship, D. D., Greenbaum, J. S., Gourmelen, N., Dow, C. F., Richter, T. G., et al. (2020). Getz Ice Shelf melt enhanced by freshwater discharge from beneath the West Antarctic Ice Sheet. *The Cryosphere, 14*(4), 1399-1408. https://doi.org/10.5194/tc-14-1399-2020

Wenman, C. P., Harry, D. L., & Jha, S. (2020). Post Middle Miocene Tectonomagmatic and Stratigraphic Evolution of the Victoria Land Basin, West Antarctica. *Geochemistry, Geophysics, Geosystems, 21*(3). https://doi.org/10.1029/2019GC008568

Whitehead, J., Quilty, P., Mckelvey, B. C., & O'Brien, P. (2006). A review of the Cenozoic stratigraphy and glacial history of the Lambert Graben—Prydz Bay region, East Antarctica. *Antarctic Science, 18*(1), 83-99. https://doi.org/10.1017/S0954102006000083

Willan, R. C. R. (2003). Provenance of Triassic-Cretaceous sandstones in the Antarctic Peninsula: Implications for terrane models during Gondwana breakup. *Journal of Sedimentary Research, 73*(6), 1062-1077. https://doi.org/10.1306/050103731062

Williams, S. E., Whittaker, J. M., Granot, R., & Müller, D. R. (2013). Early India-Australia spreading history revealed by newly detected Mesozoic magnetic anomalies in the Perth Abyssal Plain. *Journal of Geophysical Research: Solid Earth, 118*(7), 3275-3284. https://doi.org/10.1002/jgrb.50239

Williams, S. E., Whittaker, J. M., Halpin, J. A., & Müller, R. D. (2019). Australian-Antarctic breakup and seafloor spreading: Balancing geological and geophysical constraints. *Earth-Science Reviews, 188*, 41-58. https://doi.org/10.1016/j.earscirev.2018.10.011

Wilson, C. G., Bond, C. E., & Shipley, T. F. (2019). How can geologic decision-making under uncertainty be improved? *Solid Earth, 10*(5), 1469-1488. https://doi.org/10.5194/se-10-1469-2019

Wilson, D. S., Jamieson, S. S. R., Barrett, P. J., Leitchenkov, G., Gohl, K., & Larter, R. D. (2012). Antarctic topography at the Eocene-Oligocene boundary. *Palaeogeography, Palaeoclimatology, Palaeoecology, 335-336*, 24-34. https://doi.org/10.1016/j.palaeo.2011.05.028

Wilson, D. S., & Luyendyk, B. P. (2006). Bedrock platforms within the Ross Embayment, West Antarctica: Hypotheses for ice sheet history, wave erosion, Cenozoic extension, and thermal subsidence. *Geochemistry, Geophysics, Geosystems, 7*(12). https://doi.org/10.1029/2006GC001294

Wilson, G., Damaske, D., Moller, H. D., Tinto, K., & Jordan, T. (2007). The geological evolution of southern McMurdo Sound - New evidence from a high-resolution aeromagnetic survey. *Geophysical Journal International, 170*(1), 93-100. https://doi.org/10.1111/j.1365-246X.2007.03395.x

Wilson, T. J. (1999). Cenozoic structural segmentation of the Transantarctic Mountains rift flank in southern Victoria Land. *Global and Planetary Change, 23*(1-4), 105-127. https://doi.org/10.1016/S0921-8181(99)00053-3

Wright, A. P., Siegert, M. J., Le Brocq, A. M., & Gore, D. B. (2008). High sensitivity of subglacial hydrological pathways in Antarctica to small ice-sheet changes. *Geophysical Research Letters, 35*(17). https://doi.org/10.1029/2008GL034937

Yakymchuk, C., Brown, C. R., Brown, M., Siddoway, C. S., Fanning, C. M., & Korhonen, F. J. (2015). Paleozoic evolution of western Marie Byrd Land, Antarctica. *Bulletin of the Geological Society of America, 127*(9-10), 1464-1484. https://doi.org/10.1130/b31136.1

Young, A., Flament, N., Maloney, K., Williams, S., Matthews, K., Zahirovic, S., & Müller, R. D. (2019). Global kinematics of tectonic plates and subduction zones since the late Paleozoic Era. *Geoscience Frontiers, 10*(3), 989-1013. https://doi.org/10.1016/j.gsf.2018.05.011

Young, D. A., Blankenship, D. D., & Holt, J. W. (2017a). *Gravity disturbance data over central Marie Byrd Land, West Antarctica (GIMBLE.GGCMG2) U.S. Antarctic Program (USAP) Data Center https://doi.org/10.15784/601003*. https://doi.org/10.15784/601003.

Young, D. A., Blankenship, D. D., & Holt, J. W. (2017b). *Magnetic anomaly data over central Marie Byrd Land, West Antarctica (GIMBLE.GMGEO2) U.S. Antarctic Program (USAP) Data Center. doi: https://doi.org/10.15784/601002*. https://doi.org/10.15784/601002.

Young, D. A., Schroeder, D. M., Blankenship, D. D., Kempf, S. D., & Quartini, E. (2016). The distribution of basal water between Antarctic subglacial lakes from radar sounding. *Philosophical Transactions of the Royal Society A: Mathematical, Physical and Engineering Sciences, 374*(2059). https://doi.org/10.1098/rsta.2014.0297

Young, T. J., Schroeder, D. M., Christoffersen, P., Lok, L. B., Nicholls, K. W., Brennan, P. V., et al. (2018). Resolving the internal and basal geometry of ice masses using imaging phase-sensitive radar. *Journal of Glaciology, 64*(246), 649-660. https://doi.org/10.1017/jog.2018.54

Zhang, Y., Person, M., Voller, V., Cohen, D., McIntosh, J., & Grapenthin, R. (2018). Hydromechanical Impacts of Pleistocene Glaciations on Pore Fluid Pressure Evolution, Rock Failure, and Brine Migration Within Sedimentary Basins and the Crystalline Basement. *Water Resources Research, 54*(10), 7577-7602. https://doi.org/10.1029/2017wr022464

Zhou, Z., Wiens, D. A., Shen, W., Aster, R. C., Nyblade, A., & Wilson, T. J. (2022). Radial Anisotropy and Sediment Thickness of West and Central Antarctica Estimated From Rayleigh and Love Wave Velocities. *Journal of Geophysical Research: Solid Earth, 127*(3), e2021JB022857. https://doi.org/10.1029/2021JB022857

11 Figure Captions

Figure 1: a) Map of representative data coverage in Antarctica indicating outcropping geology (Cox et al., 2023) and locations of onshore and offshore drill core sites, onshore passive seismic stations, MT surveys (Hill, 2020), and active seismic surveys (line centroids) and marine seismic reflection lines. Bedmap3 data coverage mostly represents the presence of airborne RES data (Frémand, Fretwell, et al., 2022), and not all surveys measured gravity or magnetic data. A close-up of the data-rich Ross Island area is available in Figure S1. b) Approaches to detection and characterization of sedimentary basins, including the direct characterization of rocks from drillcore and outcrop, and indirect characterization from geophysical data. MT – magnetotelluric, RES – Radio Echo Sounding, UAV- Unmanned Aerial Vehicle, AUV – Autonomous Underwater Vehicle. Modified from Kennicutt et al. (2019).

Figure 2: Key models and datasets for defining basin distribution in Antarctica including a) model of sedimentary basin likelihood from machine learning (Li et al., 2022), b) along-track roughness using airborne RES data compiled from Eisen et al. (2020) and additional data. Along track roughness ν was calculated using a spatial technique as in Eisen et al. (2020), c) bed elevation and d) its large-scale spatial variability defined as standard deviation in a 30 km by 30 km window; both from BedMachine Antarctica (M. Morlighem, 2020). e) Airy isostatic residual gravity anomaly and f) spatial variability (standard deviation, 30 km window) of Bouguer gravity anomaly. Gravity data after AntGG (Scheinert et al., 2016) and additional data (Forsberg et al., 2018; Kvas et al., 2021; Olesen et al., 2020; G. J. G. Paxman et al., 2019; Sandwell et al., 2014; Tinto et al., 2019; D. A. Young et al., 2017a) g) magnetic field intensity anomaly and h) its large-scale spatial variability (standard deviation, 30 km window). Magnetic data after ADMAP-2 (A. V. Golynsky et al., 2018) and additional data (F. Ferraccioli et al., 2020; Forsberg et al., 2018; G. J. G. Paxman et al., 2019; Tinto et al., 2019; D. A. Young et al., 2017b). Major sedimentary basin regions used for classification are outlined. CWA – Central West Antarctica, EW – Ellsworth Whitmore, SC – Siple Coast, CL, TAM – Transantarctic Mountains, DML-Dronning Maud Land, GSM – Gamburtsev Subglacial Mountains, EML- Enderby-Mac Robertson Land, PEL – Princess Elizabeth Land, QML – Queen Mary Land, LD – Law Dome.

Figure 3: Classification of geological bed type in Antarctica showing the main classes of Type 1 and Type 2 basins, intra-basin volcanics, and crystalline basement, as well as regions of mixed class. Major sedimentary

basin regions are outlined in grey. The coastline shows both the ice sheet grounding line and the ice shelf edge. Dashed lines A, B and C indicate locations of annular profiles (Fig 6). PL – Palmer Land, RFIS – Ronne-Filchner Ice Shelf, BI – Berkner Island, HG – Haag Block, EWM – Ellsworth Whitmore Mountains, PM – Pensacola Mountains, BSB – Byrd Subglacial Basin, MBL – Marie Byrd Land IB – Iselin Bank, CL – Coats Land, PPB – Pensacola-Pole Basin, RB – Recovery Basin, RSH – Recovery Subglacial Highlands, JS – Jutulstraumen, DML-Dronning Maud Land, WRT-West Ragnhild Trough, FSH – Fuji Subglacial Highlands, AIS – Amery Ice Shelf, SPCM – Southern Prince Charles Mountains, GSM – Gamburtsev Subglacial Mountains, SPB – South Pole Basin, LV – Lake Vostok, ASB – Aurora Subglacial Basin, VSB – Vincennes Subglacial Basin, WSB – Wilkes Subglacial Basin. An unannotated version of this figure is available in Figure S2.

Figure 4: Relative effect sizes for selected datasets for a) crystalline basement vs Type 1 basins, b) crystalline basement vs Type 2 basins, c) Type 1 basins vs Type 2 basins. For each, datasets are ordered by Cohen's effect size indicating the ability of the dataset to discriminate those classes. The listing on the right highlights the datasets in rank order. Effect sizes above 0.8 may be considered a large effect, and below 0.5 a small effect.

Figure 5: Interpreted ages for a) the base of the basin sequence and b) the top of the basin sequence. Locations of selected age information for volcanic, sedimentary, and metasedimentary rocks are derived from PetroChron Antarctica (Sanchez et al., 2021), and broadly indicate where basin ages are better constrained.

Figure 6: Annular profiles of basin structure. a) shows the location of the three profiles A, B and C (see also Figure 3) at latitudes of 82.5°S, 77.5°S and 72.5°S. b), c) and d) show the profile data for profiles A, B and C respectively including in the upper panel the basin likelihood model of (Li et al., 2022). The lower panel shows bed topography (M. Morlighem, 2020) and base-of-basin elevation for several basin thickness model (Baranov et al., 2021; Haeger & Kaban, 2019; K. Hochmuth et al., 2020; Lindeque, Gohl, Wobbe, et al., 2016; Straume et al., 2019; Tankersley et al., 2022; Zhou et al., 2022). SPB – South Pole Basin, WSB – Wilkes Subglacial Basin, VH- Vostok Highlands, TAH – Terre Adelie Highlands TAM – Transantarctic Mountains, EWM – Ellsworth Whitmore Mountains, PM – Pensacola Mountains, RSH – Recovery Subglacial Highlands, GSM – Gamburtsev Subglacial Mountains, ASB – Aurora Subglacial Basin, MBL – Marie Byrd Land, LV – Lake Vostok, BI- Berkner Island, CL – Coats Land, FSH – Fuji Subglacial Highland, SPCM – Southern Prince Charles Mountains, VSB – Vincennes Subglacial Basin, IB – Iselin Bank, TI – Thurston Island, PL – Palmer Land, JS – Jutulstraumen, WRT-West Ragnhild Trough, AIS – Amery Ice Shelf.

Figure 7: Sedimentary basins of the Ross Sea and Siple Coast regions, showing basin regions and reinterpreted basin structures, rift parallel (blue) and transverse (red). Basin faults are reinterpreted from prior studies (Fred J. Davey et al., 2021; Lindeque, Gohl, Wobbe, et al., 2016; Pérez et al., 2021; Sauli et al.,

2021; M. Studinger et al., 2001; Tankersley et al., 2022; D. S. Wilson et al., 2012; T. J. Wilson, 1999). Also shown are the interpreted East Antarctica-West Antarctica basement boundary (black) (Tinto et al., 2019), and the seismically defined extents of thick basin cover (Zhou et al., 2022) (purple). UMB – Upstream MacAyeal Basin, MB- MacAyeal Basin, TD- Trunk D Basin, ACB – Amundsen Coast Basin, CT- Crary Trough, SDB- Siple Dome Basin, TR – Terror Rift, VLB – Victoria Land Basin, P3 – Polar 3 Anomaly, RI – Roosevelt Island, SG – Shackleton Glacier, SMIS – Southern McMurdo Ice Shelf, NG – Nimrod Glacier, BG – Byrd Glacier, CW – Cape Washington, DG – David Glacier, E- Erebus

Figure 8: Sedimentary basins of the a) Central West Antarctica and b) Antarctic Peninsula Drake and eastern Weddell Sea regions. Structures in a) are reinterpreted from prior studies (Bell et al., 1998; Bingham et al., 2012; Haeger & Kaban, 2019; Jordan, Ferraccioli, Ross, et al., 2013; Jordan, Ferraccioli, Vaughan, et al., 2010; Jordan et al., 2020; M. Studinger et al., 2001) as associated with the WARS (blue) and WSRS (red). PI – Pine Island Rift Basin, FR – Ferrigno Rift, BSB – Byrd Subglacial Basin, BST – Bentley Subglacial Trough, EWM- Ellsworth Whitmore Mountains, SR – Sinuous Ridge, PSZ – Pagano Shear Zone, SST – South Shetland Trench, BB – Bransfield Basin, PB – Powell Basin, JB – Jane Basin, SOS – South Orkney Shelf, TPG – Trinity Peninsula Group, LMG – LeMay Group, JRB – James Ross Basin.

Figure 9: Sedimentary basins of the Weddell and Weddell Coast regions. Structures are reinterpreted from prior studies including (Bamber et al., 2006; F. Ferraccioli, Jones, Curtis, Leat, et al., 2005; Jones et al., 2002; T. A. Jordan et al., 2017; Jordan, Ferraccioli, Ross, et al., 2013; G. J. G. Paxman et al., 2017; G. J. G. Paxman et al., 2019; Riedel et al., 2012). Blue lines indicate structures parallel with the SWRS, Red lines structures aligned transverse to the SWRS, parallel to the Pagano Shear Zone. Orange lines indicate structures of other orientations. Purple lines indicate magnetic trends of the NWRS including the Orion and Explora Anomalies. ER- Evans Rift, RR- Rutford Rift, EWM – Ellsworth Whitmore Mountains, WRA – Weddell Rift Anomaly, BIR – Bungenstock Ice Rise, FB – Foundation Basin, PR Patuxent Range, PM – Pensacola Mountains, AR – Argentina Range, SR-Shackleton Range, TM – Theron Mountains, U&A – Urfjell and Amelang Groups, PT- Pencksokket Trough, RSG – Ritscherflya Supergroup, JS – Jutulstraumen, FIS – Fimbul Ice Shelf

Figure 10: Sedimentary basins of the Enderby-Mac. Robertson and Lambert regions. Red structures indicate structures aligned with the main north-south Lambert Rift trend while purple structures are aligned with the east-west trend. Blue structures are aligned with Precambrian structures including the Gamburtsev Suture (F. Ferraccioli et al., 2011), the Ruker anomaly and Proterozoic basins in the southern Prince Charles Mountains (McLean et al., 2008). Orange lines indicate structures associated with the Fuji Subglacial Highlands block. SR – Sør Rondane, WRT – West Ragnhild Trough, CRT – Central Ragnhild Trough BLB – Beaver Lake Basin, FG – Fisher Glacier, MG – Mellor Glacier, LG – Lambert Glacier, ME – Mawson Escarpment, LSE – Lake Snow Eagle, WIIB – Wilhelm II Basin.

Figure 11: Sedimentary basins of the Vostok, Queen Mary Land, Aurora, and Terre Adelie regions. Purple lines indicate older structures associated with collisional events (Michael Studinger et al., 2003) while the blue lines indicate interpreted EARS structures (F. Ferraccioli et al., 2011). Black and Red structures indicate Paleozoic-Mesozoic structures linked to the Knox, Aurora, Vincennes and Sabrina subglacial basins. Orange structures indicate structures associated with the Wilkes Subglacial Basin, with slightly different trend. Structures reinterpreted from prior studies (A. R. A. Aitken et al., 2016; A. R. A. Aitken et al., 2014; Cianfarra & Salvini, 2016; Maggi et al., 2016; Maritati et al., 2016; Tabacco et al., 2006). LS – Lake Sovetskaya, L90E – Lake 90°E, LV – Lake Vostok, WIIB – Wilhelm II Basin, SIS – Shackleton Ice Shelf, SG – Sandow Group.

Figure 12: The Transantarctic Mountains and the Wilkes and South Pole subglacial sedimentary basins. Blue lines indicate major rift structures of the Wilkes and South Pole subglacial basins and red lines major cross-basin discontinuities. Orange lines indicate structures from other events. Structures reinterpreted from (Fausto Ferraccioli et al., 2009; Fausto Ferraccioli & Bozzo, 2003; Frederick et al., 2016; Jordan, Ferraccioli, Armadillo, et al., 2013; T. J. Wilson, 1999). WR – Wisconsin Range, QMR – Queen Maud Range, MR – Miller Range

Figure 13: Structure of the Antarctic lithosphere showing basins over a) Moho depth (Pappa, Ebbing, & Ferraccioli, 2019), b) lithosphere-asthenosphere boundary depth (Hazzard et al., 2023), 1 to 6 indicate lithospheric embayments around the East Antarctic margin c) multidata lineament analysis (Stål et al., 2019) and d) multiscale gravity edge analysis. All images show the WARS bounding TAM front and East Antarctic lineament sets in dashed black. Labelling: a to d cross-rift structures in the WARS, 1 to 9 cross-basin structures in the Beacon Basin, PLL – Palmer Land Lineament, FTL – Filchner Trough Lineament, CLL – Coats Land Lineament, RL – Ruker Lineament, GS – Gamburtsev Suture, KBL Knox Basin Lineament, AL-Aurora lineament, HBL – Highland B Lineament, CL – Concordia lineament, ATL-Adventure Trough Lineament, WAL – Wilkes-Adelie Lineament, MGL – Matusevich Glacier Lineament. WSRS – Weddell Sea Rift System, NG – Nimrod Glacier, RG – Reedy Glacier, GR – Gunnerus Ridge, FSH – Fuji Subglacial Highlands, WIS – West Ice Shelf, DML – Dronnning Maud Land, VH – Vostok Highland, AB – Aurora Subglacial Basin, SWB – Southern Wilkes Basin, TAM – Transantarctic Mountains, AP-Antarctic Peninsula, CWA – Central West Antarctica, MBL – Marie Byrd Land, SC – Siple Coast, EB- Eastern Basin, TR – Terror Rift, SP – South Pole Basin, RSH – Recovery Subglacial Highlands, SGB – Slessor Glacier Basin, LR – Lambert Rift, GSM- Gamburtsev Subglacial Mountains. An unannotated version of this figure is available in Fig S3.

Figure 14: Tectonic reconstruction snapshots a) 265 Ma, b) 120 Ma, c) 65 Ma and d) 34 Ma showing the context of basin formation since Pangea (Müller et al., 2019; A. Young et al., 2019). East Antarctica is held fixed in this reconstruction which does not include rift block motions not involving ocean spreading. Basins are shown from their base-of-basin age to their top-of-basin age, with basin age indicating the time elapsed since the former. Each image also shows the major lithospheric boundaries (see Fig 13). Past plate

trajectories (PPTs) are shown for departing plates for the following time periods a) 280 to 265 Ma 1-Cimmeria, b) 180 to 120 Ma 1 – South America, 2 – Africa, 3 – Madagascar, 4-Greater India, 5- Australia c) 90 to 65 Ma 1 – South America, 2 – Africa, 3 – Madagascar, 4-Greater India, 5 – Australia, 6 – Zealandia, and d) 64 to 34 Ma, 1 – South America, 2 – Africa, 3 –Indo-Australia 4 – Zealandia/Pacific. TP – Trinity Peninsula, EM – Ellsworth Mountains (inferred location) PrB – Prydz Bay, GIV - George IV land, KP – Kerguelen Plateau, PAP-Perth Abyssal Plain, PeB – Perth Basin, DP – Drake Passage, SS – Scotia Sea, AB – Adare Basin TG – Tasman Gateway. An unannotated version of this figure is available in Fig S4.

Figure 15: a) Paleotopography at the Eocene Oligocene boundary (Guy J. G. Paxman et al., 2019) and b) the difference with the present day. Negative values indicate surface lowering due to tectonic subsidence and or glacial erosion.

Figure 16: Influences on ice-sheet dynamics showing basins over a) geothermal heat flux estimated from geophysical data (Lösing & Ebbing, 2021) b) surface ice sheet velocity derived from InSAR phase mapping (Mouginot et al., 2019) c) inferred basal friction coefficient derived by inverting for basal conditions using the Ice sheet and Sea level System Model (Dawson et al., 2022) and d) subglacial hydrology, including subglacial lakes (Livingstone et al., 2022), and a modern-day drainage network (Le Brocq et al., 2013). Numbers indicate ice stream systems with sedimentary basins beneath fast flowing ice including 1 – Mercer and Whillans, 2 – Bindschadler and MacAyeal, 3 – Institute , 4- Academy and Support Force, 5 – Jutulstraumen, 6 – West and Central Ragnhild, 7 – Cook. Letters indicate ice stream systems with basins upstream including a – Thwaites and Pine Island, b – Recovery and Slessor, d – Lambert, Mellor and Fisher, d – Denman and Scott, e – Totten, f – David, Skelton and Byrd. FR – Ferrigno Rift, PIRB – Pine Island Rift Basin, BIR – Bungenstock Ice Rise, AC – Amundsen Coast Basin, FB – Foundation Basin, SPB – South Pole Basin, AVB – Aurora-Vincennes Basin, SWB – Southern Wilkes Basin, NWB – Northern Wilkes Basin, RL- Recovery Lakes, LV- Lake Vostok, DC – Dome C. An unannotated version of this figure is available in Fig S5.

Figure 1.

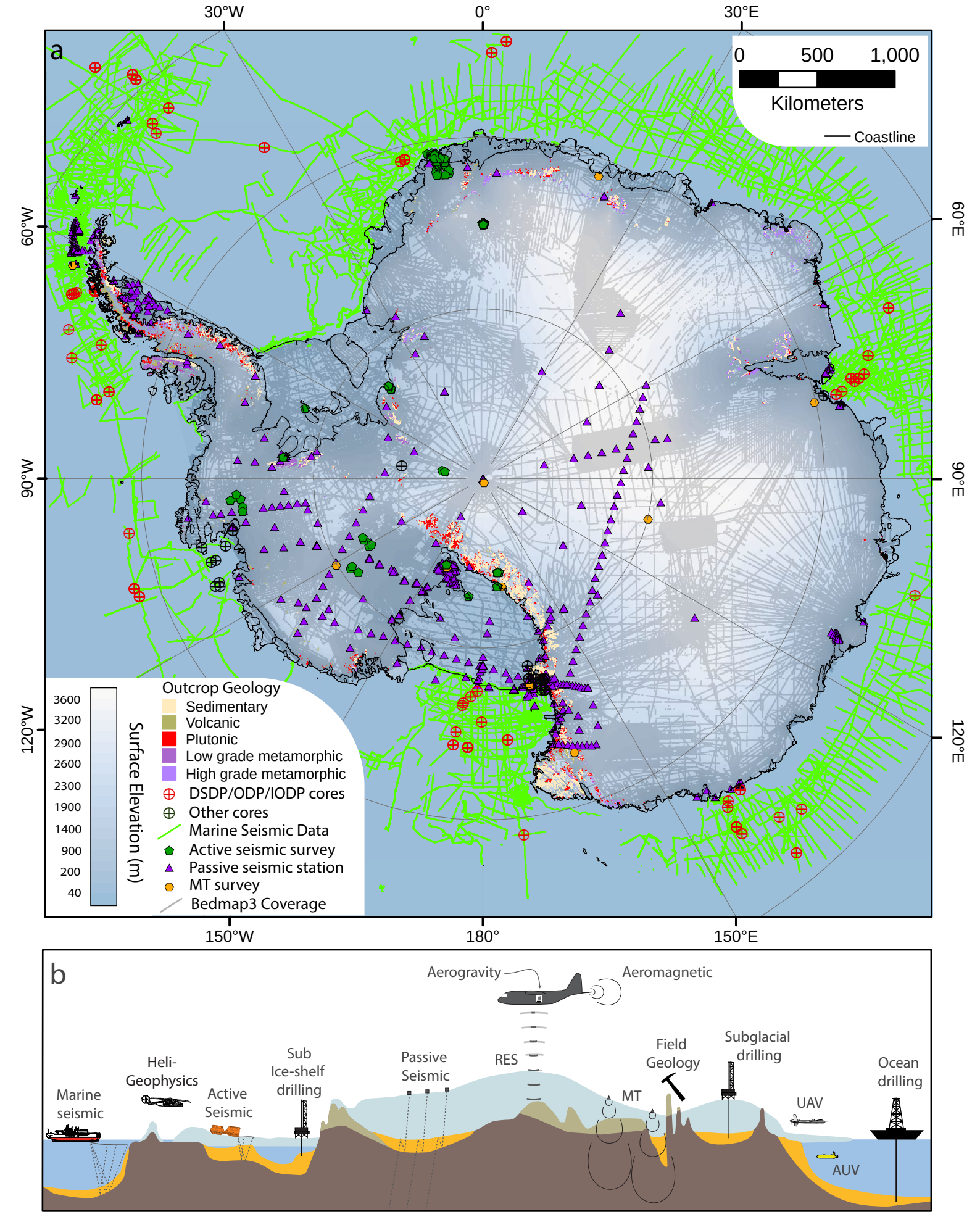
a
30°W
0°
30°E
60°W
90°W
120°W
60°E
90°E
120°E
150°W
180°
150°E
0
500
1,000
Kilometers
Coastline
Outcrop Geology
Sedimentary
Volcanic
Plutonic
Low grade metamorphic
High grade metamorphic
DSDP/ODP/IODP cores
Other cores
Marine Seismic Data
Active seismic survey
Passive seismic station
MT survey
Bedmap3 Coverage
Surface Elevation (m)
3600
3200
2900
2600
2300
1900
1400
900
200
40

b
Aerogravity
Aeromagnetic
Heli-
Geophysics
Sub
Ice-shelf
drilling
Passive
Seismic
RES
Field
Geology
Subglacial
drilling
Ocean
drilling
Marine
seismic
Active
Seismic
MT
UAV
AUV

Figure 2.

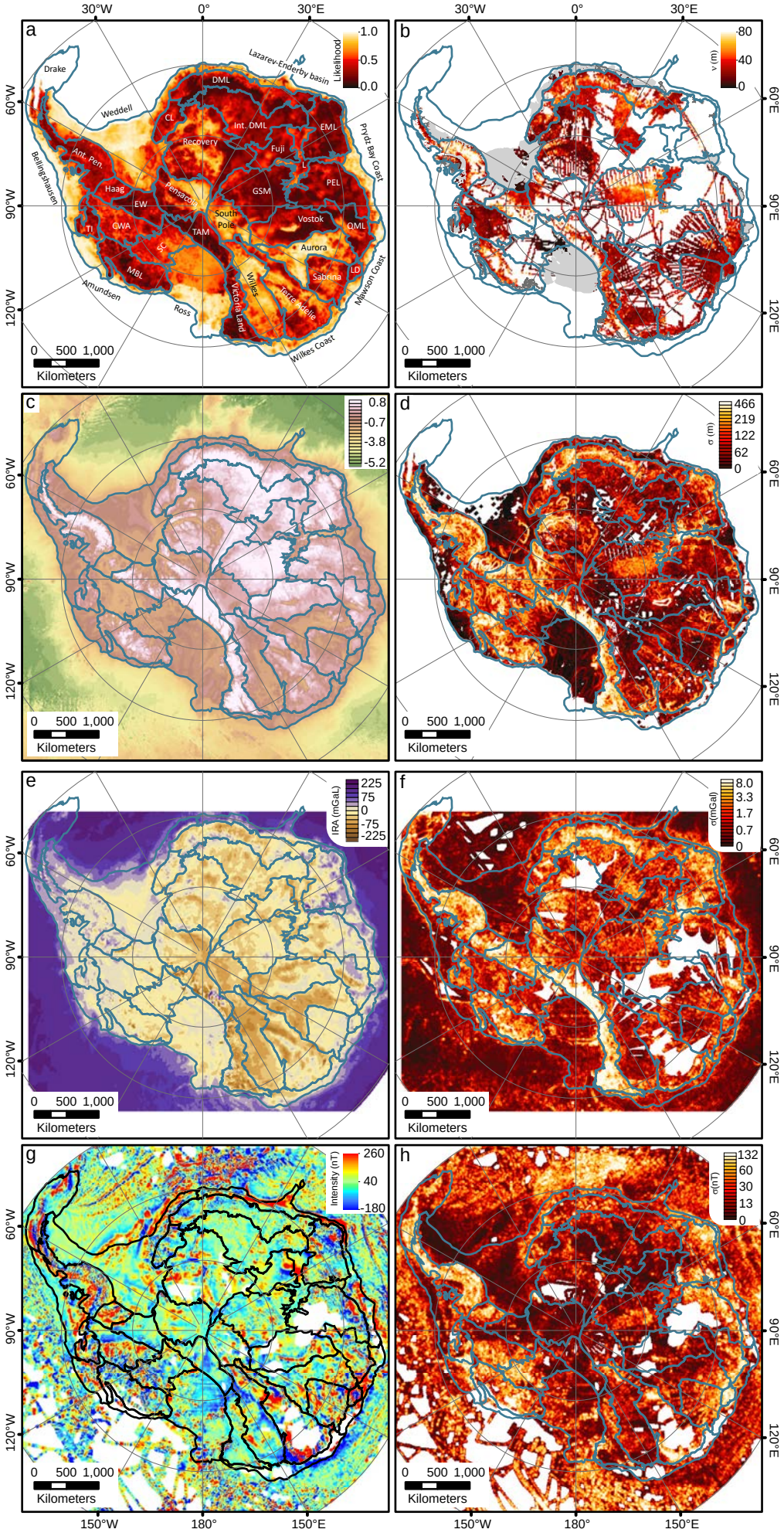
a
b
c
d
e
f
g
h
30°W
0°
30°E
150°W
180°
150°E
60°W
90°W
120°W
60°E
90°E
120°E
Likelihood
1.0
0.5
0.0
v (m)
80
40
0
0.8
-0.7
-3.8
-5.2
σ (m)
466
219
122
62
0
IRA (mGaL)
225
75
0
-75
-225
σ(mGal)
8.0
3.3
1.7
0.7
0
Intensity (nT)
260
40
-180
σ(nT)
132
60
30
13
0
0 500 1,000
Kilometers
Drake
Weddell
Lazarev-Enderby basin
Prydz Bay Coast
Mawson Coast
Wilkes Coast
Amundsen
Ross
Bellingshausen
Ant. Pen.
Haag
EW
TI
GWA
SY
MBL
CL
DML
Int. DML
EML
Recovery
Fuji
L
PEL
GSM
Pensacola
South Pole
TAM
Vostok
OML
Aurora
Sabrina
LD
Wilkes
Victoria Land
Terre Adelie

Figure 3.

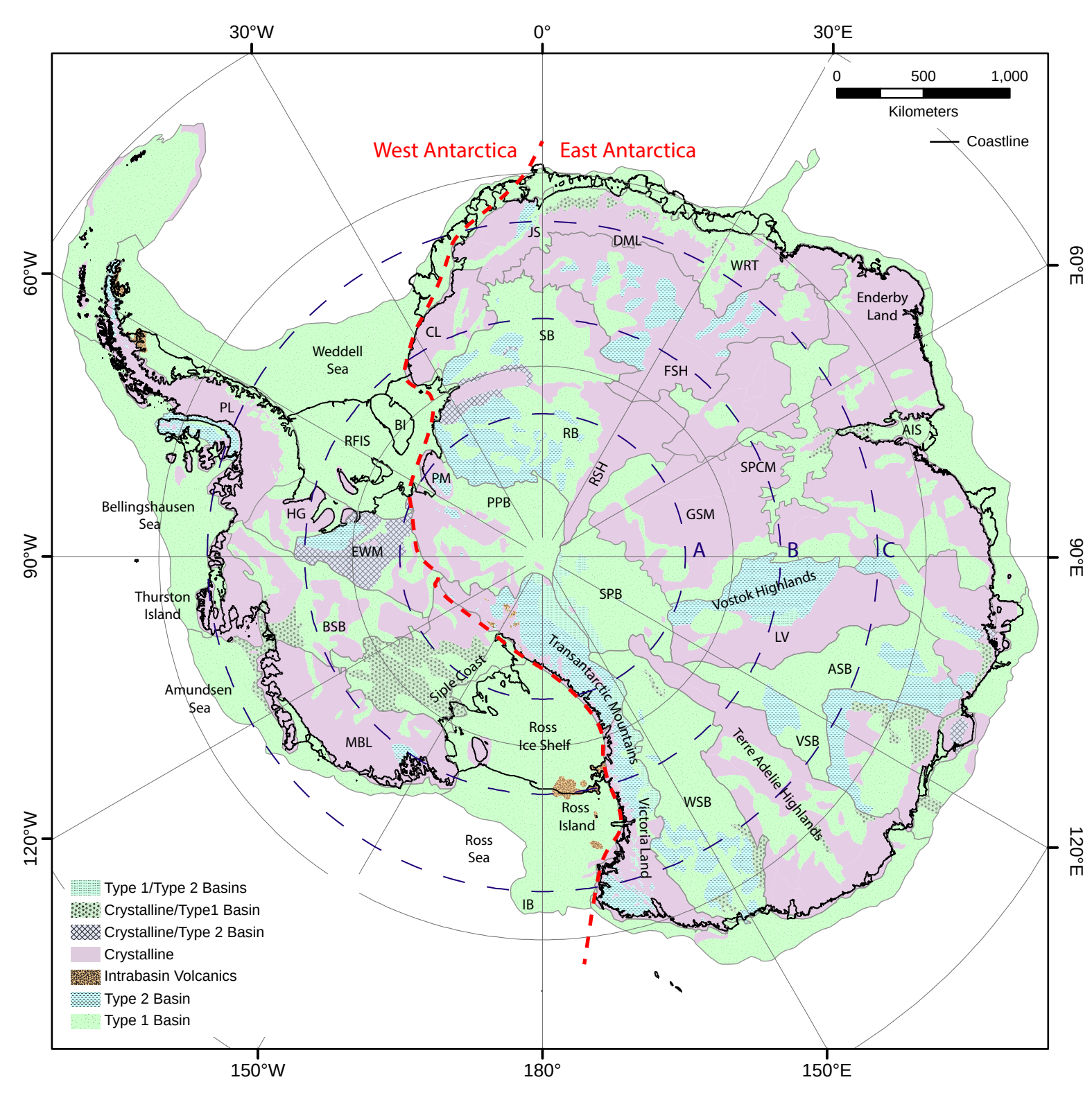
30°W
0°
30°E
60°W
60°E
90°W
90°E
120°W
120°E
150°W
180°
150°E
0
500
1,000
Kilometers
Coastline
West Antarctica
East Antarctica
JS
DML
WRT
Enderby Land
CL
SB
Weddell Sea
FSH
PL
BI
RFIS
RB
AIS
PM
RSH
SPCM
Bellingshausen Sea
HG
PPB
GSM
EWM
A
B
C
Thurston Island
SPB
Vostok Highlands
BSB
LV
Transantarctic Mountains
ASB
Siple Coast
Amundsen Sea
Ross Ice Shelf
VSB
MBL
Terre Adelie Highlands
WSB
Ross Island
Victoria Land
Ross Sea
IB
Type 1/Type 2 Basins
Crystalline/Type1 Basin
Crystalline/Type 2 Basin
Crystalline
Intrabasin Volcanics
Type 2 Basin
Type 1 Basin

Figure 4.

a)

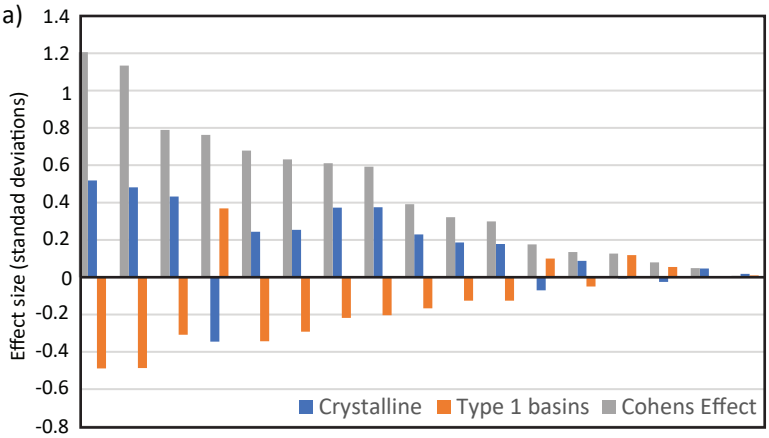

Rank	Dataset	Variable
1	Topography	Elevation
2	Topography	Rebounded elevation
3	Gravity	Free air anomaly
4	Gravity	Bouguer anomaly
5	Topography	Rebounded elevation variation (30 km)
6	Gravity	Bouguer variation (30 km)
7	GOCE	Mean curvature
8	GOCE	Structure Index
9	Magnetic	Magnetic intensity variation (30 km)
10	Gravity	High-pass Airy IRA (1000km)
11	Magnetic	Magnetic total gradient
12	Gravity	High-pass Bouguer Anomaly (1000km)
13	Magnetic	Magnetic total anomaly
14	Gravity	Airy IRA
15	Magnetic	High-pass pseudogravity (1000 km)
16	Magnetic	Pseudogravity
17	Magnetic	Magnetic Intensity RTP

b)

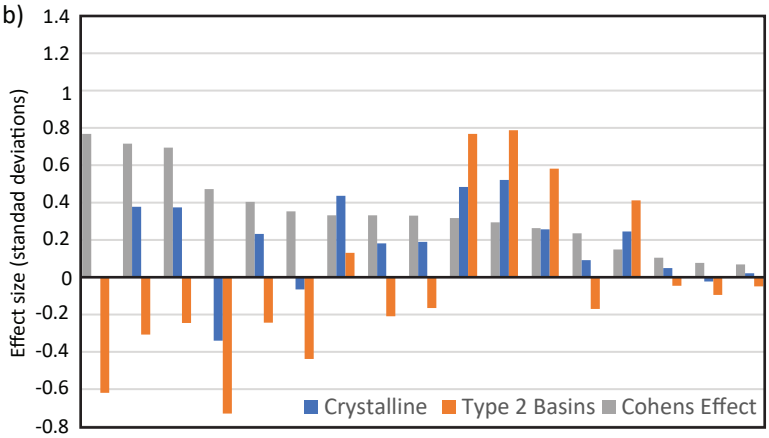

Rank	Dataset	Variable
1	Gravity	Airy IRA
2	GOCE	Structure Index
3	GOCE	Mean curvature
4	Gravity	Bouguer anomaly
5	Magnetic	Magnetic intensity variation (30 km)
6	Gravity	High-pass Bouguer Anomaly (1000km)
7	Gravity	Free Air Anomaly
8	Magnetic	Magnetic total gradient
9	Gravity	High-pass Airy IRA (1000km)
10	Topography	Rebounded elevation
11	Topography	Elevation
12	Gravity	Bouguer variation (30 km)
13	Magnetic	Magnetic total anomaly
14	Topography	Rebounded elevation variation (30 km)
15	Magnetic	Pseudogravity
16	Magnetic	High-pass pseudogravity (1000 km)
17	Magnetic	Magnetic Intensity RTP

c)

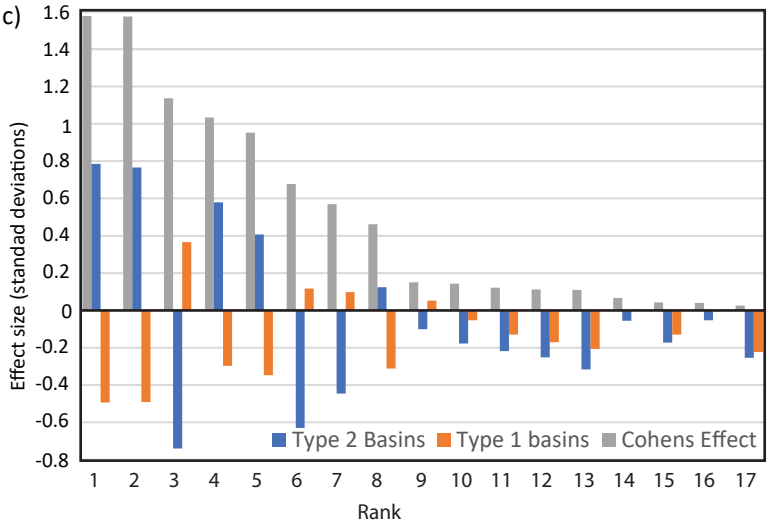

Rank	Dataset	Variable
1	Topography	Elevation
2	Topography	Rebounded elevation
3	Gravity	Bouguer anomaly
4	Gravity	Bouguer variation (30 km)
5	Topography	Rebounded elevation variation (30 km)
6	Gravity	Airy IRA
7	Gravity	High-pass Bouguer Anomaly (1000km)
8	Gravity	Free Air Anomaly
9	Magnetic	High-pass pseudogravity (1000 km)
10	Magnetic	Magnetic total anomaly
11	Magnetic	Magnetic total gradient
12	Magnetic	Magnetic intensity variation (30 km)
13	GOCE	Structure Index
14	Magnetic	Magnetic Intensity RTP
15	Gravity	High-pass Airy IRA (1000km)
16	Magnetic	Pseudogravity
17	GOCE	Mean curvature

Figure 5.

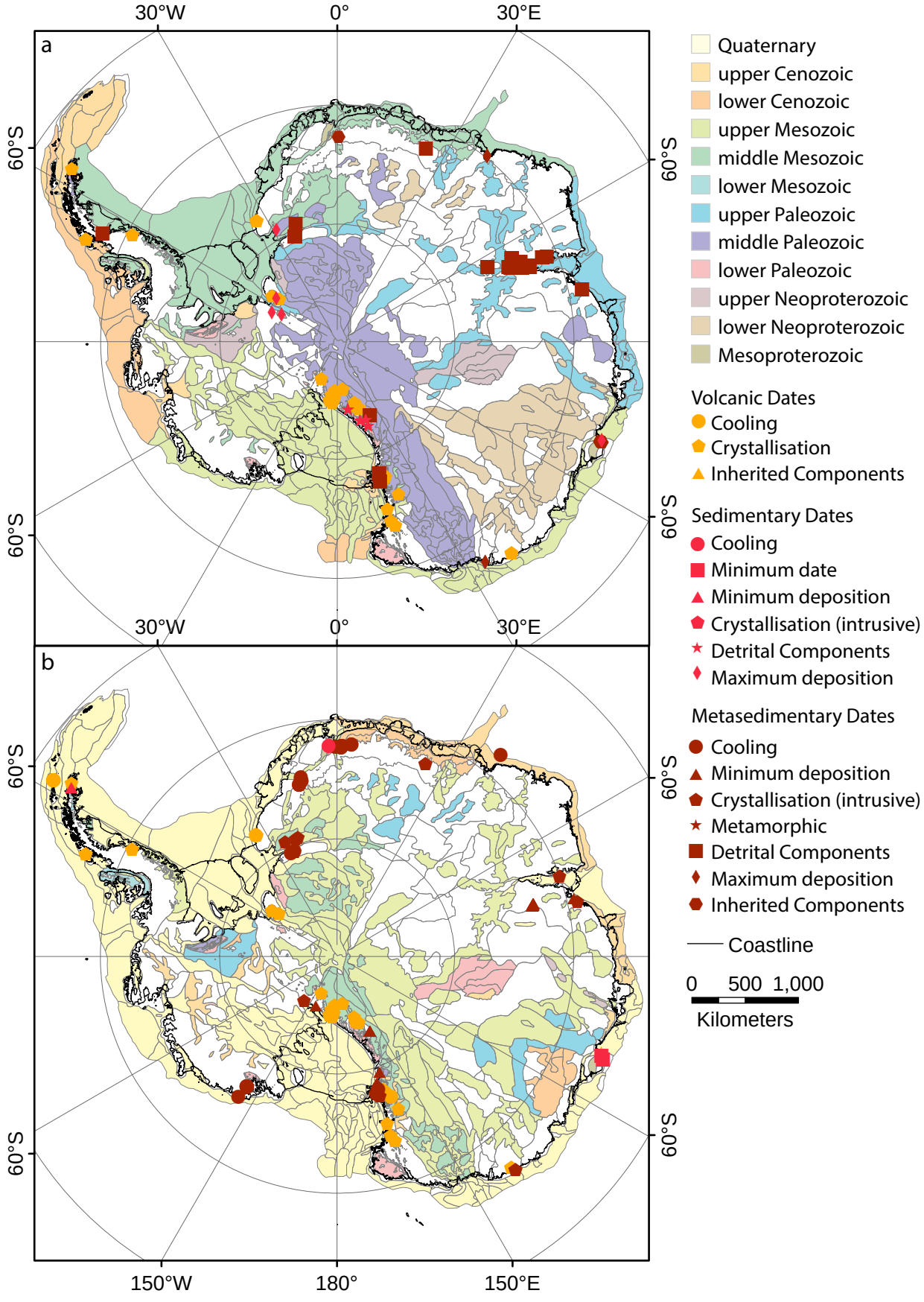
a
b
30°W
0°
30°E
60°S
150°W
180°
150°E
Quaternary
upper Cenozoic
lower Cenozoic
upper Mesozoic
middle Mesozoic
lower Mesozoic
upper Paleozoic
middle Paleozoic
lower Paleozoic
upper Neoproterozoic
lower Neoproterozoic
Mesoproterozoic
Volcanic Dates
Cooling
Crystallisation
Inherited Components
Sedimentary Dates
Cooling
Minimum date
Minimum deposition
Crystallisation (intrusive)
Detrital Components
Maximum deposition
Metasedimentary Dates
Cooling
Minimum deposition
Crystallisation (intrusive)
Metamorphic
Detrital Components
Maximum deposition
Inherited Components
Coastline
0 500 1,000
Kilometers

Figure 6.

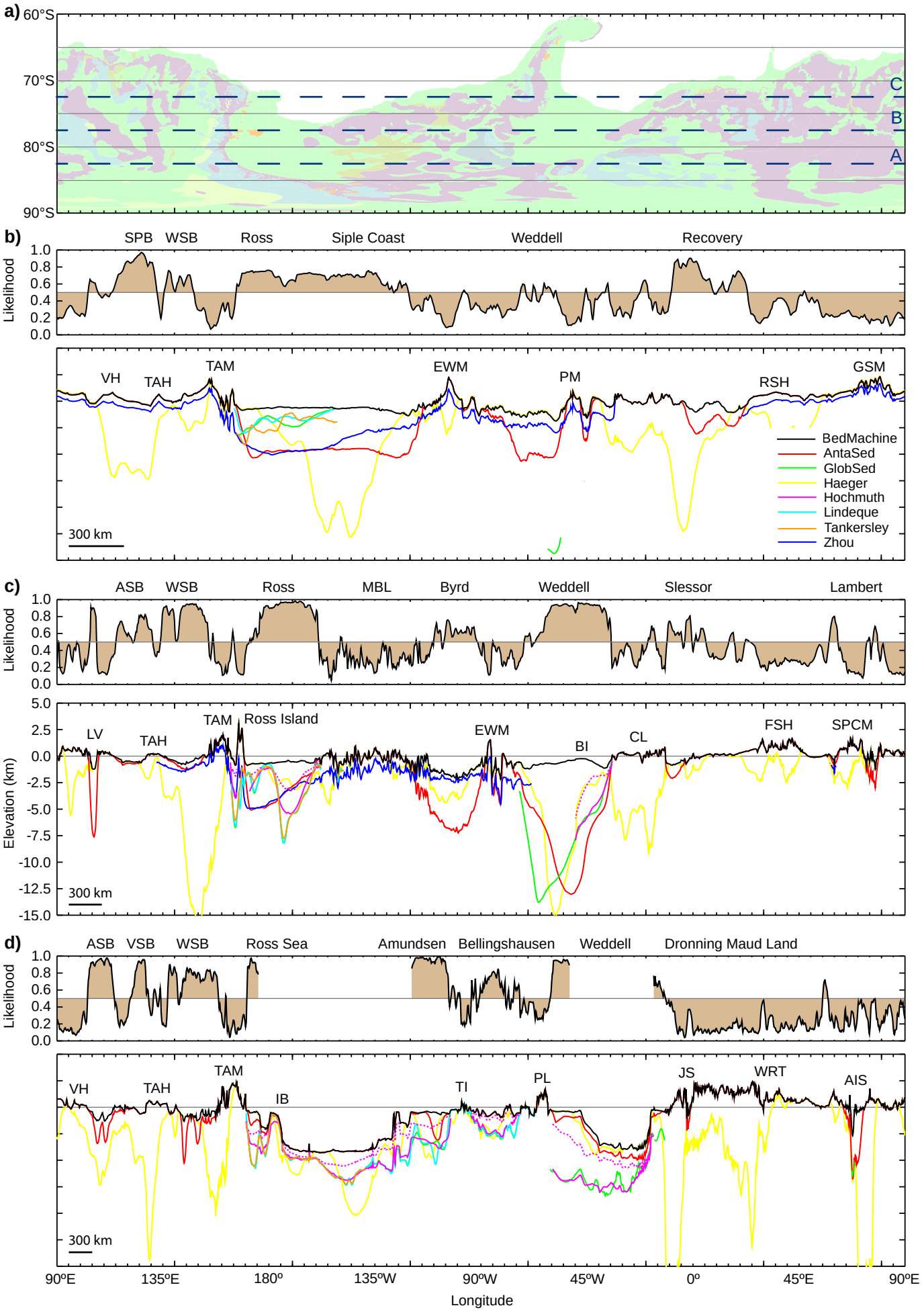
a)
60°S
70°S
80°S
90°S
C
B
A
b)
SPB
WSB
Ross
Siple Coast
Weddell
Recovery
Likelihood
1.0
0.8
0.6
0.4
0.2
0.0
VH
TAH
TAM
EWM
PM
RSH
GSM
BedMachine
AntaSed
GlobSed
Haeger
Hochmuth
Lindeque
Tankersley
Zhou
300 km
c)
ASB
WSB
Ross
MBL
Byrd
Weddell
Slessor
Lambert
Likelihood
1.0
0.8
0.6
0.4
0.2
0.0
Elevation (km)
5.0
2.5
0.0
-2.5
-5.0
-7.5
-10.0
-12.5
-15.0
LV
TAH
TAM
Ross Island
EWM
BI
CL
FSH
SPCM
300 km
d)
ASB
VSB
WSB
Ross Sea
Amundsen
Bellingshausen
Weddell
Dronning Maud Land
Likelihood
1.0
0.8
0.6
0.4
0.2
0.0
VH
TAH
TAM
IB
TI
PL
JS
WRT
AIS
300 km
90ºE
135ºE
180º
135ºW
90ºW
45ºW
0º
45ºE
90ºE
Longitude

Figure 7.

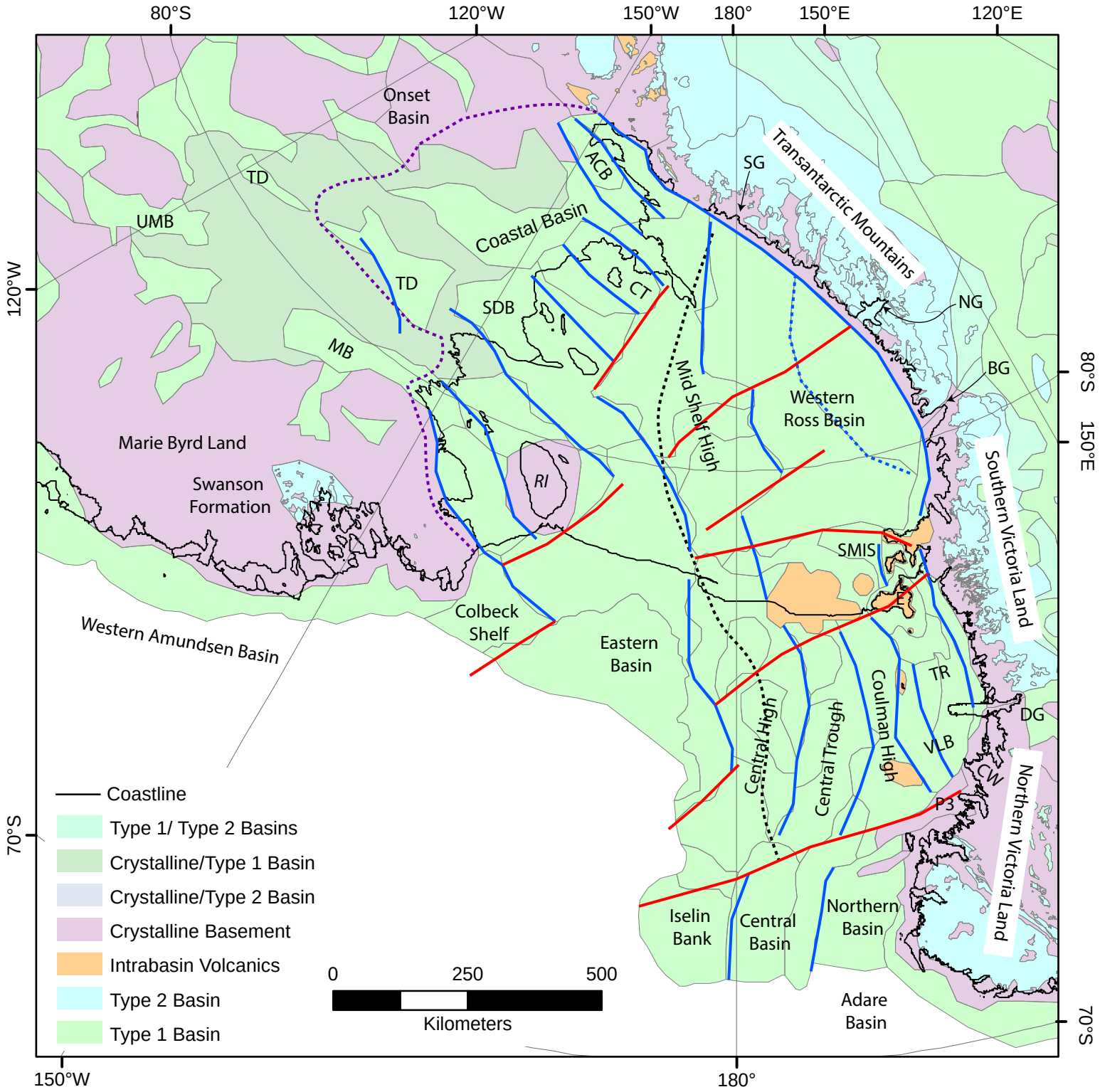
80°S
120°W
150°W
180°
150°E
120°E
70°S
Onset Basin
TD
UMB
ACB
SG
Transantarctic Mountains
Coastal Basin
CT
TD
SDB
NG
MB
Mid Shelf High
BG
Western Ross Basin
Marie Byrd Land
Swanson Formation
RI
Southern Victoria Land
SMIS
Colbeck Shelf
Western Amundsen Basin
Eastern Basin
TR
DG
Central High
Central Trough
Coulman High
VLB
CW
P3
Northern Victoria Land
Iselin Bank
Central Basin
Northern Basin
Adare Basin
Coastline
Type 1/ Type 2 Basins
Crystalline/Type 1 Basin
Crystalline/Type 2 Basin
Crystalline Basement
Intrabasin Volcanics
Type 2 Basin
Type 1 Basin
0
250
500
Kilometers

Figure 8.

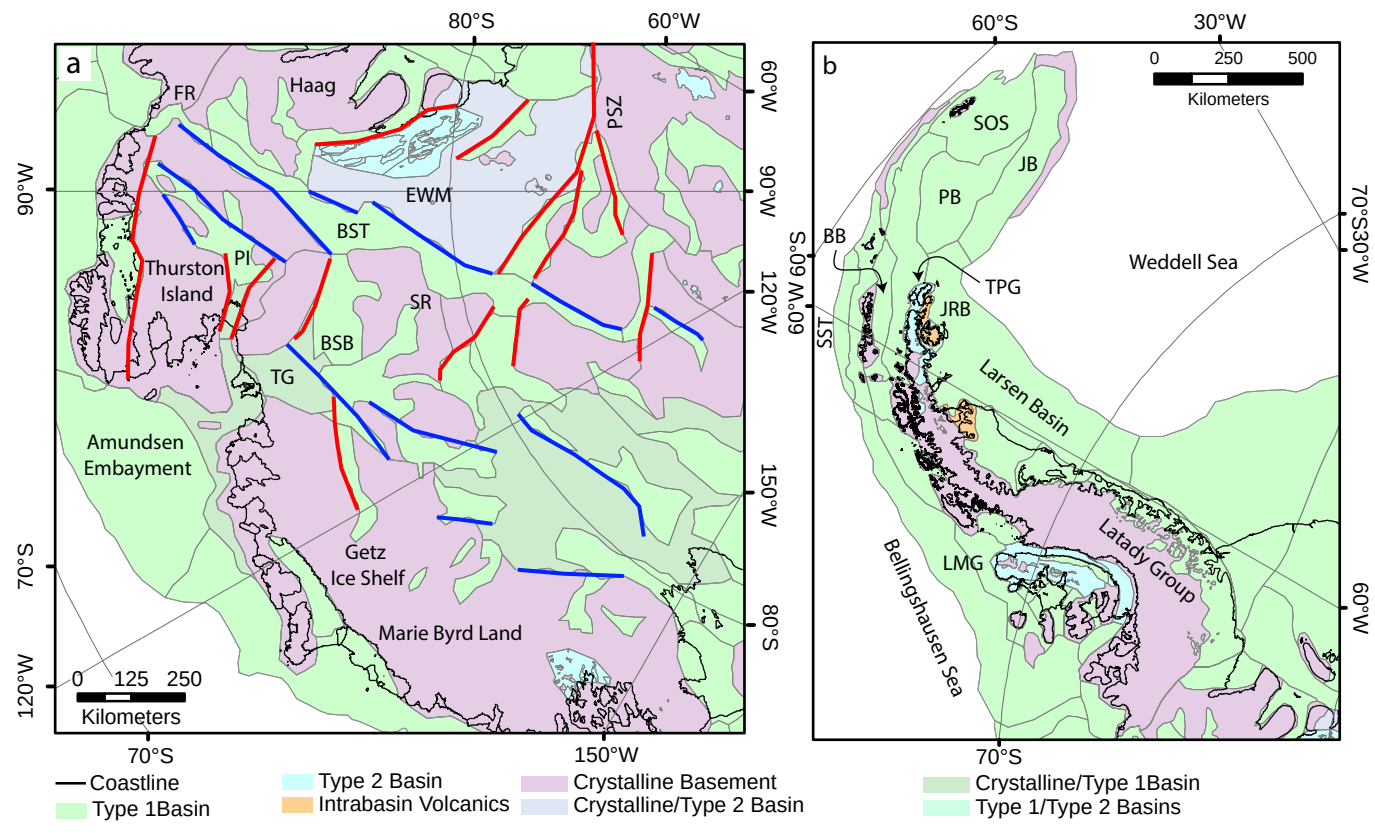
a
b
FR
Haag
PSZ
EWM
BST
PI
Thurston
Island
SR
BSB
TG
Amundsen
Embayment
Getz
Ice Shelf
Marie Byrd Land
0 125 250
Kilometers
80°S
60°W
90°W
120°W
150°W
70°S
60°S
30°W
0 250 500
Kilometers
SOS
JB
PB
BB
TPG
JRB
SST
Weddell Sea
Larsen Basin
Latady Group
LMG
Bellingshausen Sea
70°30'W
60°W
Coastline
Type 1Basin
Type 2 Basin
Intrabasin Volcanics
Crystalline Basement
Crystalline/Type 2 Basin
Crystalline/Type 1Basin
Type 1/Type 2 Basins

Figure 9.

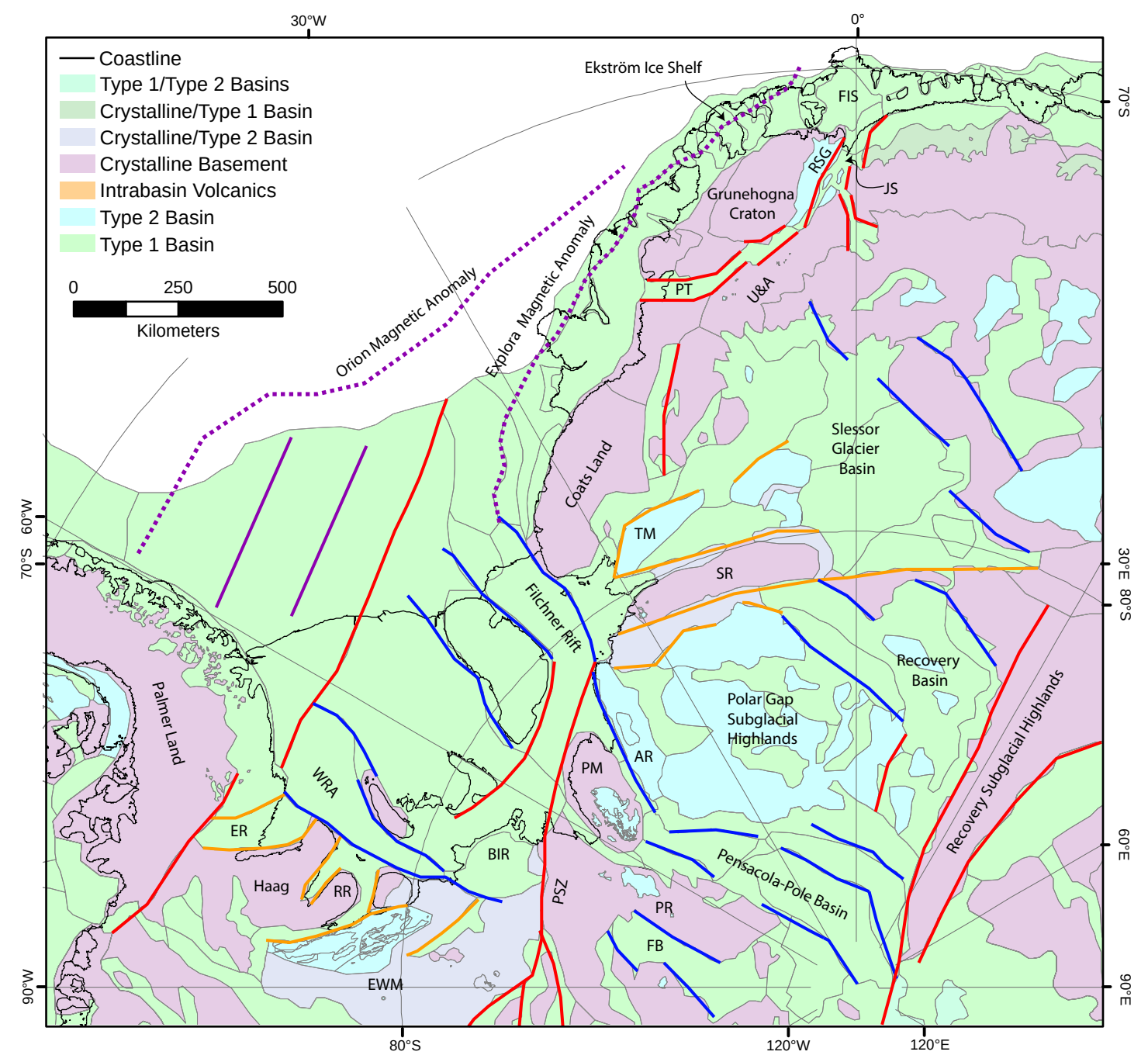
Coastline
Type 1/Type 2 Basins
Crystalline/Type 1 Basin
Crystalline/Type 2 Basin
Crystalline Basement
Intrabasin Volcanics
Type 2 Basin
Type 1 Basin
0
250
500
Kilometers
30°W
0°
70°S
60°W
30°E
80°S
90°W
90°E
80°S
120°W
120°E
Ekström Ice Shelf
FIS
RSG
JS
Grunehogna Craton
PT
U&A
Orion Magnetic Anomaly
Explora Magnetic Anomaly
Coats Land
Slessor Glacier Basin
TM
SR
Filchner Rift
Recovery Basin
Polar Gap Subglacial Highlands
Recovery Subglacial Highlands
Palmer Land
WRA
ER
Haag
RR
BIR
PM
AR
PSZ
Pensacola-Pole Basin
PR
FB
EWM

Figure 10.

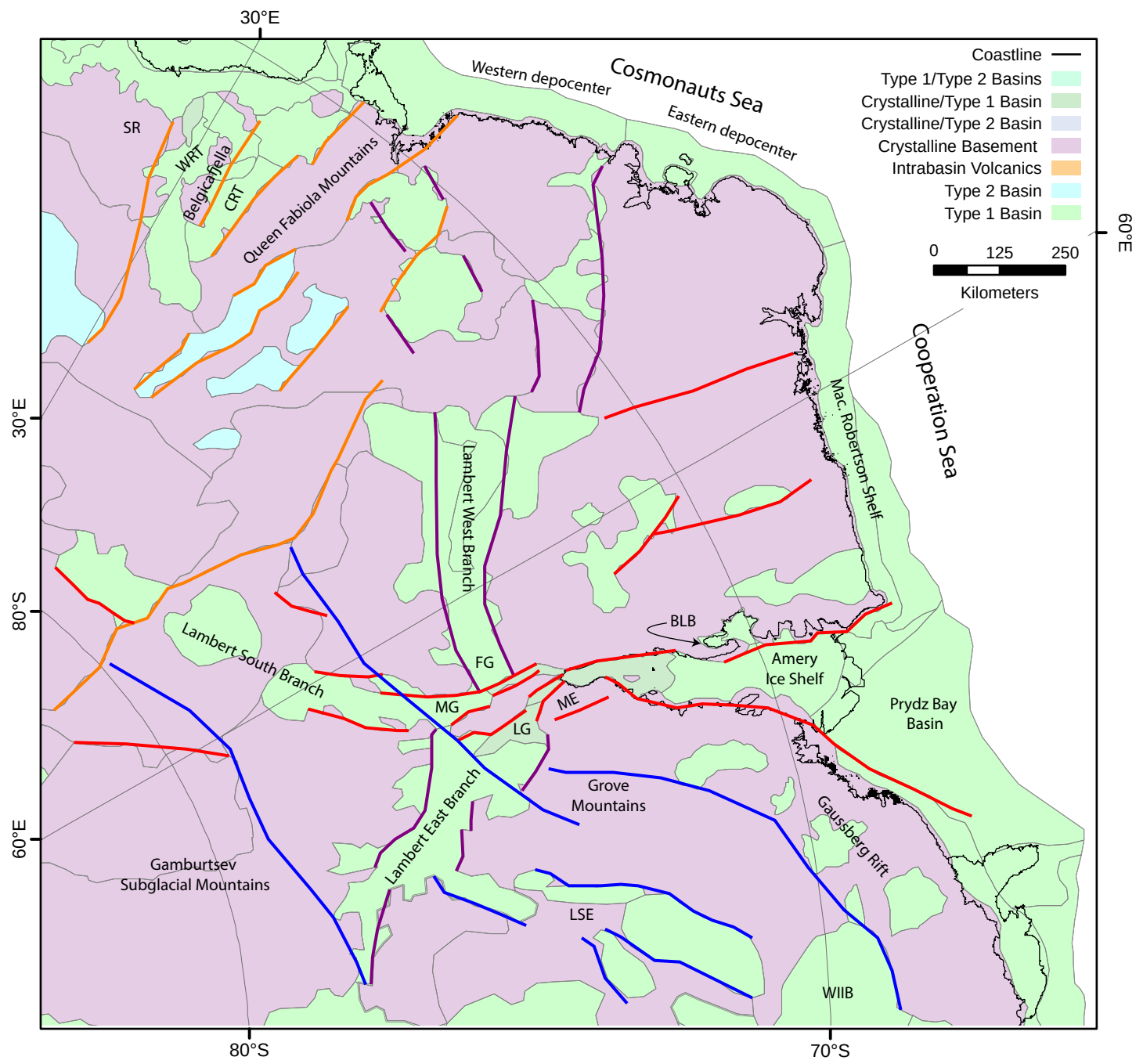
30°E
60°E
80°S
70°S
Coastline
Type 1/Type 2 Basins
Crystalline/Type 1 Basin
Crystalline/Type 2 Basin
Crystalline Basement
Intrabasin Volcanics
Type 2 Basin
Type 1 Basin
0
125
250
Kilometers
Cosmonauts Sea
Western depocenter
Eastern depocenter
Cooperation Sea
SR
WRT
Belgicafjella
CRT
Queen Fabiola Mountains
Lambert West Branch
Lambert South Branch
Lambert East Branch
Mac. Robertson Shelf
BLB
FG
MG
LG
ME
Amery
Ice Shelf
Prydz Bay
Basin
Grove
Mountains
Gaussberg Rift
Gamburtsev
Subglacial Mountains
LSE
WIIB

Figure 11.

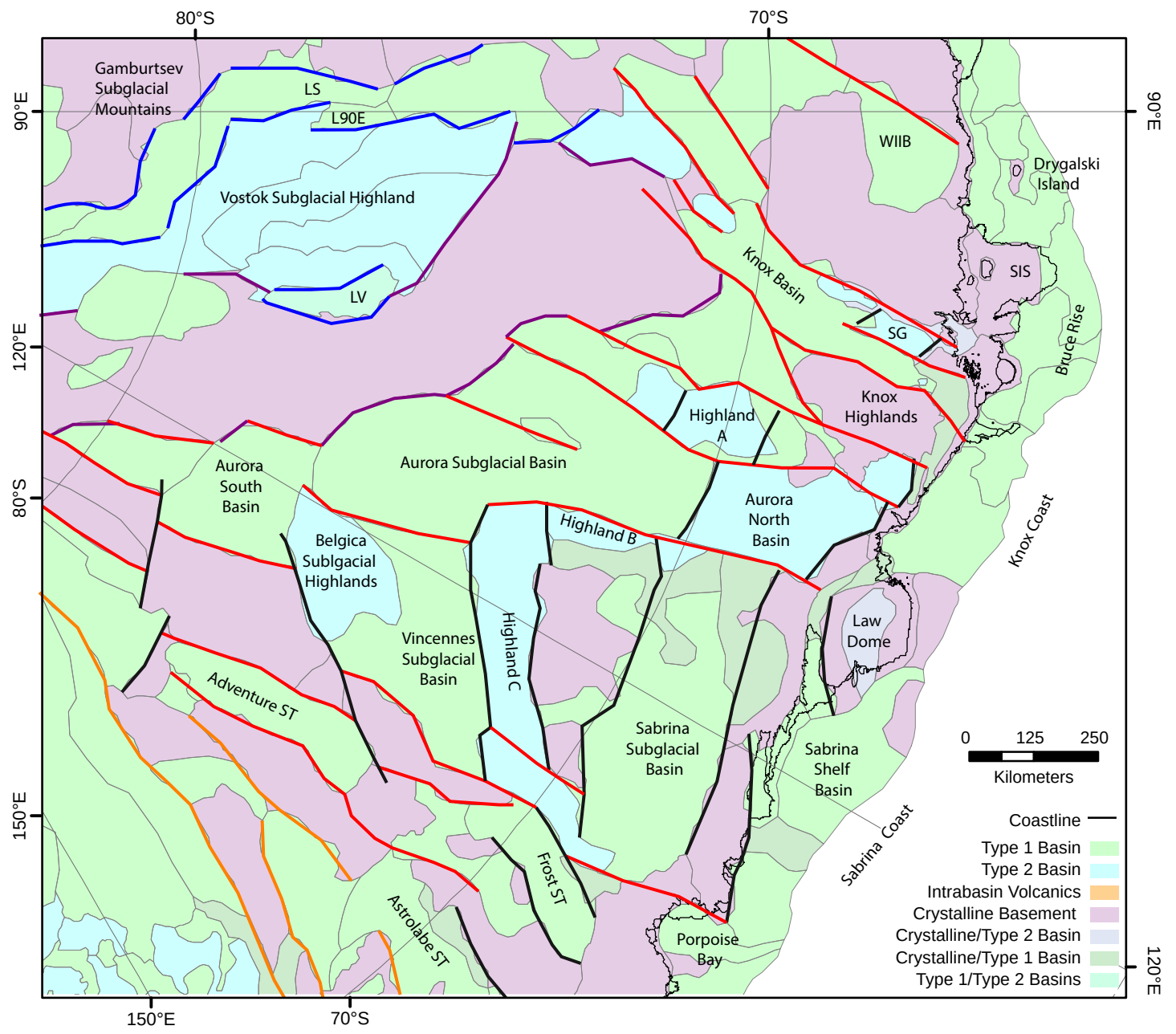
80°S
70°S
90°E
120°E
150°E
Gamburtsev Subglacial Mountains
LS
L90E
Vostok Subglacial Highland
LV
WIIB
Drygalski Island
SIS
Knox Basin
SG
Bruce Rise
Knox Highlands
Highland A
Aurora South Basin
Aurora Subglacial Basin
Aurora North Basin
Knox Coast
Belgica Sublgacial Highlands
Highland B
Highland C
Vincennes Subglacial Basin
Law Dome
Adventure ST
Sabrina Subglacial Basin
Sabrina Shelf Basin
Sabrina Coast
Frost ST
Astrolabe ST
Porpoise Bay
0
125
250
Kilometers
Coastline
Type 1 Basin
Type 2 Basin
Intrabasin Volcanics
Crystalline Basement
Crystalline/Type 2 Basin
Crystalline/Type 1 Basin
Type 1/Type 2 Basins

Figure 12.

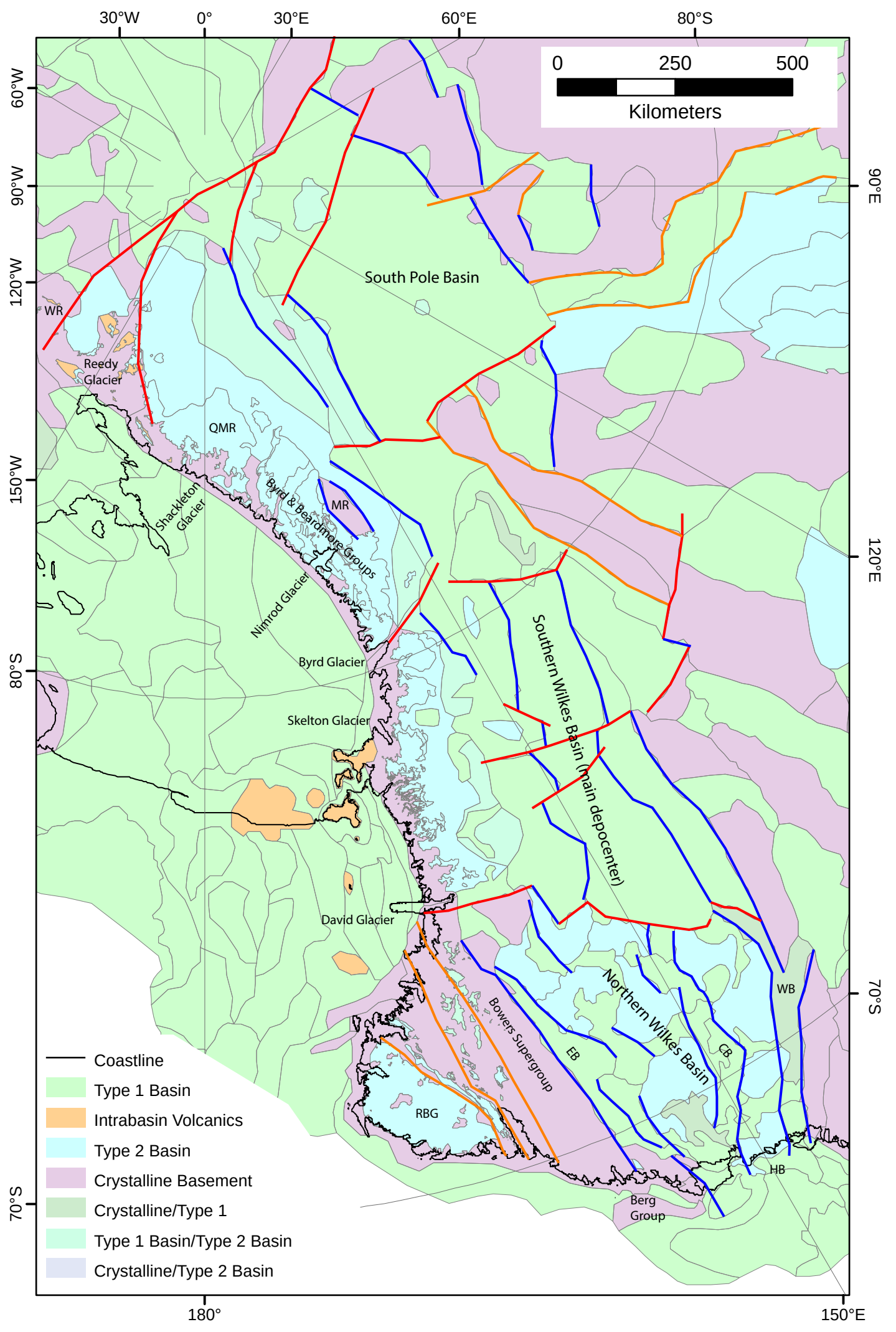
30°W
0°
30°E
60°E
80°S
60°W
90°W
120°W
150°W
80°S
70°S
90°E
120°E
70°S
180°
150°E
0
250
500
Kilometers
South Pole Basin
WR
Reedy Glacier
QMR
Shackleton Glacier
Byrd & Beardmore Groups
MR
Nimrod Glacier
Byrd Glacier
Skelton Glacier
Southern Wilkes Basin (main depocenter)
David Glacier
Northern Wilkes Basin
Bowers Supergroup
EB
CB
WB
HB
RBG
Berg Group
Coastline
Type 1 Basin
Intrabasin Volcanics
Type 2 Basin
Crystalline Basement
Crystalline/Type 1
Type 1 Basin/Type 2 Basin
Crystalline/Type 2 Basin

Figure 13.

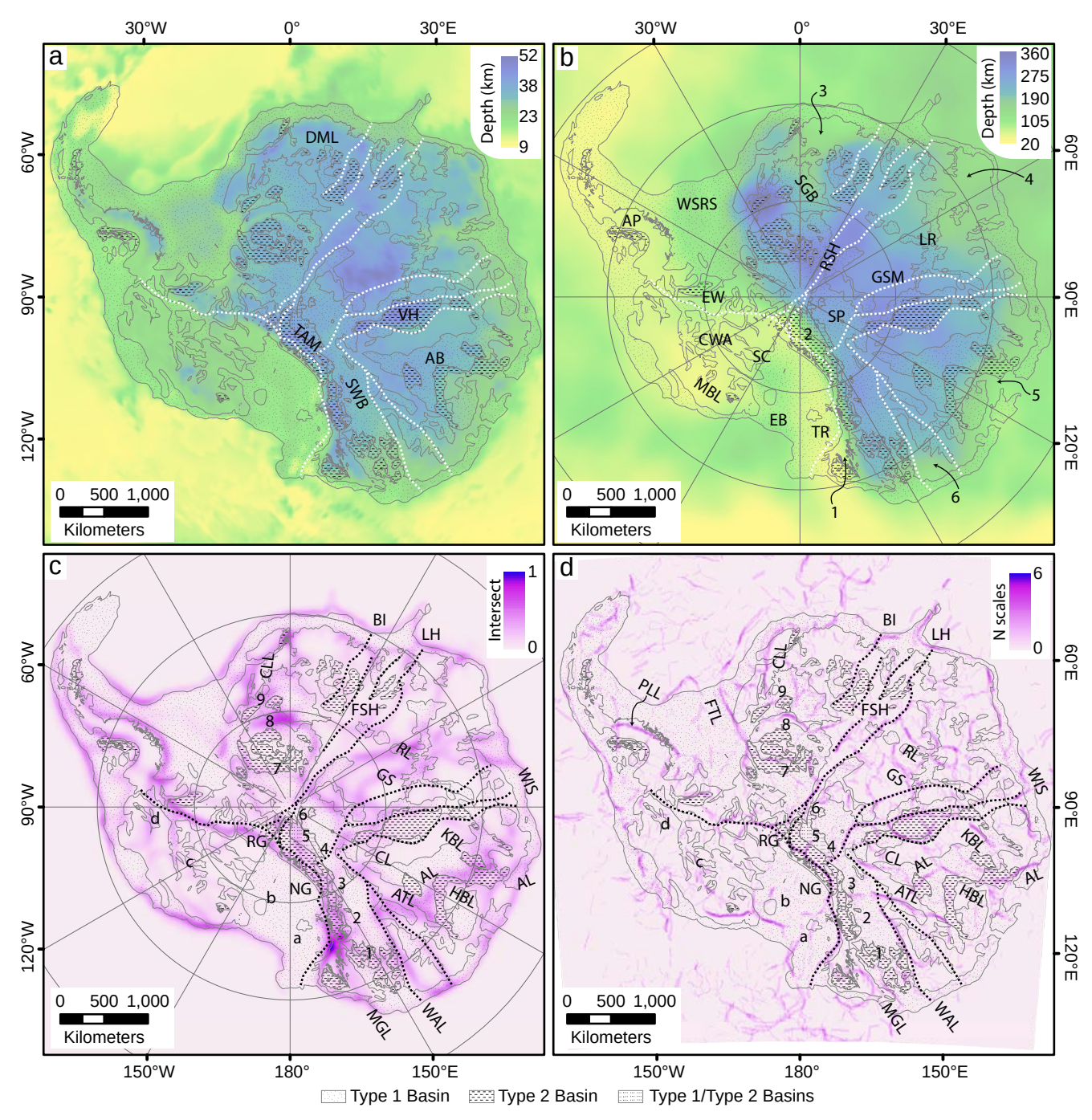
a
b
c
d
30°W
0°
30°E
150°W
180°
150°E
60°W
90°W
120°W
60°E
90°E
120°E
Depth (km)
52
38
23
9
360
275
190
105
20
Intersect
1
0
N scales
6
0
DML
TAM
VH
AB
SWB
WSRS
AP
SGB
RSH
LR
GSM
EW
SP
CWA
SC
MBL
EB
TR
BI
LH
CLL
FSH
RL
GS
WIS
RG
KBL
CL
AL
NG
ATL
HBL
PLL
FTL
MGL
WAL
0 500 1,000
Kilometers
Type 1 Basin
Type 2 Basin
Type 1/Type 2 Basins

Figure 14.

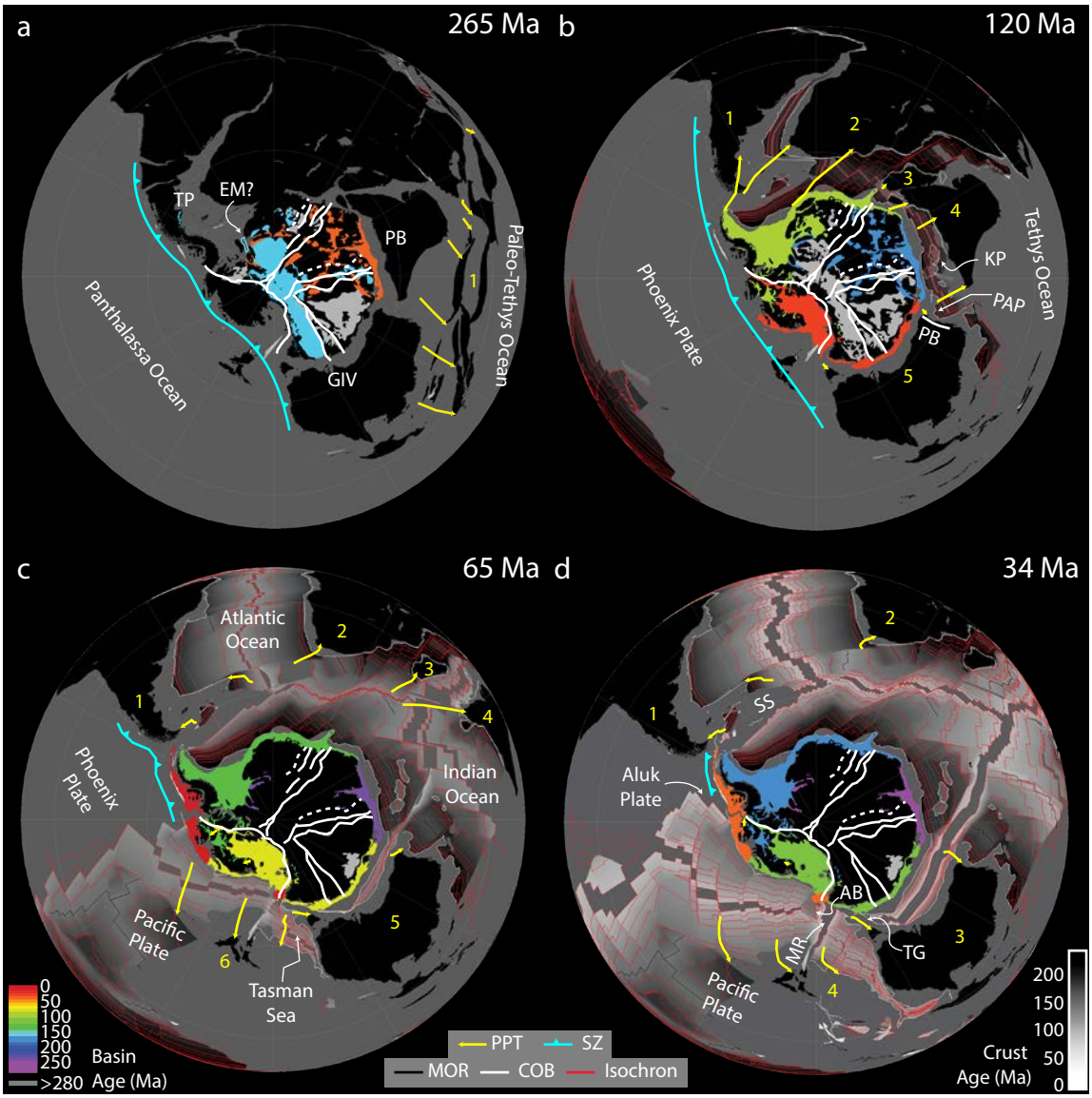
a
265 Ma
b
120 Ma
TP
EM?
PB
Paleo-Tethys Ocean
Panthalassa Ocean
GIV
1
2
3
4
KP
PAP
PB
5
Phoenix Plate
Tethys Ocean
c
65 Ma
d
34 Ma
Atlantic Ocean
Indian Ocean
Phoenix Plate
Pacific Plate
Tasman Sea
6
SS
Aluk Plate
AB
MR
TG
0
50
100
150
200
250
>280
Basin Age (Ma)
PPT
SZ
MOR
COB
Isochron
200
150
100
50
0
Crust Age (Ma)

Figure 15.

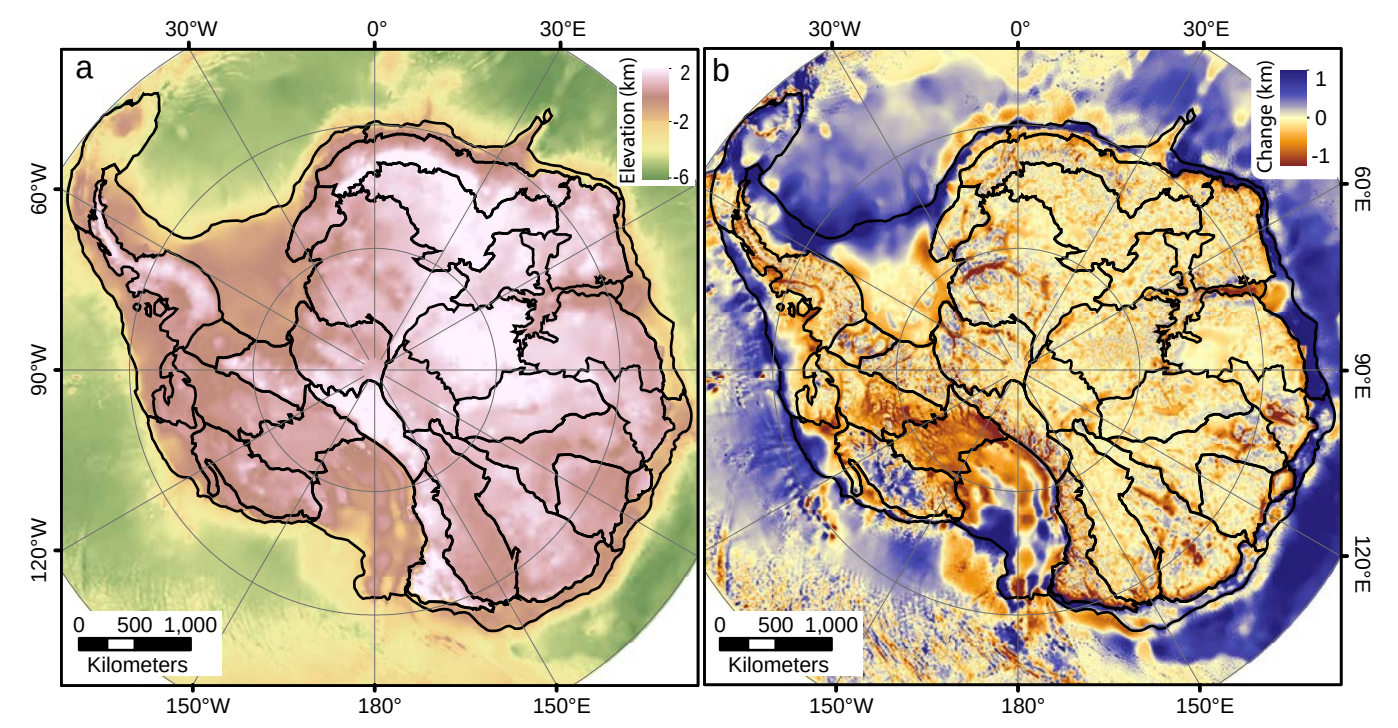
a
b
30°W
0°
30°E
60°W
90°W
120°W
60°E
90°E
120°E
150°W
180°
150°E
Elevation (km)
2
-2
-6
Change (km)
1
0
-1
0 500 1,000
Kilometers

Figure 16.

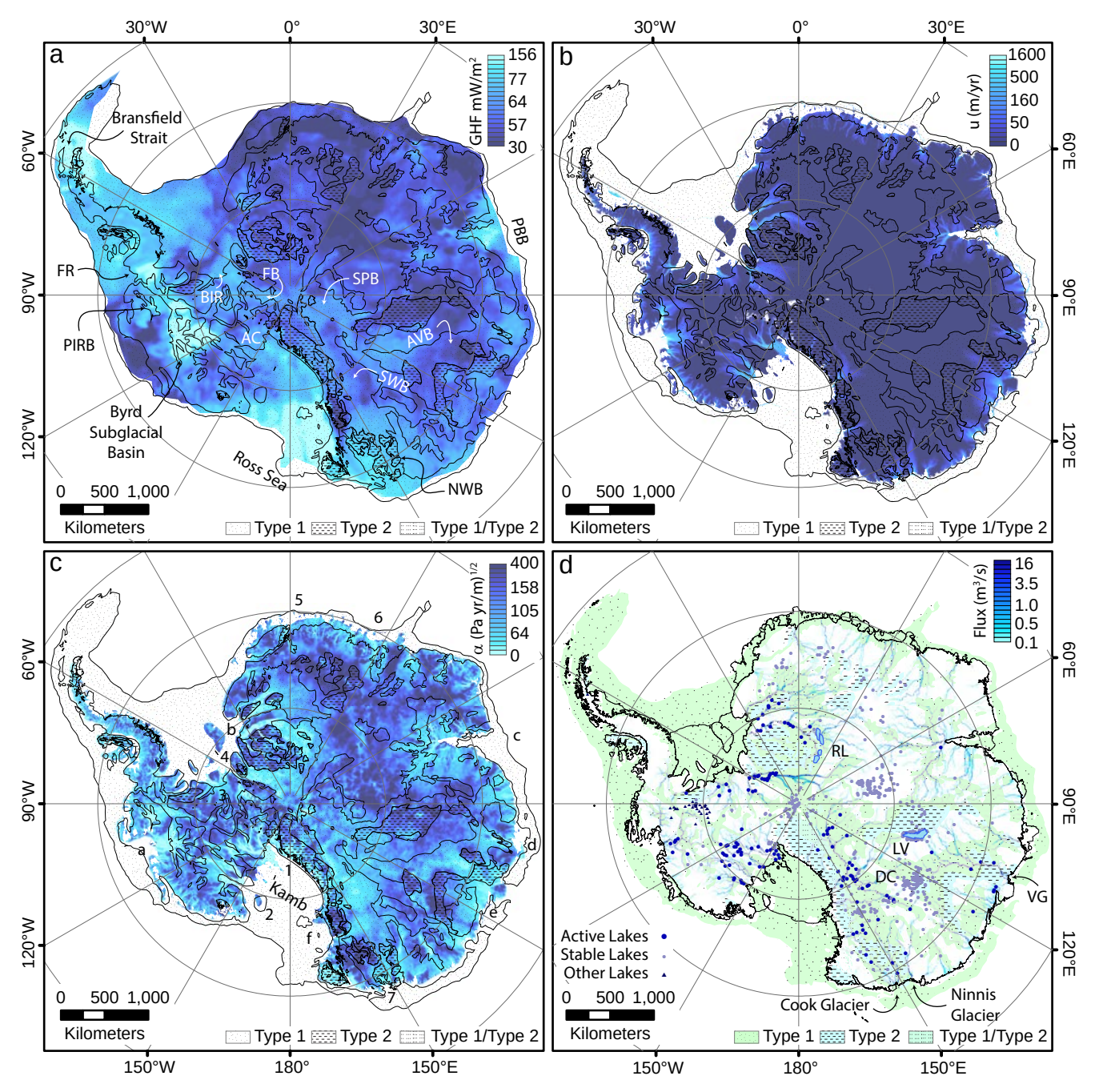
a
GHF mW/m²
156
77
64
57
30
Bransfield Strait
PBB
FR
FB
SPB
BIB
PIRB
AC
AVB
SWB
Byrd Subglacial Basin
Ross Sea
NWB
0 500 1,000
Kilometers
Type 1
Type 2
Type 1/Type 2
b
u (m/yr)
1600
500
160
50
0
c
α (Pa yr/m)^1/2
400
158
105
64
0
Kamb
d
Flux (m³/s)
16
3.5
1.0
0.5
0.1
RL
LV
DC
VG
Active Lakes
Stable Lakes
Other Lakes
Cook Glacier
Ninnis Glacier
30°W
0°
30°E
60°W
90°W
120°W
60°E
90°E
120°E
150°W
180°
150°E

Reviews of Geophysics

Supporting Information for

Antarctic sedimentary basins and their influence on ice sheet dynamics

A.R.A. Aitken[1,2], L. Li[1], B. Kulessa[3,4], D. Schroeder[5,6], T.A. Jordan[7], J.M. Whittaker[8], S. Anandakrishnan[9], E.J. Dawson[5], D. A. Wiens[10], O. Eisen[11,12], M.J. Siegert[13,14]

1. School of Earth Sciences, The University of Western Australia, Perth, Western Australia, Australia
2. Australian Centre of Excellence for Antarctic Science, The University of Western Australia, Perth, Western Australia, Australia
3. School of Biosciences, Geography and Physics, Swansea University, Wales, UK
4. School of Geography, Planning and Spatial Sciences, The University of Tasmania, Hobart Tasmania, Australia
5. Department of Geophysics, Stanford University, Stanford, California, USA
6. Department of Electrical Engineering, Stanford University, Stanford, California, USA
7. British Antarctic Survey, Cambridgeshire, UK
8. Institute for Marine and Antarctic Studies, University of Tasmania, Hobart, Tasmania, Australia
9. College of Earth and Mineral Sciences, Pennsylvania State University, Pennsylvania, USA
10. Department of Earth & Planetary Sciences, Washington University, St. Louis, Missouri, USA
11. Glaciology, Alfred Wegener Institute, Helmholtz Centre for Polar and Marine Research, Bremerhaven, Germany
12. Department of Geosciences, University of Bremen, Bremen, Germany
13. Grantham Institute and Department of Earth Science and Engineering, Imperial College London, London, UK
14. Tremough House, University of Exeter, Penryn, Cornwall, UK

Contents of this file

Additional Supporting Information (Files uploaded separately)

Movie S1: Tectonic reconstruction showing the context of basin formation since 410 Ma (Müller et al., 2019; Young et al., 2019). East Antarctica is held fixed in this reconstruction which also does not include rift block motions or internal plate deformation. Sedimentary

basins are shown from their base-of-basin age to their top-of-basin age, with basin age indicating the time elapsed since the former. Continent-ocean boundaries (COB), oceanic crust age and isochrons and mid-ocean ridges (MOR) are also shown. Reconstruction was made using GPlates reconstruction software

Introduction

Supplementary figures included here show additional representations of the data shown in the main text including in Fig S1 an equivalent of Figure 1, zoomed into the data-rich McMurdo Sound region, and unannotated versions of Figures 3, 13, 14 and 16. All data and visualization are equivalent.

The tectonic reconstruction shows the context of Antarctica's basin s during the dispersal of plates from a Pangean configuration, beginning 410 Ma. The reconstruction was implemented in GPlates reconstruction software using the combined rotations of Müller, Cao, and Young (Cao et al., 2022; Müller et al., 2019; Young et al., 2019) with the Torsvik et al. (2019) correction applied for the Pacific. The rotations do not contain all block motions discussed in the text nor any explicit model of internal plate deformations.

As well as Antarctic basins (this study), we include in the reconstruction mid-ocean ridges from Müller et al. (2016), continent ocean boundaries from Müller et al. (2019) and the oceanic age grid and ocean crust isochrons from Seton et al. (2020). All these files are available by default in later versions of GPlates (version 2.3 was used here). The reconstruction uses East Antarctica as the fixed plate and shows relative motions to that plate. The animation is generated from a series of snapshots at 1 Ma intervals.

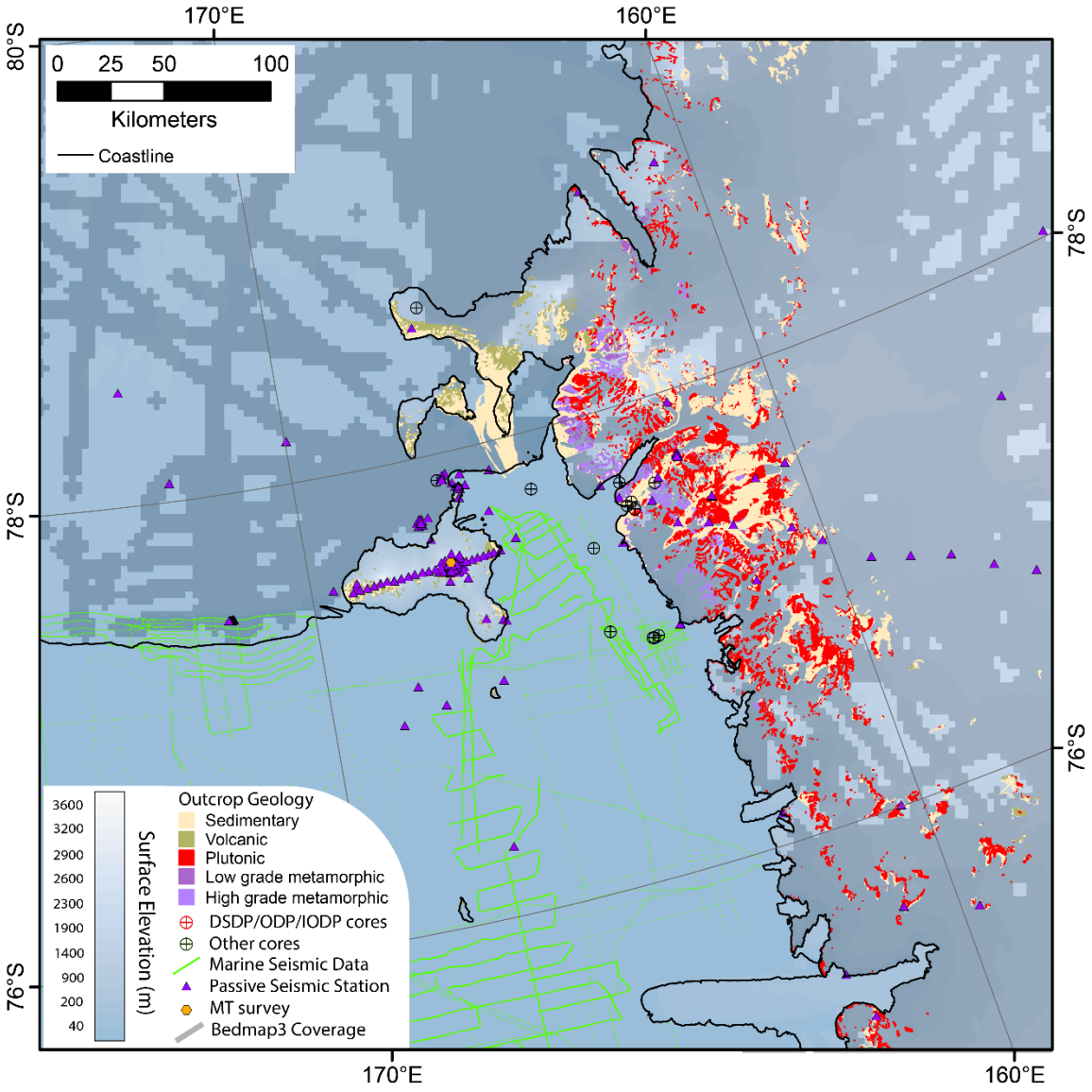

Figure S1. *Representative data coverage in the vicinity of McMurdo Sound and Ross Island, indicating outcropping geology, drill core sites, onshore passive seismic and MT stations, and marine seismic reflection lines offshore. Bedmap3 data coverage is shown only for onshore ice-covered areas.*

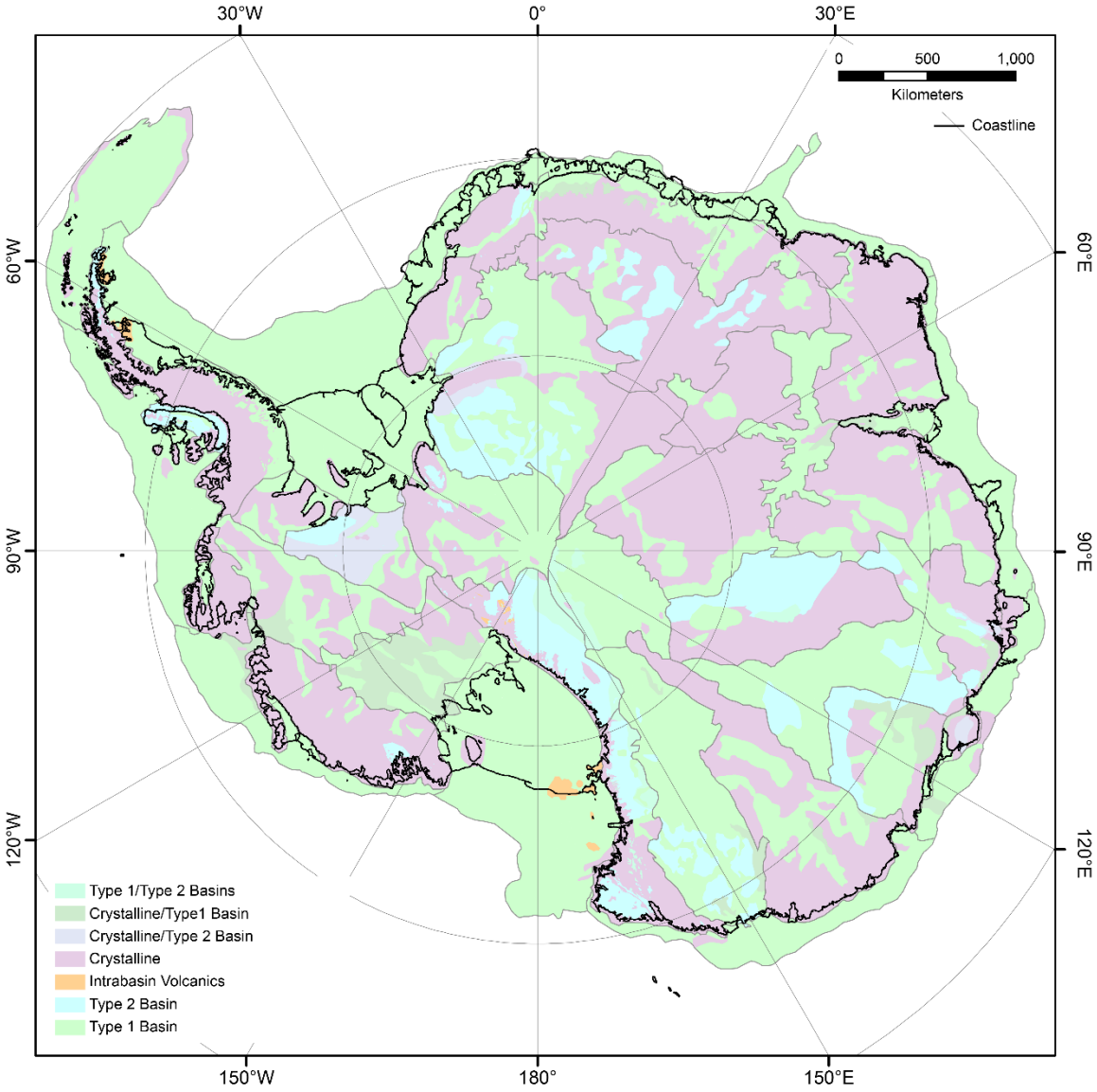

Figure S2: *Classification of geological bed type in Antarctica showing the main classes of Type 1 and Type 2 basins, intra-basin volcanics, and crystalline basement, as well as regions of mixed class without annotations. Major sedimentary basin regions are outlined in grey. The coastline shows both the ice sheet grounding line and the ice shelf edge.*

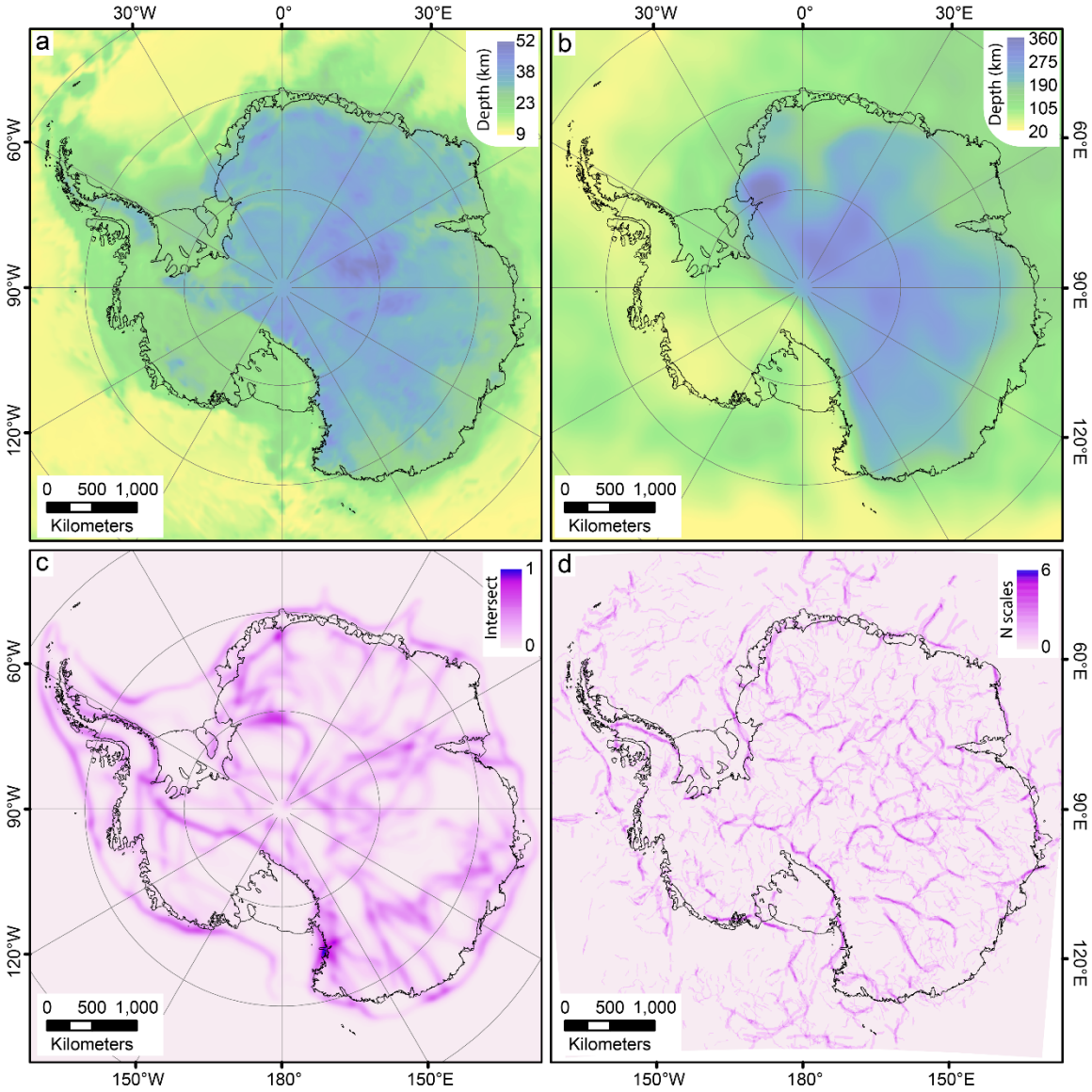

Figure S3: *Structure of the Antarctic lithosphere showing a) Moho depth (Pappa et al., 2019), b) lithosphere-asthenosphere boundary depth (Hazzard et al., 2023), c) multidata lineament analysis (Stål et al., 2019) and d) multiscale gravity edge analysis.*

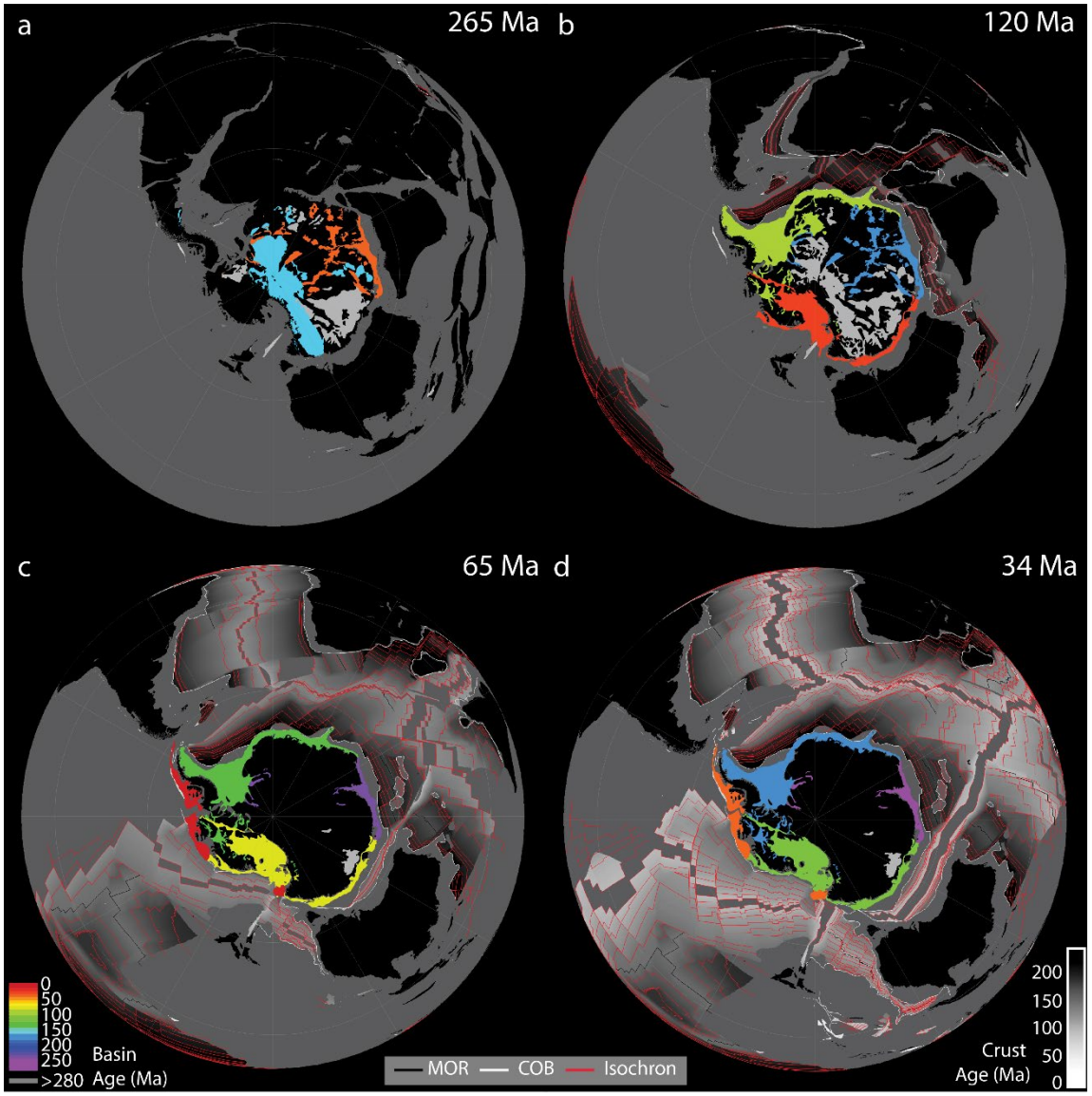

Figure S4: *Unannotated tectonic reconstruction snapshots a) 265 Ma, b) 120 Ma, c) 65 Ma and d) 34 Ma showing the context of basin formation since Pangea (Müller et al., 2019; Young et al., 2019).*

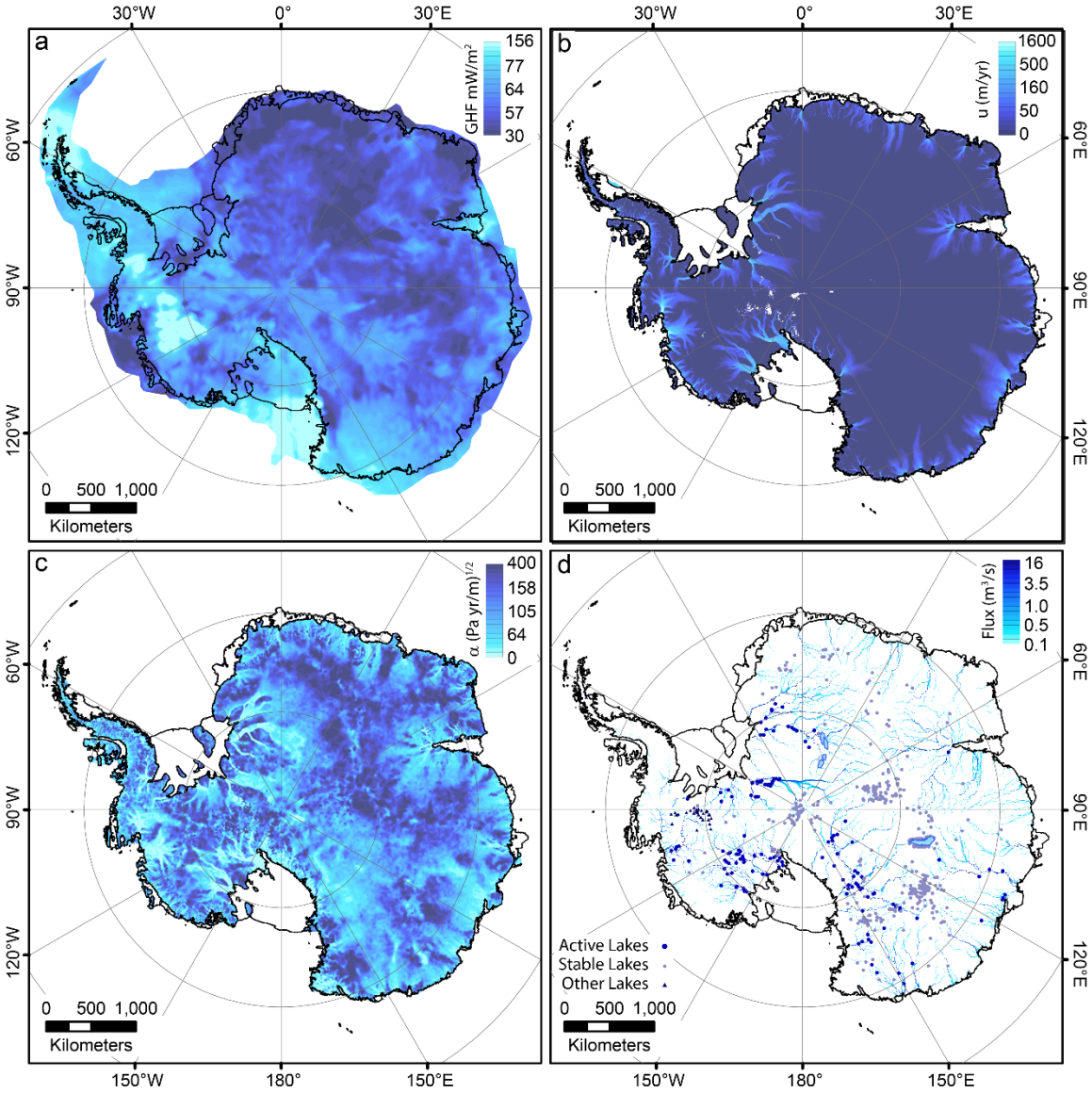

Figure S5: *Unannotated influences on ice sheet dynamics showing a) deep-seated geothermal heat flux (Lösing & Ebbing, 2021) b) surface ice sheet velocity from InSAR phase mapping (Mouginot et al., 2019) c) inferred basal friction coefficient derived by inverting for basal conditions using the Ice sheet and Sea level System Model (Dawson et al., 2022), and d) subglacial hydrology, including subglacial lakes (Livingstone et al., 2022), and a modern-day drainage network (Le Brocq et al., 2013).Figure S5: Unannotated influences on ice sheet dynamics showing a) deep-seated geothermal heat flux (Lösing & Ebbing, 2021) b) surface ice sheet velocity from InSAR phase mapping (Mouginot et al., 2019) c) inferred basal friction coefficient derived by inverting for basal conditions using the Ice sheet and Sea level System Model (Dawson et al., 2022), and d) subglacial hydrology, including subglacial lakes (Livingstone et al., 2022), and a modern-day drainage network (Le Brocq et al., 2013).*

References

Cao, X., Zahirovic, S., Li, S., Suo, Y., Wang, P., Liu, J., & Müller, R. D. (2022). A deforming plate tectonic model of the South China Block since the Jurassic. Gondwana Research, 102, 3-16. https://doi.org/10.1016/j.gr.2020.11.010

Dawson, E. J., Schroeder, D. M., Chu, W., Mantelli, E., & Seroussi, H. (2022). Ice mass loss sensitivity to the Antarctic ice sheet basal thermal state. Nature Communications, 13(1), 4957. https://doi.org/10.1038/s41467-022-32632-2

Hazzard, J. A. N., Richards, F. D., Goes, S. D. B., & Roberts, G. G. (2023). Probabilistic Assessment of Antarctic Thermomechanical Structure: Impacts on Ice Sheet Stability. Journal of Geophysical Research: Solid Earth, 128(5), e2023JB026653. https://doi.org/10.1029/2023JB026653

Le Brocq, A. M., Ross, N., Griggs, J. A., Bingham, R. G., Corr, H. F. J., Ferraccioli, F., et al. (2013). Evidence from ice shelves for channelized meltwater flow beneath the Antarctic Ice Sheet. Nature Geosci, 6(11), 945-948. https://doi.org/10.1038/ngeo1977

Livingstone, S. J., Li, Y., Rutishauser, A., Sanderson, R. J., Winter, K., Mikucki, J. A., et al. (2022). Subglacial lakes and their changing role in a warming climate. Nature Reviews Earth & Environment, 3(2), 106-124. https://doi.org/10.1038/s43017-021-00246-9

Lösing, M., & Ebbing, J. (2021). Predicting Geothermal Heat Flow in Antarctica With a Machine Learning Approach. Journal of Geophysical Research: Solid Earth, 126(6), e2020JB021499. https://doi.org/10.1029/2020JB021499

Mouginot, J., Rignot, E., & Scheuchl, B. (2019). Continent-Wide, Interferometric SAR Phase, Mapping of Antarctic Ice Velocity. Geophysical Research Letters, 46(16), 9710-9718. https://doi.org/10.1029/2019gl083826

Müller, R. D., Seton, M., Zahirovic, S., Williams, S. E., Matthews, K. J., Wright, N. M., et al. (2016). Ocean Basin Evolution and Global-Scale Plate Reorganization Events Since Pangea Breakup. Annual Review of Earth and Planetary Sciences, 44(1), 107-138. 10.1146/annurev-earth-060115-012211

Müller, R. D., Zahirovic, S., Williams, S. E., Cannon, J., Seton, M., Bower, D. J., et al. (2019). A Global Plate Model Including Lithospheric Deformation Along Major Rifts and Orogens Since the Triassic. Tectonics, 38(6), 1884-1907. https://doi.org/10.1029/2018TC005462

Pappa, F., Ebbing, J., & Ferraccioli, F. (2019). Moho Depths of Antarctica: Comparison of Seismic, Gravity, and Isostatic Results. Geochemistry, Geophysics, Geosystems, 20(3), 1629-1645. https://doi.org/10.1029/2018GC008111

Seton, M., Müller, R. D., Zahirovic, S., Williams, S., Wright, N. M., Cannon, J., et al. (2020). A Global Data Set of Present-Day Oceanic Crustal Age and Seafloor Spreading Parameters. Geochemistry, Geophysics, Geosystems, 21(10), e2020GC009214. https://doi.org/10.1029/2020GC009214

Stål, T., Reading, A. M., Halpin, J. A., & Whittaker, J. M. (2019). A Multivariate Approach for Mapping Lithospheric Domain Boundaries in East Antarctica. Geophysical Research Letters, 46(17-18), 10404-10416. https://doi.org/10.1029/2019GL083453

Torsvik, T. H., Steinberger, B., Shephard, G. E., Doubrovine, P. V., Gaina, C., Domeier, M., et al. (2019). Pacific-Panthalassic Reconstructions: Overview, Errata and the Way Forward. Geochemistry, Geophysics, Geosystems, 20(7), 3659-3689. https://doi.org/10.1029/2019GC008402

Young, A., Flament, N., Maloney, K., Williams, S., Matthews, K., Zahirovic, S., & Müller, R. D. (2019). Global kinematics of tectonic plates and subduction zones since the late Paleozoic Era. Geoscience Frontiers, 10(3), 989-1013. https://doi.org/10.1016/j.gsf.2018.05.011